NON-DESTRUCTIVE EVALUATION OF SOIL MOISTURE IN EVAPOTRANSPIRATION COVER SYSTEM

by

MD. ISHTIAQUE HOSSAIN

Presented to the Faculty of Civil Engineering of

The University of Texas at Arlington in Partial Fulfillment

of the Requirements

for the Degree of

DOCTOR OF PHILOSOPHY

THE UNIVERSITY OF TEXAS AT ARLINGTON

December 2017

ACKNOWLEDGEMENTS

I would like to express my sincere appreciation to my supervising professor, Dr. Sahadat Hossain, for his constant guidance and encouragement, without which this dissertation would not have been possible. For his unwavering support, I am truly grateful. I would also like to thank all of the professors of the Department of Civil Engineering for their guidance and valuable lectures.

I would like to acknowledge the City of Denton Municipal Solid Waste Landfill for funding this project. I am especially thankful for City of Denton Municipal Solid Waste Officials, for their generous support. I also like to convey my appreciation to Dr. Xinbao Yu, Dr. Hyeok Choi, and Dr. Ashfaq Adnan for devoting their time to serving as committee members. I really appreciate their valuable suggestions and constructive comments.

Special thanks to all my friends and research team members for their cooperation and assistance throughout my graduate studies. Their friendship, moral support, and helpful discussions have been highly appreciated during the whole process. I would specially thank Dr. Sonia Samir, Dr. Zahangir Alam, Dr. MD. Faysal, Dr. Golam Kibria, Dr. Sadik Khan, and Masrur Mahedi for being there whenever I needed them.

Most importantly, I express my deepest gratitude to my superman-like father, wonder-woman-like mother, sweetest sister, and my loving wife for their immeasurable encouragement and heartiest support. Everything I have done and everything I am today is because of them. Finally, I want to dedicate this work to my family and I feel privileged to have had the strength and patience to pursue a doctoral degree.

November 10, 2017

ABSTRACT

NON-DESTRUCTIVE EVALUATION OF SOIL MOISTURE IN EVAPOTRANSPIRATION COVER SYSTEM

Md Ishtiaque Hossain, PhD

The University of Texas at Arlington, 2017

Supervising Professor: MD Sahadat Hossain

A conventional landfill cover system is designed as a barrier layer system, with low hydraulic conductivity, to minimize the percolation of water from the cover to the waste. Evapotranspiration (ET) covers are currently becoming a popular alternative that are acceptable to landfill authorities, due to their cost effectiveness and nature-friendly performance. The principle function of the ET cover is to store the infiltrated water, using the water balance technique, until it is transpired by plants into the atmosphere, thus minimizing percolation. The performance of the final cover system is assessed by monitoring the soil moisture in the ET cover and the percolation of water into the waste. Current methods, which use small-scale field lysimeters equipped soil instrumentations to assess soil moisture, provide only discrete information and are unable to provide an accurate spatial or depthwise variation. Therefore, the development of a more efficient system for monitoring a full-scale ET cover system is vitally important. Electrical resistivity imaging (ERI) is an alternative method for evaluating soil moisture. A substantial number of studies have been carried out in laboratories and the field to correlate soil moisture and electrical resistivity; however, very few have correlated these parameters for the ET cover system, and there have been no significant studies on the relationship between soil moisture sensors and ERI. Therefore, the ERI method has the potential to be employed

in the ET cover system to estimate the moisture storage and hence percolation of the ET covers system.

To study the soil moisture in an ET cover system using ERI, it is necessary to acknowledge the differences in the soil conditions of the conventional cover system and the ET cover system. These differences can be attributed to the presence of planned vegetation and the resulting plant root systems. Therefore, the objective of this study is to perform detailed statistical analyses for the different soil conditions and develop field scale relationships between soil moisture and ERI. Model parameters will be developed to enable the estimation of soil moisture without the presence of other soil moisture instrumentation. Factors that might influence the ERI values are closely investigated to explain the differences in the soil conditions. Finally, a novel approach has been taken to evaluate the percolation rate in the lysimeters, using base layer moisture estimation and the field capacity of the cover soil.

For this investigation six lysimeter sections, along with a control section of vegetated and non-vegetated sections, were constructed in the City of Denton Landfill, in Denton, TX. Monthly monitoring was performed; using soil moisture sensors and the ERI instrument, and the physical and chemical properties of the cover soil, along with vegetation's and weather conditions, were monitored and recorded.

Two years of investigations indicated a good correlation between soil resistivity and soil moisture, and two separate relationships were proposed: a compacted clay model with an R^2 value of 0.92 and a vegetated clay model with an R^2 of 0.87. Further model validation showed that the percentage of error remained within 5% for the developed models. Qualitative analysis of data showed the variations of different factors in the field, and the use of the ERI showed the comprehensive differences between vegetated and non-vegetated landfill covers. The changes in excess soil moisture at the

base layer of the lysimeter showed a direct correlation with the rate of percolation of the lysimeters (r squared = 0.9324). The establishment of this trend made it possible to predict the rate of percolation, using the base layer moisture change, and constituted a novel approach to using ERI to predict the soil moisture of ET cover systems.

.

Table of Contents

Acknowledgements iii

Abstract iv

List of Illustrations xii

List of Tables xvii

Chapter 1 INTRODUCTION 1

BACKGROUND 1

PROBLEM STATEMENT 3

RESEARCH OBJECTIVES 4

DISSERTATION ORGANIZATION 4

Chapter 2 EVAPOTRANSPIRATION COVER AND ELECTRICAL RESISTIVITY: A REVIEW 1

OF LANDFILL COVER SYSTEMS 1

Requirements for Landfill Covers 1

Conventional vs Alternative Cover System 2

Cost Comparison 3

EVAPOTRANSPIRATION LANDFILL COVERS 5

Design Characteristics of Evapotranspiration Cover 6

Soil properties 7

Flow properties for saturated soil: 7

Flow properties for unsaturated soil 8

Soil Water Movement and Water-Holding Capacities 11

Soil Chemical Properties - Soil pH, Soil Nutrients, Cation Exchange Capacity, and Humus 15

Plants and Plant Roots- Plant Selection, Soil Density, Root Distribution, and Root Growth 16
Climate, Weather and Water Balance –Ambient conditions, evapotranspiration, and hydrologic water balance/water balance 19
Performance Criteria –Site selection, site-specific design 21
Suitability of Clay as Evapotranspiration Cover Soil 21
MONITORING SYSTEMS OF EVAPOTRANSPIRATION COVERS 22
Field Instrumentation Methods 23
Point Measurement of Soil Moisture Profiles 25
Methodology of Soil Moisture Sensors 26
Limitations of using Soil Moisture Sensors 27
ELECTRICAL RESISTIVITY OF COMPACTED CLAY 28
Soil Pore Water Characterization 28
Electrical Conduction in Clays 29
Clay Water Interface 31
Concept of Electrical Resistivity 32
Soil Resistivity models 33
RELATIONSHIP OF SOIL PROPERTIES WITH ELECTRICAL RESISTIVITY 33
Moisture content 34
Soil Density and Degree of Saturation 44
Soil Temperature 49
Soil Index properties 52
Cation Exchange Capacity and Specific Surface Area 53
Soil Texture and Soil Composition 54

Clay Content 55
Hydraulic Conductivity 56
Soil pH and Nutrient Availability 58
Plant and Plant roots 59
ELECTRICAL RESISTIVITY MEASUREMENT 61
Laboratory Measurement Systems 61
Field Measurement Systems 64
Electrode Configuration 65
Comparison of Different Array Methods 66
Dimensions of Resistivity Survey 68
Resistivity Data Interpretation 70
Chapter 3 FIELD-SCALE QUANTIFICATION OF SOIL MOISTURE USING ELECTRICAL RESISTIVITY IN EVAPOTRANSPIRATION COVER SYSTEM 72
ABSTRACT 72
INTRODUCTION 73
MATERIAL AND METHODS 77
Study Area 77
Lysimeter Construction and Field Instrumentation 78
Data collection 81
DATA ANALYSIS 84
Correlation analysis 84
Regression analysis 85
RESULTS AND DISCUSSION 86
Soil Electrical Resistivity Versus Soil Moisture Sensor Measurements 87
Correlation Analysis Between Soil Moisture and ERI 91

Regression Model Development for Soil Moisture and ERI 97
Comparison with Established Model and Proposed Modified Model 100
SUMMARY AND CONCLUSION 102
Chapter 4 EVALUATION OF FACTORS INFLUENCING ELECTRICAL RESISTIVITY IN EVAPOTRANSPIRATION COVER SOIL 105
ABSTRACT 105
INTRODUCTION 106
MATERIALS AND METHODOLOGY 109
Site Description 109
Field Investigation 112
RESULTS AND ANALYSIS 116
(1) Cover Soil Characterization 116
(2) Soil Compaction 119
(3) Soil pH 122
(4) Soil Temperature 123
(5) Soil Moisture 125
(6) Electrical Resistivity Imaging (ERI) 129
Evapotranspiration 133
ERI and Cover Soil Moisture 135
DISCUSSION AND CONCLUSIONS 137
Chapter 5 NON-DESTRUCTIVE APPROACH TO ESTIMATING SOIL WATER STORAGE AND PERCOLATION IN EVAPOTRANSPIRATION COVER SYSTEM 140
ABSTRACT 140
INTRODUCTION 141

MATERIAL AND METHODS 143
Site Description 143
ET Cover Soil Characterization 144
Sensor Nests 145
Electrical Resistivity Tests in the Field 146
RESULTS AND DISCUSSION 148
Monitoring ET Lysimeters 148
Moisture Distribution Using ERI to Predict Moisture flow in the Lysimeters 151
Relationship between ERI and Soil Moisture 152
Excess Base Layer Moisture and Percolation 153
Estimation of Percolation 158
SUMMARY AND CONCLUSIONS 161
Chapter 6 SUMMARY AND CONCLUSIONS 163
Appendix A ERI Profiles of ET Lysimeters 166
References 175
Biographical Information 192

LIST OF ILLUSTRATIONS

Figure 2-1 Conventional vs alternative landfill covers (Benson and Bareither, 2012) 3
Figure 2-2 Ideal cycle for annual soil moisture variation (Bendient et al., 2008) 7
Figure 2-3 Saturated hydraulic conductivity measured through a porous media (modified from Albright et al., 2004) 8
Figure 2-4 Illustration of suction concepts (Albright et al., 2004) 9
Figure 2-5 Schematic showing the relationship between pore diameter, suction at which water is held in pores of various sizes, and water content (Albright et al., 2004) 10
Figure 2-6 Relationship between soil suction and hydraulic conductivity (Albright et al., 2004) 11
Figure 2-7 Simplified representation of the relationship between soil moisture and the pore space that controls hydraulic conductivity (Albright et al., 2004) 11
Figure 2-8 Illustration of the void space concept (Albright et al., 2004) 14
Figure 2-9 Illustration of the field capacity concept (Albright et al., 2004) 14
Figure 2-10 Illustration of the wilting point concept (Albright et al., 2004) 14
Figure 2-11 Possible distributions of living roots at different times during the growing season 18
Figure 2-12 Ion chromatography (IC) test procedures (http://www.metrohm.co.uk) 29
Figure 2-13 Diffuse double layer (DDL), Stern layer, and precipitated ions in clays (http://geophysics.geoscienceworld.org) 31
Figure 2-14 Relationship of soil moisture and electrical resistivity 35
Figure 2-15 Relationship between the electrical resistivity and the volumetric soil moisture 39
Figure 2-16 Relationship between ratio of bulk soil and pore water conductivity with volumetric moisture content (Kalinsky and Kelly 1993) 41

Figure 2-17 ERT during the year of 2007 (Brunet et al., 2010) 43
Figure 2-18 Comparison of ERT and TDR predicted water content at depths (a) 0-20 cm, (b) 20-40 cm, and (c) 40-70 cm (Brunet et al., 2010) 44
Figure 2-19 Phase diagram of soil 45
Figure 2-20 Effect of degree of saturation on conductivity at different electrolyte concentrations 46
Figure 2-21 Iso conductivity contour of compacted sample (Parentheses show electrical conductivity in mho/m.) (Rinaldi and Cuestas, 2002) 47
Figure 2-22 Relationship between electrical resistivity, molding water content, and compaction effort for different soils (Abu Hassanein et al., 1996) 49
Figure 2-23 Relationship between electrical resistivity and temperature (Abu Hassanein et al., 1996) 50
Figure 2-24 Conductivity of clay soil at different frequencies (Rinaldi and Cuestas, 2002) 51
Figure 2-25 Relationship between electrical resistivity and Atterberg limits at optimum water content (Abu Hassanein et al. 1996) 56
Figure 2-26 Correlation between microscopic and hydraulic permeability coefficients during consolidation (Arulanandan, 1968) 58
Figure 2-27 (a) Root dry mass per unit soil volume (RMD) as a function of electrical resistivity (ρ). (b) RMD calculated with the logistic regression model (RMD_c) versus measured RMD (RMD_m) (Amato et al., 2008) 61
Figure 2-28 Two-electrode electrical resistivity measurement system 62
Figure 2-29 Four-electrode electrical resistivity measurement system 63

Figure 2-30 During field investigations, four electrodes are typically positioned at arbitrary locations. For the four-electrode system, the resistivity is measured by the following equation: 64
Figure 2-31 Sensitivity and resolution diagrams of electrode configurations. (a) Pole-pole, (b) dipole-dipole, (c) pole-dipole, (d) Gamma-array, (e) pole-bipole, (f) Wenner- Beta, (g) Wenner, (h) gradient array, (i) Schlumberger, and (j) midpoint-potential-referred (Dahlin & Zhou, 2004). 68
Figure 2-32 2D resistivity measurement (Samoulien et al. 2005) 69
Figure 2-33 Schematic of iterative inversion modelling (Sharma, 1997) 71
Figure 3-1 Location of ET lysimeters (on left) and field installation setup (on right) 77
Figure 3-2 Steps of Lysimeter Construction (a) Embankment construction, (b) Embankment excavation, (c) Geomembrane placement (d) Percolation collection system installation, (e) Geo-composite drain placement, (f) Compacted clay placement, (g) Topsoil placement, (h) Vegetation and erosion mat placement, (i) ET cover lysimeter after completion 79
Figure 3-3 ET cover soil properties for different lysimeters at different depths 80
Figure 3-4 ERI profile along the lysimeters showing moisture sensor locations 81
Figure 3-5 Soil resistivity and soil moisture relationship of all the measured data for this investigation (a) Temperature-corrected resistivity vs. soil moisture (b) Temperature-corrected natural log resistivity vs. soil moisture 93
Figure 3-6 Measured soil resistivity and volumetric soil moisture data grouped by lysimeters 94
Figure 3-7 Measured soil resistivity and volumetric soil moisture data grouped by different depths 95

Figure 3-8 Relationship between Soil Resistivity and Volumetric Soil Moisture for Compacted clay and vegetated clay 100
Figure 3-9 Comparison of present study with two-parameter model (a) non-vegetated clay, (b) vegetated clay 102
Figure 4-1 Pilot zone section and schematic of sensors placed in the field 110
Figure 4-2 (a) Location of ET lysimeters in City of Denton landfill, TX, USA (b) Plan view of the lysimeters and the pilot scale study area. 111
Figure 4-3 (a) Soil compaction tester; (b) Field compaction testing using soil compaction tester 113
Figure 4-4 (a) ET chamber schematic and (b) the equipment being used in the field .. 116
Figure 4-5 Plant root mass density in the vegetated cover soil of the control section .. 119
Figure 4-6 Compaction level variations at different depths (a) Non-vegetated cover soil (b) Vegetated cover soil 120
Figure 4-7 Field compaction level profiles for vegetated and non-vegetated landfill cover soils 121
Figure 4-8 Soil compaction level in the lysimeters 122
Figure 4-9 Soil pH variations in (a) ET lysimeters and (b) pilot section 123
Figure 4-10 Soil temperature variations at different depths of the pilot scale cover soil (a) Non-vegetated (b) Vegetated 124
Figure 4-11 Soil moisture variations at different depths of the control section cover soil (a) Non-vegetated (b) Vegetated 126
Figure 4-12 Soil moisture variations after a single rainfall event. 129
Figure 4-13 ERI profiles of vegetated and non-vegetated cover soil after 16.256 mm precipitation 131

Figure 4-14 ERI profiles of vegetated and non-vegetated cover soil after 7 days without any rainfal 132
Figure 4-15 Evapotranspiration rate variations in vegetated and non-vegetated cover soil and the weather components which influence process in the field. 134
Figure 4-16 Evapotranspiration rate variations in ET lysimeters 135
Figure 5-1 Location of the ET cover project in the City of Denton Landfill, TX 144
Figure 5-2 Location of moisture sensors in the cover soil 146
Figure 5-3 Electrical resistivity imaging along the lysimeters 147
Figure 5-4 Measured rate of runoff of the lysimeters for two-year period 149
Figure 5-5 Measured percolation rates for two-year period of the lysimeters 150
Figure 5-6 I Section investigation for moisture conditions in lysimeters 152
Figure 5-7 Rainfall events in the ET lysimeter from the beginning of operation (October 2014 to June 2015) 153
Figure 5-8 Moisture variation of the base layer in the ET lysimeters from October 2014 to June 2015 155
Figure 5-9 Relationship between base layer excess moisture and the rate of percolation for the ET lysimeter 156
Figure 5-10 ERI profile of all the lysimeters for January 2017 158
Figure 5-11 ERI profile of Lysimeter 1 for January 2017 159
Figure 5-12 Observed cumulative percolation in the lysimeters 160

LIST OF TABLES

Table 2-1 Advantages and Disadvantages of ET Landfill Covers 4

Table 2-2 Non-destructive soil water monitoring devices for ET covers (USEPA, 2011) . 24

Table 2-3 Major types of soil moisture sensors and their relative advantages and disadvantages (Walker et al., 2004) 27

Table 2-4 Relationships between soil moisture and electrical resistivity (Calamita et al., 2012) 37

Table 2-5 Typical ranges of LL, PL, and activity of minerals (Mitchell and Soga, 2005) . 52

Table 3-1 ET cover soil characterization summary..... 80

Table 3-2 Vegetation mixes used in the ET lysimeters..... 80

Table 3-3 Moisture and temperature sensors installed in the ET cover soil..... 80

Table 3-4 Summary of descriptive statistical parameters for soil resistivity and soil moisture (a) data grouped by lysimeters (b) data grouped by depth and (c) data grouped by soil condition (SD: standard deviation, CV: coefficient of variation, Min.: minimum, Qu.: quartile, IQR: interquartile range 89

Table 3-5 Correlation analysis between soil resistivity and volumetric soil moisture for different data sets measured in this investigation (r*: Spearman correlation coefficient, r: Pearson's correlation coefficient, C.I. 95%: 95% confidence interval, # of points: sample size) 96

Table 3-6 Regression analysis between soil resistivity and volumetric soil moisture for different data sets measured in this investigation (SE: standard errors, C.I. 95%: 95% confidence interval of regression parameters, RMSE: root mean square error, R^2: coefficient of determination, SD (MC): standard deviations of soil moisture measurements, SD R: standard deviation of resistivity measurements, N: # of samples) 99

Table 3-7 Developed Model for different soil condition..... 100

Table 3-8 Established and proposed model for non-vegetated and vegetated cover soil respectively. 101

Table 4-1 Location of moisture sensor placed in the pilot zone..... 111

Table 4-2 Summary of soil compaction testing in the control section..... 113

Table 4-3 Geotechnical Characterization of Pilot Section Soil Samples 118

Table 4-4 Developed models for different soil condition..... 136

Table 4-5 Model validation in the control section..... 137

Table 5-1 Geotechnical Characterization of ET Lysimeter Base Layer Soil..... 145

Table 5-2 Resistivity log of lysimeter 1 cross-section (x= 26 feet) on 30th January, 2017 159

Table 5-3 Rate of percolation predicted from the excess moisture 161

Chapter 1

INTRODUCTION

BACKGROUND

Economic and environmentally sound management of generated waste is a major concern for engineers, landfill operators, and government officials (Squillace, et. al. 2012), and the placement of landfill cover systems is vital to reducing the environmental damage that the landfill might pose. An impermeable cover or final cover system is usually designed and installed in landfills to alleviate any possible long-term risk that the landfilled waste may pose to the environment (USEPA, 2006). These covers serve specific purposes, such as minimizing infiltration and further percolation of water into the waste, promoting surface runoff, controlling gas emissions and odors, and preventing erosion (Barnswell and Dwyer, 2011; USEPA, 2006). Conventional landfill covers are constructed of materials having low permeability to minimize the downward migration of water through the cover; however, they are expensive to construct and maintain (Hauser, 2008). Therefore, evapotranspiration (ET) cover systems or water balance cover systems, are becoming an increasingly popular alternative because of their efficiency in satisfying the cover system performance requirements at less cost.

An ET cover system is a more natural and cost-effective alternative to a conventional cover. They rely on ET and the water storage capacity of soil to minimize infiltration into the waste, which allows them to act very similar to nature (Benson et al., 2002). This natural mechanism is more likely to be sustainable in the long-term than the conventional cover. The primary principle of an ET cover is to store the infiltrated water from rainfall in the cover soil and transpire the water through plants during drier periods (Barnswell and Dwyer, 2011; Benson et al., 2002). Hence, the performance of an ET cover largely depends on the water storage capability of the cover soil and the

percolation of water through it. ET covers are becoming more common for full-scale use due to potential problems with the long-term durability of fine-grained barrier layers and the relatively high cost of conventional covers (Albright et al., 2004).To monitor the field performance of an ET cover system, lysimeters are installed to measure the water flowing through the bottom of the cover. They may also be equipped with soil water monitoring tools, and are commonly used as a secondary or indirect monitoring tool to verify the effectiveness of the lysimeters in terms of moisture storage and percolation (Malusis and Benson, 2006). The soil moisture instruments are typically placed at discrete locations and at different depths to provide information about the availability of soil moisture and to evaluate changes over time in vertical and horizontal gradients. A high water content suggests that the cover is approaching the storage capacity, thereby increasing the possibility of percolation (Madalinski et al., 2003).

Monitoring and maintaining an ET cover system efficiently is essential to the preservation of the integrity and effectiveness of the cover system for long-term use. Drainage lysimeters and soil water monitoring devices are the most common methods used for performance monitoring. Several other moisture monitoring methods are available also, such as capacitance sensors, thermal dissipation units, psychrometers, tensiometers, and time domain reflectrometry (USEPA, 2011), but are not deemed to be as accurate. Benson et al., 2001, concluded that methods for measuring percolation, such as trend analysis of soil moisture sensors, tracers method, and the water balance method have higher levels of discrepancies than the lysimetry method.

Several studies on detecting soil moisture have proposed the use of geophysical methods such as electrical resistivity imaging (ERI) as a non-destructive method for subsurface investigation (Liang et al., 2007; Nijland et al., 2010; Schnabel et al., 2012). Studies conducted by Abu Hassanein et al., 1996, and Kibria, et al., 2012 showed a

significant correlation between moisture content and electrical resistivity in different types of soil in laboratory scale investigations. Therefore, the use of electrical resistivity might be considered a suitable alternative for evaluating the soil moisture content of ET covers.

PROBLEM STATEMENT

Drainage lysimeters are a reliable method for evaluating the soil moisture storage and percolation of ET covers in the field (Gee and Hillel, 1988; Benson et al., 2001). Non-destructive soil moisture monitoring devices are also frequently used (Malusis and Benson, 2006). Interestingly, moisture monitoring devices are often installed in drainage lysimeters as a secondary method for determining the soil moisture and hence the moisture storage of the cover soil (USEPA, 2006). However, if the currently available non-destructive methods, such as moisture sensors, are used to monitor the soil water storage only for discrete locations, the overall performance of the covers might be overlooked (Schnabel et. al, 2012). Another downside is that it is expensive to install sensors in the cover soil, and they are not suitable for long-term moisture monitoring due to their short lifetime warranty (Rock, S et.al, 2012).

In summary, a non-destructive, extensive, and inexpensive method such as electrical resistivity, which uses a multi-electrode array to measure the soil electrical resistivity, might be considered a suitable tool for ET cover monitoring. Spatially and temporally variable data, using the electrical conduction phenomenon of soil, provides moisture variations and detects heterogeneity of the subsurface. The use of ERI has been studied by researchers to detect moisture variations in conventional landfill liners (Kibria et. al, 2012); however, no significant studies have been conducted to correlate electrical resistivity with the moisture variations in ET covers. Furthermore, a soil moisture sensor which uses dielectric constant to measure the volumetric soil moisture has never been compared with the electrical resistivity method. Therefore, it is important

to establish a cost-effective, non-destructive, and efficient method which could be used in the field to monitor moisture content of ET cover soil.

Six ET cover lysimeters were constructed in the City of Denton landfill to assess the moisture content of ET cover soil, using the ERI method. The relationships between resistivity and moisture content were investigated to estimate the moisture storage and hence estimate the percolation.

RESEARCH OBJECTIVES

The overall objective of the current study was to evaluate the moisture content in evapotranspiration covers, using electrical resistivity imaging, and to assess the potential of its applications. The specific tasks required to establish electrical resistivity as a moisture monitoring tool for an ET cover system are as follows:

- Selection of the study area
- Construction of the lysimeters
- Field Instrumentation in the ET cover lysimeters
- Data collection
- ERI investigation of the lysimeters
- Development of statistical relationship between ERI and soil moisture
- Moisture content prediction in the field, using currently available models
- Model validation
- Determination of percolation in ET cover by moisture estimation, using ERI

DISSERTATION ORGANIZATION

Chapter 1 begins with an introduction, followed by a problem statement and objectives of the research. An extensive literature review is presented in Chapter 2. The rest of the dissertation is divided into three papers. The first paper describes a detailed

statistical analysis of the electrical resistivity and soil moisture data for an ET cover. Two separate exponential models are proposed for vegetated and non-vegetated clay, and field scale verification is carried out for the models. The second paper discusses the variable factors that make it necessary to have two separate models: one for vegetated and one for non- vegetated clay. The most influential factors are explored, explaining the differences in the two ERI soil moisture models. Finally, the third paper describes the application of using soil moisture sensor data to estimate the rate of percolation, suggesting that soil water storage can be estimated by using ERI, and that base layer moisture changes will provide the percolation for the ET lysimeters. These papers are followed by a summary and conclusions.

Chapter 2

EVAPOTRANSPIRATION COVER AND ELECTRICAL RESISTIVITY: A REVIEW OF LANDFILL COVER SYSTEMS

According to the USEPA (2011), a landfill cover is a critical component of a landfilling operation and is vitally important to reducing the environmental damage that a landfill might pose. It is very important that the nature and process of application of the cover at each landfill be appropriate to accomplish the general objectives of controlling possible threats that may arise. Landfill cover technology can be either conventional or innovative, but it must work well with the other parts of landfill containment system, which includes gas collection, groundwater protection, and leachate management (Koerner, 1997). There are many types of landfill covers: daily cover, intermediate cover, and final cover. The daily cover is used on the working face of the landfill, where a thin layer of soil is placed, after the working hours of the landfill, to deter the presence of rodents and birds and to prevent the odor and litter from spreading. Intermediate covers are placed in inactive parts of the landfill, where the future wastes may be disposed of. The final cover; which is the most significant cover type for the landfill because it is a part of the landfill remediation process, is placed when the landfill reaches the design capacity and final waste grade (McBean et al., 1995, Dunn, 1995). This cover system is referred to as the final cover system in this paper.

Requirements for Landfill Covers

Several essential and technical reasons dictate the placement of a cover in a landfill. The design is selected according to the regulations. The major purposes of the cover system are to (Hauser, 2009):

- Minimize infiltration of water into the landfilled waste and percolation of the contaminated water into the groundwater;

- Quarantine wastes, thus preventing movement due to wind and water, so that that they don't enter the environment;
- Regulate the emission of landfill gases.

Conventional vs Alternative Cover System

In the United States, conventional final cover systems are designed according to the regulations set by the Resource Conservation and Recovery Act (RCRA). Individual states may modify the RCRA act for their final cover system. The regulations generally require a cover which is less permeable than the landfill bottom liner in order to avoid the "bathtub effect." As soil itself is not capable of reaching low permeability, the regulations require the placement of a geomembrane in the cover system to match the permeability of the geomembrane placed in the bottom liner layer. In a conventional cover system, this is usually accomplished by placing a geomembrane layer over a compacted clay liner or low-permeability soil (with the order of 10^-5 to 10^-7 cm/sec). In certain locations, where clay soil is not available to achieve this low permeability, a geosynthetic clay liner is used. The cover soil is installed above all these layers (Goldenberg, 2017). Exceptions are only observed in older landfills which were constructed without a geomembrane layer.

The evapotranspiration (ET) cover is a nature-friendly system. It works with the components of nature to prevent water from infiltrating the landfilled waste. The most significant characteristics of the ET cover are that it is does not have barrier layers and that it functions efficiently for a long period of time. It is comprised of a layer of cover soil in which native grasses have been planted. Natural processes include the cover soil acting as the water reservoir layer and the combined effect of evaporation and evapotranspiration, transpiring the reserved water into the atmosphere.

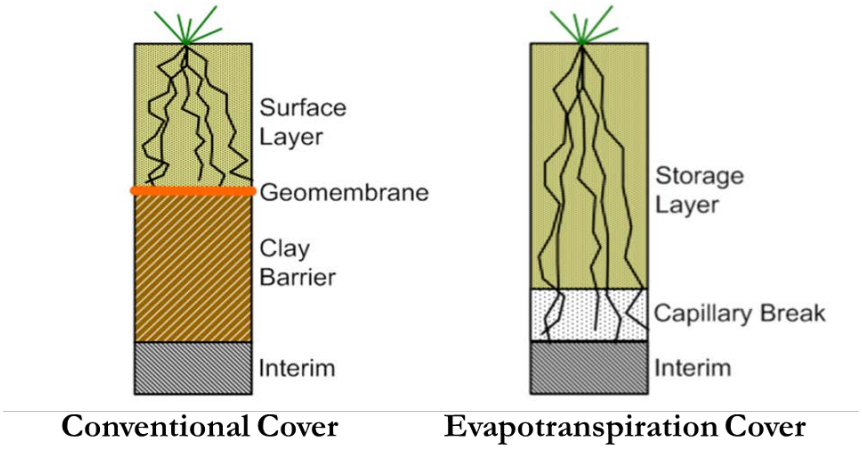

Figure 2-1 Conventional vs alternative landfill covers (Benson and Bareither, 2012)

Cost Comparison

Construction costs for conventional landfills are reported to be from $319,000 to $571,000 per acre of surface cover (Hauser et al., 1999). The report also concluded that the cost of placing an ET cover in the same location is about half of that of the conventional cover. Another study conducted by Hauser et al., 2001 concluded that the construction costs of ET covers vary from 35% to 72% of the cost of conventional covers. In addition, the repair and maintenance costs of ET covers are less than those of the conventional covers.

Advantages and Disadvantages of ET Landfill Covers

An ET cover is an efficient, natural, and self-sustaining cover that is capable of meeting the cover requirements for a site and costs approximately half the amount of a conventional cover. Various waste containment facilities such as municipal, industrial, and hazardous landfills are suitable for ET covers, depending on the site conditions, and various functions can be performed by them, depending on the site requirements. For example, if the site requires no or minimal percolation the ET covers can be designed as such. On the contrary, due to flexibility of design and construction, it can also allow water

to infiltrate for bioreactor landfill purposes. Table 2-1 summarizes the advantages and disadvantages of the ET cover.

Table 2-1 Advantages and Disadvantages of ET Landfill Covers

Advantages	**Disadvantages**
Natural System	Requires site-specific design
Greater potential for long term success	Requires adequate soil availability nearby
Long life	Restriction for reusable use
More protective to human and environment	
Easy maintenance	
Low construction cost	
Easily adaptable to bioreactor systems	

Several site-specific parameters apply when designing and constructing an ET cover. These include the climatic conditions, available soils and their water storage capacities, the required soil thickness, and the ability of the available plant species to uptake water. Each site needs to be evaluated with care to ensure that an ET design will control the water intake. With proper design, the potential benefits of an ET cover are a much lower cost because barrier or drainage layers are not needed and the use of less energy for mixing and engineering, as well as the placement and compaction of soil. ET covers may not be appropriate at facilities with insufficient evapotranspiration to remove the precipitation from the soil column, where the geology is unfavorable, where they aren't accepted by a regulatory agency, or where there are increased costs associated with the test pads. In 1998, the USEPA initiated the Alternate Cover Assessment Program (ACAP) to evaluate the field performance of traditional and alternate landfill covers (Albright et al. 2010). ET covers were installed at 12 sites and showed highly variable performances, with percolation rates ranging from 0 to 207 mm/yr. The performances were strongly related to the site climate, with the lowest percolation rates occurring in arid or semi-arid climates, and the highest rates were measured in sub-

humid and humid climates. The cost of an ET cover is low only if the required soils are available nearby. Because of their increased thickness, almost 3 meters in some cases, the cost to transport a large quantity of soil may exceed the cost to construct a traditional composite cover system. Even after considering their possible limitations, it can be concluded that ET covers can be effective in providing adequate low-permeability covers in dry climates, provided that they are designed and constructed with appropriate soils, thicknesses, and sustainable vegetation. They are engineered systems that are capable of meeting regulatory requirements at much lower costs than the traditional cover systems.

EVAPOTRANSPIRATION LANDFILL COVERS

Final covers are used to reduce the infiltration of water into contaminated soil and waste, thereby reducing the rate of leachate generation and ground water contamination. Resistive characteristics of landfill covers contribute to hydraulic impedance, which restricts flow into underlying waste. Many regulations permit are maintained for alternative cover designs that would provide equivalent hydraulic properties to the prescribed cover. Equivalency in hydraulic properties signifies that the alternative cover allows less or equal percolation from the base of its cover than a prescriptive cover. In most of cases, the cost for an alternative cover is much less than for a prescriptive cover, but it is equally effective. (Ankeny et al., 1997). One of the most common alternative covers is the “alternative earthen final cover” (AEFC), which utilizes the water storage capacity of fine-grained soils and the water expulsion capability of vegetation. (Benson and Khire, 1995; Stormont and Morris, 1998; Nyhan et al., 1997). Alternative earthen final covers are also known as “evapotranspiration or ET” covers. Water stored in the AEFC must eventually be removed by evaporation or transpiration for the cover to be working effectively. In this type of cover, the role of vegetation is very important because water

uptake by the roots is the basic means of removing the water which is stored in the cover. Thus, in the context of remediation via containment, AEFCs are classified as a phytoremediation technology.

Design Characteristics of Evapotranspiration Cover

The idealized annual relationship between potential ET (PET), soil-moisture, and precipitation (rainfall) is provided in Figure 2.2. Infiltrated water is removed from the soil (from the atmospheric/soil boundary down) during times when the PET is greater than the rainfall, which is basically during the spring and summer. During autumn and winter, when the amount of rainfall is greater than the PET, the water tends to infiltrate the soil from the atmospheric/soil boundary and cause the water content in the soil to increase. Ideally the entire soil system will not reach field capacity prior to the PET becoming greater than the amount of rainfall. ET cover systems act as a sponge to manage water,

. The basic ideas behind this concept are:

- Provides enough water storage capacity within the soil system to prevent percolation from the bottom of the cover system during periods when rainfall (precipitation) exceeds PET,
- Removes a sufficient amount of stored water from the cover system during periods when ET exceeds rainfall (precipitation).

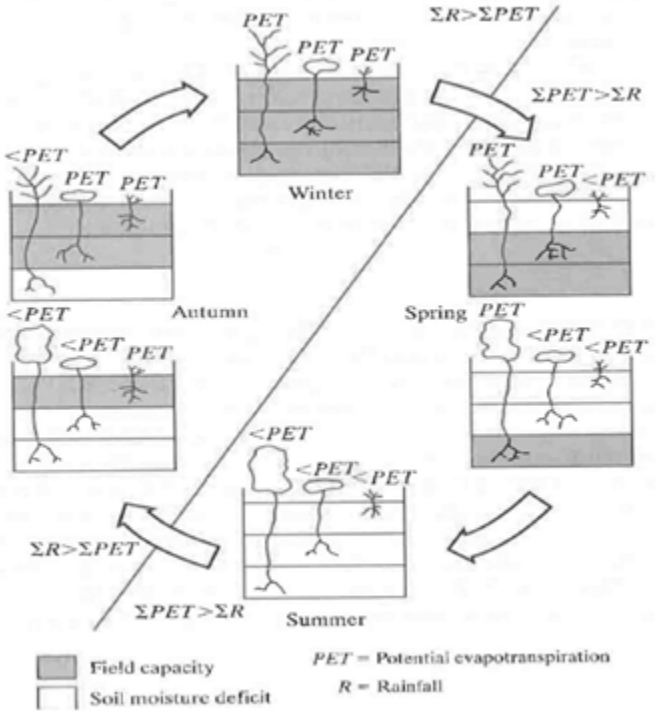

Figure 2-2 Ideal cycle for annual soil moisture variation (Bendient et al., 2008)

Soil properties

Flow properties for saturated soil:

Water flow in saturated soil can be explained by Darcy's Law during the time period when the cover is saturated due to storage of a large quantity of water. Figure 2.3 illustrates the saturated hydraulic conductivity schematic. The law describes the relationship between the flow rate of water (Q); hydraulic gradient (i), which is the difference in hydraulic potential (H) acting over the length (L) of the flow path; saturated hydraulic conductivity (ks); and the cross-sectional area (A) of the soil through which flow is occurring, as follows:

$$Q = Ks\frac{\Delta H}{L}A = KsiA$$

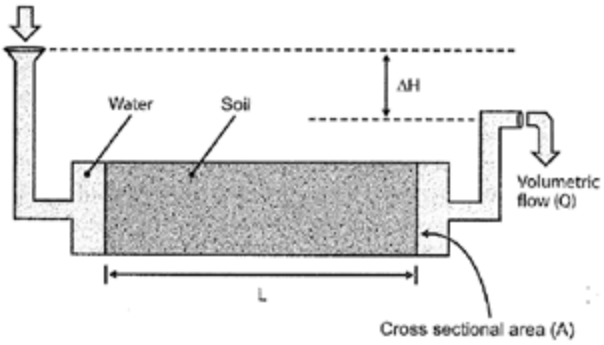

Figure 2-3 Saturated hydraulic conductivity measured through a porous media (modified from Albright et al., 2004)

Flow properties for unsaturated soil

The water pressure in the soil pores of the cover system is negative in unsaturated soil, as the water remains in tension. This negative pressure of water in the soils is called matric suction (ψ), but is usually simply referred to as suction. The common suction concept is shown in Figure 2-4 below. There is negative suction above the water surface within the tube, due to the holding of water by capillary forces under tension; there is positive water pressure below the water surface. By creating suction with capillary forces, water is retained in the soil. In unsaturated soil, adsorptive forces within soil surface and water molecules hold water (Albright et al. 2004).

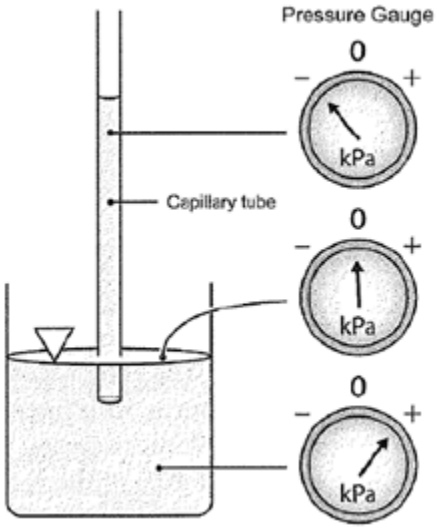

Figure 2-4 Illustration of suction concepts (Albright et al., 2004)

The soil water retention curve (SWCC) describes soil water content as a function of suction. The relationship is shown in Figure 2-5 below. The SWCC incorporates the following terms and definitions:

- Saturated water content (θs) – condition of soil at zero suction
- Residual water content (θr) – driest condition of the soil, which corresponds to the water content below which water removal becomes practically impossible
- Air entry value (ψa) – suction at which the large pores desaturate
- Field capacity (θc) – generally determined as the moisture content at a suction of 33 kPa
- Wilting point (θm) – generally described as the moisture content in the soil at a suction of 1,500 kPa (Albright et al. 2004).

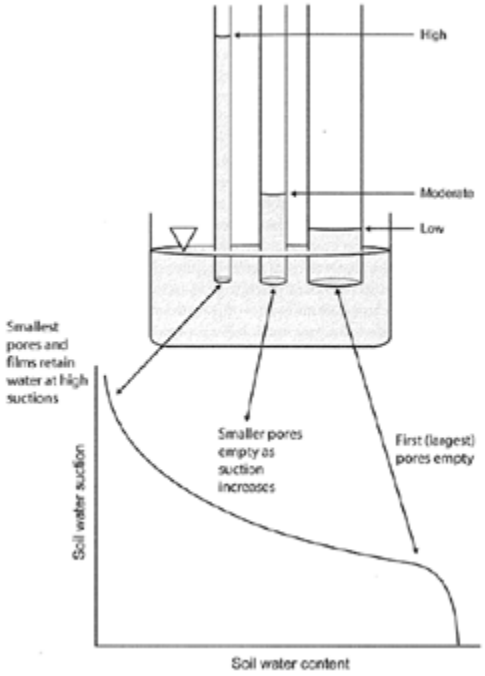

Figure 2-5 Schematic showing the relationship between pore diameter, suction at which water is held in pores of various sizes, and water content (Albright et al., 2004)

Hydraulic conductivity reduces significantly in between saturated conditions, where maximum hydraulic conductivity occurs, and dry conditions (shown, though exaggerated in Figure 2-6). When the soil moisture content in the soil decreases, suction increases. As a consequence, pore spaces in the soil become either fully or partly filled with air. Thus, the conduits which can pass water through soil, reduce in size, and the hydraulic conductivity of the soil decreases (Figure 2-7).

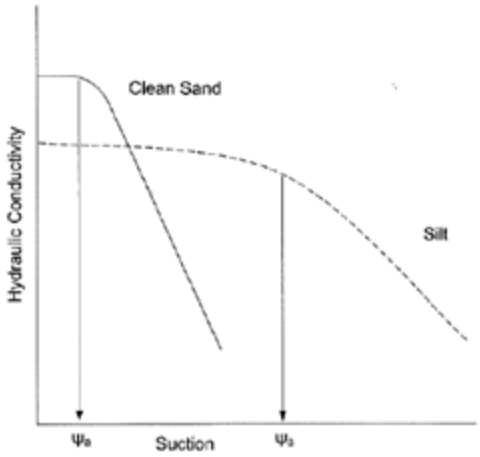

Figure 2-6 Relationship between soil suction and hydraulic conductivity (Albright et al., 2004)

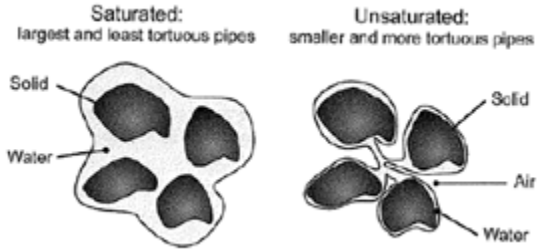

Figure 2-7 Simplified representation of the relationship between soil moisture and the pore space that controls hydraulic conductivity (Albright et al., 2004)

Soil Water Movement and Water-Holding Capacities

The system of an evapotranspiration cover acts like a sponge, preventing water from percolating through the bottom. (See Figure 2-8, Figure 2-9, and Figure 2-10.) Albright et al., (2004) explained the figures clearly, as below.

Two soils were submerged to saturation (Figure 2.6), one a clean uniform sand (relatively large particles of similar particle size) and the other a silty sand (a finer-textured and more broadly graded soil). The fraction of total soil volume occupied by pore

space varied with the soil textures, with finer-textured soils generally having a higher fraction of total soil volume as pores. However, for this example each soil was assigned a pore volume of 40%, with the remaining 60% represented by soil grains. Thus, both soils had a porosity of 0.40.

The two soils were raised out of the water and allowed to drain freely (Figure 2-8). Water will drain until the suction that develops in the pore water is large enough to resist the gravity forces causing drainage. Much more water drains from the sand than from the silt, which is intuitive. The sand has larger pores, and thus small suctions can develop to retain water within the pore structures. The amount of water remaining in the sand is about 10% of the total soil volume, whereas it is about 44% for the silty sand. (These numbers are arbitrary, but do approximate actual soils and are meant to demonstrate concepts.) The soils, which have drained freely and have reached equilibrium, are often described as being at field capacity water content (θc). A variety of definitions of field capacity exist, including (1) the amount of water the soil can hold against the force of gravity, (2) the amount of water left in the soil after draining from saturation by gravity for 24 to 48 hours, (3) the state of saturated soil when all of the soil moisture that is able to freely drain away has done so, and (4) the water content corresponds to a suction of 33 KPa. This last definition, which is quantitative, is common in practice and is used henceforth.

When plants are added and roots extend through the soil (Figure 2-9), additional water can be removed by transpiration. Plants remove water until they wilt (i.e., the cessation of transpiration). This water content is referred to as the wilting point (indicated by the arrows in Figure 2-10), and is less than the field capacity. Wilting occurs when the plant can no longer maintain plant cell turgidity against the evaporative demand placed by the atmosphere on one end of the plant (the leaf surfaces) and the tension under

which the soil water is held at the other end of the plant (the roots). Intuition may prove less useful in understanding the wilting point because, in this state, all soils may appear to be simply “dry,” with little discernable difference in water content between soil textures. However, at the wilting point, the water content of the coarse-textured sand is lower than that of the finer textured silt. Also, in this example, the water content of the silt at the wilting point is greater than that of the sand at field capacity. By convention, the wilting point is often assigned as the water content at a suction of 1,500 kPa. However, the soil water content at the wilting point varies with plant species and with climate. Desert plants often can transpire water to a much higher suction than plants from more humid environments. The 1,500 kPa definition is reasonably representative of plants in more humid environments, but the wilting point of semi-arid and arid environments can be 4,000 to 10,000 kPa.

ET covers act as storage tanks that are filled when the rate of water added by precipitation exceeds that of water removal by ET, and are emptied when ET exceeds precipitation. A full “storage tank” corresponds to field capacity (θc), and an empty tank corresponds to the wilting point (θm). The cover will not drain as long as the soil water content does not exceed field capacity, and the water content in the cover will not drop below the wilting point. The difference between these two quantities ($\theta c - \theta m$) represents the volume of pore space that is available to store water per total volume of soil. This difference is referred to as the unit available storage ($\theta u = \theta c - \theta m$) and is used to determine the thickness required to store a known amount of water.

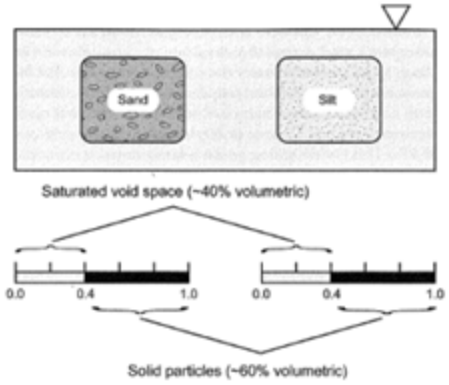

Figure 2-8 Illustration of the void space concept (Albright et al., 2004)

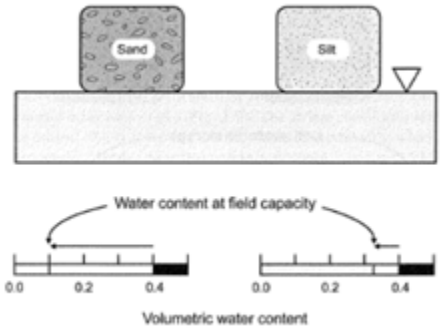

Figure 2-9 Illustration of the field capacity concept (Albright et al., 2004)

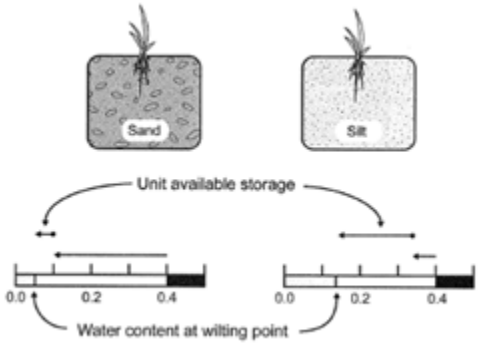

Figure 2-10 Illustration of the wilting point concept (Albright et al., 2004)

Soil Chemical Properties - Soil pH, Soil Nutrients, Cation Exchange Capacity, and Humus

Soil's ability to support vegetation is affected by the amount of nutrients, soil pH, cation exchange capacity, and organic content. Soil pH is the pH of a solution in equilibrium with soil in specific conditions. Growth of vegetation is highest at neutral pH, within a range of 6-7.5. Nitrogen is primarily available when the soil pH is 5.8 and greater, and phosphorus availability is limited below 6.2 or greater than 8.5. According to Thomas (1996), when the soil pH is greater than 7.6, there is plenty of calcium; when the pH is below 5.5-6, it is necessary to add lime. If the soil pH is 2-3, the soil contains an excessive amount of acid and is not an appropriate environment for vegetation growth. A pH value below 5.5 indicates the possible presence of toxic aluminum; a pH from 7.6 to 8.3 indicates that a calcareous environment exists in soil; and a pH greater than 8.3 is reflective of excess sodium in the soil.

The soil layers have to be capable of contributing enough nutrients to nurture vegetation growth. When there is an imbalance or lack of nutrients, additional nutrients need to be added. Nitrogen, phosphorus, and potassium are the nutrients used in the largest amounts, and if they are not present in the soil, fertilization is comparatively inexpensive, easy, and successful. Iron, manganese, boron, chorine, iodine, zinc, copper, and molybdenum are vital elements that support vegetation growth (Sauchelli, 1969).

Cation Exchange Capacity (CEC) is a very important measure of the ability of the soil to hold and exchange inherent nutrients. Cation exchange sites are located on the edges of clay and organic soil material. CEC properties are dominated by the amount of clay content because soil organic content is less than 5% for most soils and is rarely greater than 3 or 4% of soil mass. High CEC values are optimal for soils with ET covers of landfills because of their ability to store soil nutrients.

Soil humus is composed of an organic component of soil, and it takes a very long time to decay. Humus adds CEC to the soil and upgrades the soil structure, facilitating robust plant growth. Adding a small portion of organic material to the soil eventually results in humus that improves the soil over a long period of time.

Plants and Plant Roots- Plant Selection, Soil Density, Root Distribution, and Root Growth

The potential for achieving a high-performing ET cover is not only dependent on the soil moisture content. Plants absorb water and nutrients quickly when the growing conditions are good, and healthy plants minimize percolation from the bottom of the soil cover by drying out the soil. Plant growth is determined by conditions which may act independently or feed off of one another. These are the soil properties, proper selection of plant species, appropriate temperature of soil and air, diseases, humidity, and attacks of insects.

Vegetation of an ET cover stabilizes the surface of the cover, enhances transpiration, and minimizes erosion. Grasses (wheatgrass and clover), shrubs (rabbit brush and sagebrush), and trees (willow and hybrid poplar) have been used successfully on ET covers. Grass covers are preferred for some sites due to their prime erosion control and substantial fibrous root system, but woody plants are also preferred for some sites. Native plants are more tolerant of the territorial weather conditions, consume available resources effectively, and can survive for a long time even when they are grown under unfavorable conditions. Native plants can live through extensive drought, insect attacks, periodic fires, and disease. A mixture of warm-and-cold-season species is usually planted to enable water uptake for the total growing period, which promotes transpiration. Imported plants are more like to disturb the natural ecosystem than native plants and are less tolerant to unexpected incidents like sudden insect attacks and diseases.

It is not difficult to control the soil density during construction of an ET landfill cover. The mass of dry soil per unit bulk volume is called soil density (MG/m^3 or gm/cm^3), and the reduction of root growth occurs when the soil bulk density is greater than 1.5 Mg/m^3. Soil bulk density greater than 1.7 Mg/m^3 prevents root growth. Particle-size distribution, combined with soil density, controls root growth. According to Jones (1983), plant root growth lessens when the soil bulk density is greater than 1.5 Mg/m^3. Soils containing less than 70% sand with a bulk density greater than 1.7 Mg/m^3 experience 0.2 optimum root growth. Robust root growth can be found in soil bulk densities of 1.1-1.5 Mg/m^3.

ET covers of landfill are extremely dependent on the performance of plant roots since they control the amount of water removed from the soil. Many complex functions are performed by roots, including the following:

- Roots equip plants with an anchorage system
- Fleshy roots act as storage for nutrients.
- Roots supply the plant with water and nutrients from soil layers of different biological, physical, and chemical properties.

Some plants are capable of developing random shoots when the main root gets damaged. The shortest roots absorb the water and nutrients that are present in the soil and pull oxygen from the soil atmosphere. During the soil's drying period, the plants get stressed, which reduces the mass of shoots aboveground and results in the roots dying. If a favorable soil environment exists, the plants, especially native ones, can replace the dead roots quickly when favorable conditions return. It is very important for plants to produce new roots rapidly in the wet soil after rainfall event. Low soil strength, sufficient fertility, and adequate oxygen provide a favorable environment for root growth. Low

strength of soil leads to low bulk density, which is very important for healthy vegetation growth and the ultimate success of the ET cover.

The drying of each soil layer depends on the distribution and density of living plant roots. An example of a root distribution pattern for a soil with good tilth is shown in Figure 2.8 below. When all layers are wetted in the growing season, roots develop as shown in Condition 1. The majority of roots are in the upper 15-30 cm of the soil, near the surface. When soils are wet, the plants extract water and nutrients from the uppermost layer. Thus, in a natural rooting pattern, the uppermost layer dries first. And the rooting pattern moves to Condition 2 when the upper layers get dried. At the end of growing season or after severe drought, the rooting assumes the pattern of Condition 3, deep inside the soil profile. While parts of the root system die from drying of soil or other stresses, new roots grow rapidly in other layers. Soil temperature, the amount of oxygen, and some other factors limit root density and water use from a particular soil layer. The density of living and active roots change more than once during the growing season due to rapidly changing conditions.

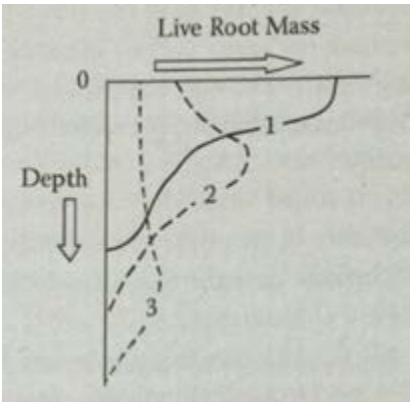

Figure 2-11 Possible distributions of living roots at different times during the growing season

When conditions are optimum, plant roots naturally grow faster. The following are some of the factors which may affect plant growth:

- Undesirable Soil pH
- Strength of soil
- Physical factors
- Soil solution salinity
- Soil water content
- Soil oxygen
- Air-filled porosity in soil
- Chemical toxicity
- Allelopathic toxicants

Climate, Weather and Water Balance –Ambient conditions, evapotranspiration, and hydrologic water balance/water balance

The main climatic factors that affect ET are precipitation, solar radiation, air temperature, wind, and relative humidity. The amount, distribution, and time of precipitation have a direct effect on the intrusion of water into the cover and, more specifically, into the waste underneath the cover. Climatic factors also control the temperature of the waste underneath the cover soil, and over time, these factors control the waste degradation rate. Precipitation and wind are the climatic factors that influence soil erosion. Basically, daily and seasonal variations of climatic factors determine the amount of deep percolation into the waste daily. If the majority of precipitation occurs during the dormant season, the risk for percolation through the bottom of the cover soil increases. It is actually good for the vegetation if the majority of precipitation occurs

during the growing season. Consecutive rainy days are more conductive to percolation than alternating dry and rainy days.

It is vital to control the amount of water that enters the cover soil in a landfill. The term “deep percolation” refers to the amount of water that percolates through the cover soil and enters the waste. This deep percolation is a part of a bigger hydrologic system. To estimate the entire hydrologic system, it is necessary to accurately assess the total hydrologic system. The system of water entering and leaving the ET cover is referred to as the mass balance; the quantity on earth is constant.

$$Incoming\ water = Outgoing\ water$$

$$P + I = ET + Q + L + \Delta SW + PRK + error$$

P=Precipitation

I=irrigation, if applied

ET= Evapotranspiration

Q= Surface runoff

L=Lateral flow

ΔSW= Change in soil water storage

PRK= Deep percolation (below cover or root zone)

Error= Lack of balance in the measured terms

ET is the most effective mechanism for removing water from the ET cover, and can be estimated by employing a given set of climatic conditions. This is the amount of water that will return to the atmosphere when abundant, freely-transpiring plants are available and the water supply is plentiful.

Performance Criteria –Site selection, site-specific design

The performance criteria of an ET cover includes:

- Control of infiltration into waste
- Isolation of waste and prevention of its movement by wind or water.
- Control of landfill gas.

Federal regulations mandate design requirements that control the water flow barrier, drainage layer, thickness, and function of soil and plant cover. Conventional covers meet these requirements. An ET cover also meets the performance criteria, as it controls infiltration into waste beneath the cover, separates waste from the cover, and prevents its movement by wind or water. In a dry climate, where the cover soil is too thin to control infiltration into waste, it is easy to increase the thickness of ET cover to rectify the problem. When needed, it is also easy to install a conventional gas extraction system within the ET cover. For fresh waste, where there will be a large amount of toxic gas or methane, a vertical gas well, which will not affect the performance of the ET cover, can be inserted to extract the gas.

It is always important to measure the risks associated with a landfill and to plot their remediation. For example, landfills located above tight shale or other low-permeability materials are less prone to harm ground water. Unfortunately, in some of the older landfills, the waste comes in contact with ground water, and the cover, while needed, cannot protect the ground water from contamination.

Suitability of Clay as Evapotranspiration Cover Soil

A compacted clay cover consists of a single compacted clay barrier layer and a drainage layer. It falls under the guidelines of the Resource Conservation and Recovery Act (RCRA), which specifies a maximum hydraulic conductivity of 1×10^{-7} cm/s (USEPA, 2006). This rate allows 32 mm of deep percolation per year if the barrier is continuously

wetted with a hydraulic gradient of 1. The liner under the landfill waste is the first application of a compacted clay barrier. The barriers perform very well when they are in wet conditions and under continuous compaction. Some covers, however, dry, freeze, and interfere with plant root activity. According to Suter et al. 1993, natural, physical, and biological processes cause clay barriers to fail in the long term. Melchoir et al., 2003 reported that wet climate clay barriers leaked 8 to 9% of precipitation, and the leakage increased even after eight years from the start of the experiment. Albright et al., 2006 monitored the performance of compacted clay barriers in three different locations for two to four years. The sites were in the desert in California; a humid area in Iowa; and a subtropical, wet location in Georgia. The inbuilt hydraulic conductivity of the clay barriers ranged from 1.6 to 4×10^{-8} cm/s. Albright also researched four additional sites and concluded that a large increase of hydraulic conductivity with time is very common.

MONITORING SYSTEMS OF EVAPOTRANSPIRATION COVERS

ET covers are monitored regularly to check their performance in minimizing the infiltration of water into waste. Percolation can be monitored using systems like lysimeters, which are installed beneath a cover. The water collected in the lysimeter is directed towards a point where the water collected is measured, using different kinds of devices like tipping buckets and pressure transducers (Benson et al., 2001). Percolation monitoring is estimated by collecting and removing leachate. One indicator for the performance of ET cover is the amount of leachate generated through the cover. The higher the percolation, the more leachate will be generated (USEPA, 2006).

Soil-moisture monitoring is a vital part of the process of establishing an ET cover (Hakonson, 1997). It is performed to determine the moisture content at particular locations on the cover and to identify changes with time, both in horizontal and vertical gradients. Procedures used to determine relative humidity, soil matrix potential, and

resistance are used to measure soil moisture. A high value for soil moisture indicates that the potential for percolation is increasing. Increasing moisture results in the cover reaching its storage capacity.

Soil moisture is a key variable in the climate system. By controlling evapotranspiration, soil moisture impacts the partitioning of incoming radiation into sensible and latent heat flux. Furthermore, it represents an important water and energy storage component of the regional climate system. Regional simulations of recent and future climate conditions indicate that a projected increase in summer temperature variability and the occurrence of heatwaves in central and eastern Europe are mainly due to soil moisture atmosphere interactions (Seneviratne et al., 2006).

For this research, during the field investigations, we explored how soil moisture varies in space and got a feeling for measurement uncertainty. For the analysis, we used available data (e.g. continuous in-situ measurements) to investigate the temporal variability of soil moisture. In-situ measurements are sparse both in time and space, and alternative techniques, such as satellite measurements, which have their own specific properties and limitations, are required for large-scale measurements.

Field Instrumentation Methods

Patterns of water use and replenishment give rise to large spatial variations in soil moisture over the depth of the soil profile. Accurate measurements of the profile water content are therefore the basis of any water budget study. When monitored accurately, profile measurements show the rates of water use, amounts of deep percolation, and amounts of water stored for plant use.

Current soil moisture monitoring can be used to define moisture content at discrete locations in cover systems and to assess changes over time in horizontal and vertical gradients. Soil water content is measured using a variety of methods and

includes methods for determining soil moisture (TDR, neutron attenuation, and resistivity); soil humidity (psychrometer); and soil matric potential (heat dissipation units or HDUs). Table 2-2 presents examples of non-destructive techniques that have been used to evaluate the soil moisture content of ET cover systems.

Table 2-2 Non-destructive soil water monitoring devices for ET covers (USEPA, 2011)

Method	Description	Instrumentation
Capacitance sensor	Uses frequency domain induced polarization to measure the dielectric properties of the soil. The dielectric of dry soil is approximately 5, and the dielectric of water is approximately 80. When soil becomes moistened by water, its dielectric increases.	Consists of a probe connected to a coaxial cable and buried at appropriate depth
Electrical resistance blocks	Measures resistance resulting from a gradient between the sensor and the soil; higher resistance indicates lower soil moisture	Consists of electrodes embedded in a gypsum, nylon, or fiberglass porous material
Gee lysimeter	Wicks water from soil around a collection container and measures the resulting water level in the container directly	Consists of a small collector body and a wick. The water level in the collector body is measured by an electronic water level gauge.
Thermal dissipation unit	Uses a heated ceramic block to determine soil moisture near the block. The rate of heat dissipation from the block is related to soil moisture—the quicker the dissipation the higher the soil moisture.	Consists of a small heater inside a porous block with a temperature sensor attached by cable to a surface meter
Neutron attenuation	Emits high-energy neutrons into the soil that collide with hydrogen atoms associated with soil water and counts the number of pulses, which is correlated to moisture content	Consists of a probe inserted into access boreholes with aluminum or polyvinyl chloride casing
Psychrometer	Measures relative humidity (soil moisture) within a soil	Generally consists of a thermocouple, a reference electrode, a heat sink, a porous ceramic bulb or wire mesh screen, and a recorder
Suction lysimeter	Collects pore (unsaturated) water directly	Constructed of a porous ceramic bulb with a cylindrical reservoir to store water. A tube to the surface allows water to be drawn and measured.
Tensiometer	Measures the matric potential of a given soil, which is converted to soil moisture content	Commonly consists of a porous ceramic cup
Time domain reflectrometry	Sends pulses through a cable and observes the reflected waveform, which is correlated to soil moisture	Consists of a cable tester (or specifically designed commercial time domain reflectrometry unit), coaxial cable, and a stainless steel probe

A high soil moisture value indicates that the water content of the cover system is reaching its storage capacity, thereby increasing the potential for percolation. Soil moisture is particularly important for capillary barrier ET cover systems. When the finer-grained layer becomes saturated, the capillary barrier can fail, resulting in water percolating through the highly permeable layer to the waste below (Hakonson, 1997). Monitoring instruments have numerous configurations, costs, and accuracies. The choice of which one to use depends on the site data quality objective.

Point Measurement of Soil Moisture Profiles

While point measurements can give continuous estimates of soil moisture variations over the entire soil profile, they are not always representative of the spatial distribution, with correlation lengths varying from 10 to 1000 m (Western et al., 1998). In order to relate point measurements of soil moisture content to the spatial variations in soil moisture content, Grayson and Western (1998) examined a concept proposed by Vauchaud et al. (1985), that says that particular sites in the field always display mean behavior, while others always display extreme values. Thus, if several time-stable sites are monitored, some with an extreme wet response, some with an extreme dry response, and some with a mean response, information may be obtained about the spatially average soil moisture content and the spatial variation of soil moisture content. They also suggested that points representing the mean spatial response are likely to be located in areas that are neither strongly convergent nor divergent, are located near the mid-slopes, and are in areas that have a topographic aspect close to average for the catchment. The procedure that has been used in the United States for making a regional assessment of soil moisture content in the pre-planting season consists of collecting soil cores and producing a soil water deficit map by contouring from the point measurements of water

deficit. The resulting maps show general patterns of variability, but do not provide specific information for individual fields (Jackson et al., 1987).

Methodology of Soil Moisture Sensors

The soil moisture sensor, Decagon 5TM, uses an electromagnetic field to measure the dielectric permittivity of the surrounding medium. The sensor delivers a 70 MHz oscillating wave to the sensor prongs that charges the dielectric of the material. The stored charge is proportional to soil dielectric and soil volumetric water content. The 5TM microprocessor measures the charge and outputs a value of dielectric permittivity from the sensor.

Each 5TM sensor is calibrated to measure dielectric permittivity (ε_a) accurately in the range of 1 (air) to 80 (water). The unprocessed raw values reported by the 5TM in standard serial communication have units of $\varepsilon_a * 50$. When used in SDI- 12 communication mode, the unprocessed values have units of ε_a (for 5TM board versions R2-04).

Several researchers have studied the relationship between dielectric permittivity and volumetric water content (VWC) in soil, resulting in numerous transfer equations that predict VWC from measured dielectric permittivity. For mineral soil calibration, the volumetric moisture content is obtained by converting raw dielectric permittivity values with the Topp equation (Topp et al. 1980).

$$\mathrm{VWC} = 4.3 * 10^{-6}{\varepsilon_a}^3 - 5.5 * 10^{-4}{\varepsilon_a}^2 + 2.92 * 10^{-2}\varepsilon_a - 5.3 * 10^{-2}$$

With a properly installed 5TM sensor in a normal mineral soil with saturation extract electrical conductivity < 10 dS/m, the Topp equation results in measurements within $\pm 3\%$ of the actual soil VWC. If more accuracy is needed or if the soil has very high electrical

conductivity or abnormal mineralogy, it may be necessary to conduct a soil-specific calibration of the 5TM sensor to improve the accuracy to 1 to 2% for any soil.

Limitations of using Soil Moisture Sensors

Soil moisture sensors are installed in the soil. The three common challenges to making high quality volumetric water content measurements by this method are: 1) installing the probe in undisturbed soil, 2) minimizing disturbance to roots and biopores in the measurement volume, and 3) eradicating preferential water flow in and around the probe. Table 2-3 discusses the advantages and disadvantages.

Table 2-3 Major types of soil moisture sensors and their relative advantages and disadvantages (Walker et al., 2004)

	Sensor Type	Advantages	Disadvantages
Soil Water Content	**Neutron Probe** (Campbell Pacific Nuclear; CPN)	Accurate. Repeatable. Samples a relatively large area. One sensor for all sites & depths.	Government required paperwork and regulations. Can't leave in field. Relatively expensive (about $4,500).
	Time Domain Transmissivity (Acclima, Gro-Point)	Less expensive ($110/sensor). Easy to log data.	Samples small area.
	Capacitance Sensors (Enviroscan, Echo Probes, Acclima, Vernier, etc..)	Easy to set up to log and/or transmit data.	Highly affected by soil conditions immediately next to the sensor. High variability. More expensive ($300 - $1,200/system).
Soil Water Tension	**Tensiometers**	Less expensive ($80/sensor)	Maintenance issues.
	Granular Matrix Sensors (Watermark)	Inexpensive ($40/sensor)	Highly variable output. Less accurate. Sensitive to temperature and soil salinity.

All dielectric probes are most delicate at the surface of the probe, and any disconnection of contact between the probe and the soil or compaction of soil at the probe surface can result in large measurement errors. Water ponding on the surface and the presence of preferential paths down probe installation holes can also lead to large

measurement errors. There are many limitations to accurately measuring soil moisture using this equipment.

ELECTRICAL RESISTIVITY OF COMPACTED CLAY

Geophysical methods can be used to efficiently assess larger volumes of soil, and electrical resistivity is one of the geophysical methods which can be conducted rapidly and nondestructively. Electrical resistivity of compacted clay is very useful because it is sensitive to compaction conditions and soil composition (McCarter 1984; Abu-Hassanien 1994). The effects of compositional changes and compaction conditions on electrical resistivity are very important for assessing the compacted clay cover with an electrical-resistivity survey. Factors like anomalies, lift interfaces, and boundaries of liners also affect electrical resistivity. Electrical resistivity is a function of soil properties; a solid constituent of solids (particle size distribution, mineralogy); arrangement of voids (porosity, pore size distribution, connectivity); degree of water saturation (water content); electrical resistivity of the fluid (solute concentration); and temperature. The air medium is an insulator (i.e. infinitively resistive), the water solution resistivity is a function of the ionic concentration, and the resistivity of the solid grains is related to the density of the electrical charges at the surface of the constituents. These parameters all affect the electrical resistivity, but in different ways and to different extents.

Soil Pore Water Characterization

An electrical current is based on an arrangement of ions in pore water. The current is basically electrolytic. The electrical current is dependent on the quantity and quality of water in the pores and is higher when dissolved salts are present. Before doing field measurements, primary calibration of volumetric water content related to electrical resistivity is done in laboratory. (McCarter, 1984; Michot et al., 2000). The electrical resistivity decreases with the increase of water content. Laboratory investigations showed

that electrical resistivity decreases rapidly with increasing water content for water content < 15 %. Ion Chromatography (IC) tests are used to analyze soil pore water. The carrier fluid is injected with the extracted pore water, and a column containing adsorbent allows the compound mixture to pass through it. The composed ions are separated due to the interaction of dissolved ions in the pore water, carrier fluid, and adsorbent. It is recommended to reduce the movement of carrier fluid and enhance the conductance of separated ions during IC tests. The schematic of the IC test method is presented in Figure 2-12.

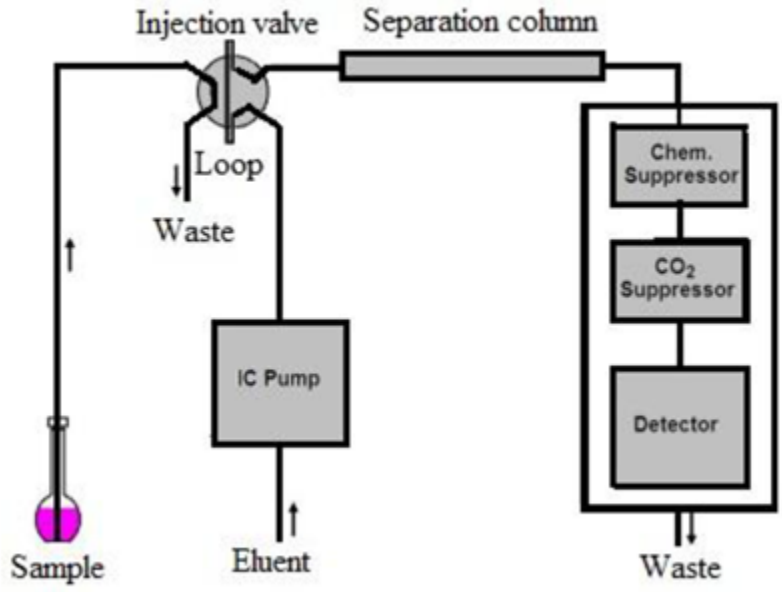

Figure 2-12 Ion chromatography (IC) test procedures (http://www.metrohm.co.uk)

Electrical Conduction in Clays

Soil is a porous media that conducts electricity through movement of ions within the void spaces and by means of a surface charge where electrolytic pore water is present (Bryson, 2005). For coarse grained soil, the conduction is mostly dependent on

the electrolytic conduction through the interconnected space granular skeleton, electrolyte conductivity, and degree of saturation (Santamarina et al., 2001). However, for a clayey soil surface, the charge is a significant component of electrical conduction. Clay particles have charge deficits due to replacement of ions at crystal structures and the acid-base reaction of silanol-aluminol (Si-O-H and Al-O-H) groups with water. Cations present adjacent to the particles are attracted to the clay particles and counter the net negative charge. Cation density is high around the solid surface, but the concentrated ion diffuses to balance the concentration all over the structure. A negative electrical field restricts the diffusion, and the ions are stimulated away because of the negative force. Consequently, both positive and negative mobile ions exist, adjoining the adsorbed layer. The combination of a charged surface and a distributed charge surface is identified as an electrical double layer. The plane where the counter ions are sturdily adsorbed with the negative charge of particles is called a Stern layer. This is an application of the external electrical field which results in charge separation in the diffuse double layer, along the Z-potential plane (Rinaldi and Cuestas, 2002). Therefore, electrical conduction in clayey soil is governed by the bulk fluid and surface conductivity. An illustration of the location of the diffuse double layer (DDL), Stern layer, and precipitated ions in clays is presented in Figure 2-13.

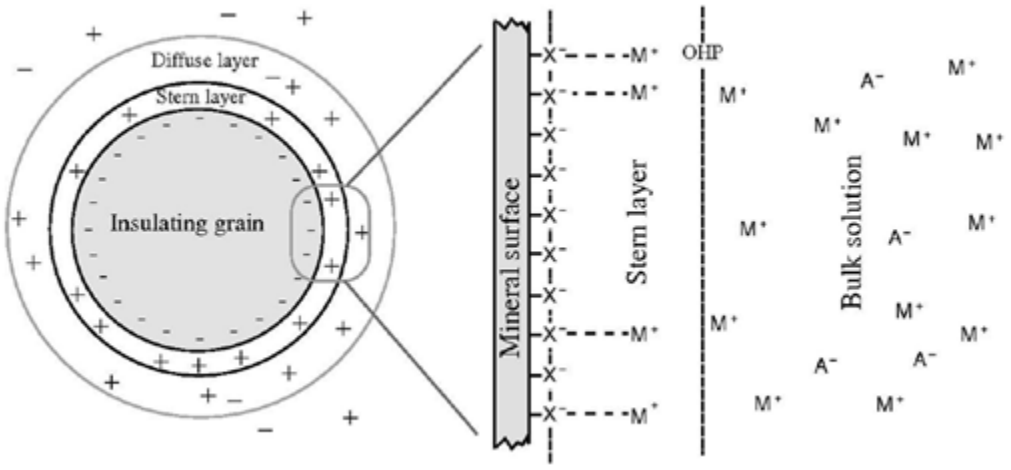

Figure 2-13 Diffuse double layer (DDL), Stern layer, and precipitated ions in clays (http://geophysics.geoscienceworld.org)

Clay Water Interface

It has been proven that the influence of moisture on physic-chemical and engineering behaviors of clay is significant. Thus, knowing the mechanism of the interaction between clay and water is very important. At dry condition, counter ions remain in an adsorbed condition in clay particles, and excess ions remain in the shape of precipitated salts. Hydration of counter ions takes place with the addition of water. Some counter ions lose their primary hydration shell (either completely or partially) during the hydration process. These counter ions develop an inner sphere complex. They exist with primary hydration shells, but also exist in the form of an outer sphere complex. Because of surface charge, the hydrated counter ions are attached to the particles. The rest of the counter ions are separated from the surface of the particles by water. Mitchell and Soga (2005) summarized the possible causes of clay water interaction, which included hydrogen bonding, attraction by osmosis, hydration of exchangeable cations, charged surface dipole attraction, and the presence of London dispersion force.

Concept of Electrical Resistivity

Electrical resistivity is understood in the context of a current flow through a subsurface medium, which consists of different layers of materials, each having individual resistivity. The resistivity of material depends on its ability to retard the flow of the electrical current and is a measure of how well the material retards the flow of the electrical current. It varies tremendously from one material to another. For example, the resistivity of a good conductor like copper is on the order of 10^{-8} Ω-m; the resistivity of an intermediate conductor like wet topsoil is 10 Ω-m; and the resistivity of poor conductors, such as sandstone, is 10^{8} Ω-m. Because of these huge variations, the measuring the resistivity of unidentified materials becomes a handy process for identifying the nature of that material without having much additional information. Other geologic lines are employed to identifying materials comprised of several layers.

The concept of resistivity is encountered when determining the resistance of an ideal cylinder of uniform composition with a length of L and a cross-sectional area of A. The resistivity seems to be a material-specific constant of proportionality in the countenance for the total resistance of the cylinder, which is

$$R = \rho \frac{L}{A}$$

The total resistance R is obtained through Ohm's law, $= \frac{V}{I}$, where V is the potential difference between the ends of the cylinder and I is the total current flowing through the cylinder. Edge effects are not considered. The resistivity of the material, an intrinsic property of the material, is then related to experimentally-measured extrinsic parameters by

$$\rho = (\frac{V}{I})(\frac{A}{L}) = RappK$$

In the above equation the resistivity is given by the product of the ‘‘apparent resistance’’ $Rapp = \frac{V}{I}$ and a ‘‘geometric factor’’ $K = \frac{A}{L}$ that carries information about the geometry of the cylinder. This type of product of an apparent resistance and a geometric factor will appear again when the resistivity of the ground is determined.

Soil Resistivity models

Soil resistivity can vary considerably due to factors such as variations in geology, temperature, water content, and water composition. When resistivity measurements are used for long-term monitoring purposes, it is important to estimate the natural variations, depending on the season, so that possible anomalies can be distinguished. The study of seasonal resistivity variations and the reasons for these are also important for several fields of applications in agriculture, environmental, and engineering geology.

RELATIONSHIP OF SOIL PROPERTIES WITH ELECTRICAL RESISTIVITY

The use of electrical resistivity imaging (ERI) in field investigations is increasing all over the world. It is a suitable and effective method for assessing spatial and temporal variations of moisture and heterogeneity of subsoils. Geotechnical engineers are able to investigate several parameters by using conventional soil boring tests; however, they can only obtain this information at discrete locations and have to perform interpolations to get a wide range of information. In contrast, ERI is able to provide an image of the subsurface, as well as qualitative information. The quantification of geotechnical properties has become a significant factor in the increasing use of ERI in engineering applications.

The development of correlations between different geotechnical properties with ERI will close the gap that currently exists between geophysical testing and geotechnical engineering, enabling geotechnical engineers to interpret the geophysical data and utilize the information for their designs, and making this method more effective for subsurface

investigation. The current study presents an investigation of geotechnical parameters that affect the electrical resistivity of compacted clays. Moisture is an important factor in the electrical conduction of soil, and its presence changes the consistency and strength of soil. This phenomenon was utilized to determine the relationship between electrical and geotechnical properties of soil. The effects of various factors on ERI were considered and are discussed below.

Moisture content

Soil moisture, either in weight or on a volume basis, is the most important parameter for geotechnical engineers. If measured by weight, it is called gravimetric moisture content. The ratio of the amount of water present in the void to the amount of solids is known as moisture content. The equation can be written as follows

$$w = \frac{Ww}{Ws} \times 100\%$$

where, Ww = Weight of water, Ws= Weight of solid soil

Volumetric moisture content measures moisture content in terms of volume of water. The moisture content is measured from the ratio of the water volume present in soil to the total volume. The equation is:

$$\theta = \frac{Vw}{Vt}$$

where, Vw = Volume of moisture, Vt = Total volume of soil mass.

Volumetric moisture content is related to gravimetric moisture content by the following expression

$$\theta = w.(\frac{\gamma_d}{\gamma_w})$$

where, γd= Dry unit weight of soil, γw= Unit weight of water.

Literature shows that moisture content is the most dominating factor influencing the electrical resistivity of soil. The electrical conduction occurs in soil mostly due to ion displacement in pore water. Adsorbed ions in the solid particles get released with the increase of moisture content from air-dry to full saturation. Mobility of the electrical charge increases with the increase of moisture. Under the application of the electric field, free electrical charges cause electrical resistivity. Electrical resistivity of soil decreases rapidly with an increase of moisture content of more than 15% (Samouelian et al., 2005). Voronin (1986) described the effect of moisture content on soil resistivity by a nonlinear curve, as presented in Figure 2-14.

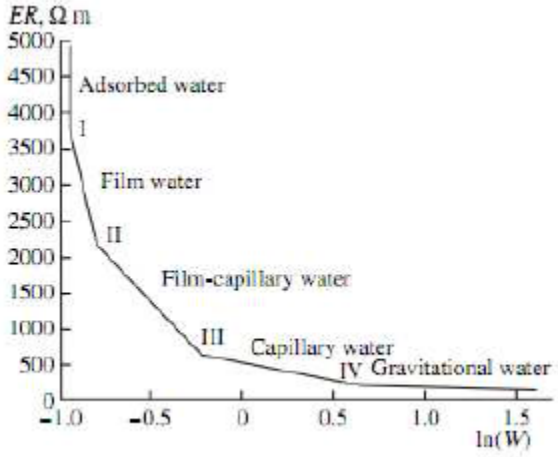

Figure 2-14 Relationship of soil moisture and electrical resistivity

Based on the condition of moisture in the soil, the moisture content and electrical resistivity curve are divided into various zones. The segments of the curve corresponding to the specific water content are adsorbed water, film water, film capillary water, capillary water, and gravitational water. Voronin explained that with an increase of moisture content, electrical resistivity decreases rapidly in the adsorption water zone, and the ions of the water molecules are immobile. A conductive path for the electrical current is created by dipolar water ions. Decrease of electrical resistivity is sharp with the increase

of moisture content in the zone of adsorption. In the film water zone, Van der Waals' force increases, resulting in a decrease in the film water zone. Water goes from film to fissure when the maximum possible thickness of water film is achieved. In the film capillary water zone, the relative portion of film water decreases, and sand capillary water increases. Capillary force is less than the molecular attraction force in this zone. The decrease of electrical resistivity is less dramatic in the film capillary and capillary water zones. In the gravitational water zone, mobility of electrical charges become independent of the movement of water molecule ions, making the electrical resistivity almost independent of water content in this particular zone.

Electrical resistivity is used to determine physical soil properties such as porosity, salinity, clay mineral content, soil moisture, etc. for the study of spatial/temporal variability (Friedman, 2005; Lapenna et al., 2005; Samouelian et al., 2005). Controlling factors influence the electrical properties of the soils (Friedman, 2005; Samouelian et al., 2005) because, commonly, the main mechanism involved in the current conduction in soils is electrolytic. The major controlling factors of bulk soil electrical resistivity are the soil solution electrical conductivity and the soil moisture (Friedman, 2005; Samouelianet al., 2005; Robinson et al., 2008). The relative proportions of air and water and the presence of connections between pores are determined by solid phase properties (Friedman, 2005; Samouelian et al., 2005). Again, depending on the relative proportions of the sizes of the soil particles, adsorbed ions on small particles (clays) can play an important role (Friedman, 2005; Samouelian et al., 2005, Robinson et al., 2008). Temperature also influences the electrolytic mechanism of current conduction (Campbell et al., 1948; Friedman, 2005). These are crucial factors for sensing the most superficial soil layers when there is a huge variability of both soil moisture and temperature. A number of theoretical (Mualem and Friedman, 1991), lab-based (Archie, 1942; Gupta

and Hanks, 1972; Rhoades et al., 1976; Kalinski and Kelly, 1993), and field-based studies (Hymer et al., 2000;Walker and Houser, 2002; Michot et al., 2003) have already determined explicit relationships between soil moisture and resistivity parameters of the unsaturated zone. A short summary of some of the most important studies relating soil moisture to resistivity is presented in Table 2-4.

Table 2-4 Relationships between soil moisture and electrical resistivity (Calamita et al., 2012)

Authors	Location	Soil texture	Land use	Size	Depth (m)	Procedure	θ–ρ relation	N	Parameter values[a]	r
McCarter (1984)		Clay				Lab	Non-linear law			
Kalinski and Kelly (1993)		Clay				Lab	Second order polynomial			
Goyal et al. (1996)					4		Linear		$a = 50$ $b = -0.1$	−0.98
Fukue et al. (1999)		Clay				Lab	Non-linear law			
Hymer et al. (2000)	US	Sandy loam	Brush		0.3	Field	Power law		$b = -0.08$ to -0.65	−0.57 to −0.94[b]
Zhou et al. (2001)	Japan	Loam			1.5	Lab	Power law	46		−0.68 to −0.93
Binley et al. (2002)	UK	Fine and medium sand	Grassland	1200 and 1800 m^2	15	Field	Power law	23	$b = -0.88$	−0.97[c]
Walker and Houser (2002)	US	Sandy loam	Bare soil	250 m	0.7	Field	Power law			~−0.59
Michot et al. (2003)	France	Loamy clay	Corn crop	6.2 m	0–0.6	Field	Linear	30–250	$a = 28.5$ to 37.7 $b = -0.05$ to -0.36	−0.46 to −0.97
Cosenza et al. (2006)	France	From coarse sand (top) to clayey silt		Borehole	2.5	Field	Power law	20	$a = 1.07$ $b = -0.41$	−0.82
Al Hagrey et al. (2004)	Italy	Loam	Olive orchard	36 m^2	0.25	Lab and field	Power law	75	$a = 1.30$ $b = -0.46$	−0.98
Zhu et al. (2007)	China	Sand	Pine forest	8 Plots	1–1.5	Field	Linear and exponential	20	$a = 0.1496$ $b = -0.0001$ (lin) $a = 0.1741$ $b = -0.0015$ (exp)	−0.80 (lin) −0.94 (exp)
Wenninger et al. (2008)	South Africa		Forested	200 m	0.5	Field	Power law	52	$b = -0.67$	−0.87
Brunet et al. (2009)	France	Sand		400 m^2		Lab and field	Power law	20	$b = -0.60$	−0.99[d]

[a] Relation: $\theta = a + b\rho$ (linear); $\theta = a\rho b$ (power law); $\theta = a \exp(b\rho)$ (exponential).
[b] The soil moisture–resistance relation was investigated.
[c] Computed from the data extracted by the manuscript.
[d] For laboratory data.

The ‘‘Archie law’’ is one of the most important formulations that relates soil moisture to soil electrical resistivity (Archie, 1942). It is a semi-empirical power law relationship that is applicable to saturated, unsaturated, and medium-to-coarse-grained soils. It does not apply to soils with a high clay mineral content. Several authors have used this law and its modified form for soil electrical resistivity measurements of different lithological formations to estimate soil moisture (Zhou et al., 2001; Binley et al., 2002; Al Hagrey et al., 2004; Cosenza et al., 2006; Brunet et al., 2009). (See Table 2-4.)

A soil electrical transmission mechanism is affected by clay minerals and involves the electricity conduction of double-layer-adsorbed ions. At low soil moisture values, smaller-size clay particles and greater specific-size particles show greater electrical conductivity than coarse soils being charged at a higher charge density. Considering the effects of surface conductivity, Rhoades et al. (1976) proposed a lab-based second order polynomial expression, relating soil moisture to soil electrical resistivity. Kalinski and Kelly (1993) used it for estimating the moisture of core samples containing 20% clay, and the estimation was highly accurate. Though it describes the soil resistivity-soil moisture relation adequately, it has strong limitations in direct field applications (Michot et al., 2003). A first order linear equation was proposed to describe the overall relationship between soil moisture and soil electrical resistivity in coarse grained soils if the number of variables is limited (Gupta and Hanks, 1972; Goyal et al., 1996; Michot et al., 2003; Zhu et al., 2007). Some authors even proposed exponential relations (Pozdnyakova, 1999; Zhu et al., 2007; Ozcep et al., 2009). Pozdnyakova (1999) highlighted the physicl basis of this law that links resistivity with the volume density of the mobile electrical charge. It has been proven by scientific literature that the non-linear models, as second order polynomial expression, power, and exponential function are most commonly used to fit the soil moisture - resistivity relationship. But there is actually

no significant difference between these three models when the variation of the variables remains within a limited range (Pozdnyakova, 1999). The relationship between soil moisture and resistivity for different studies, according to scientific literature, is shown in Figure 2-15.

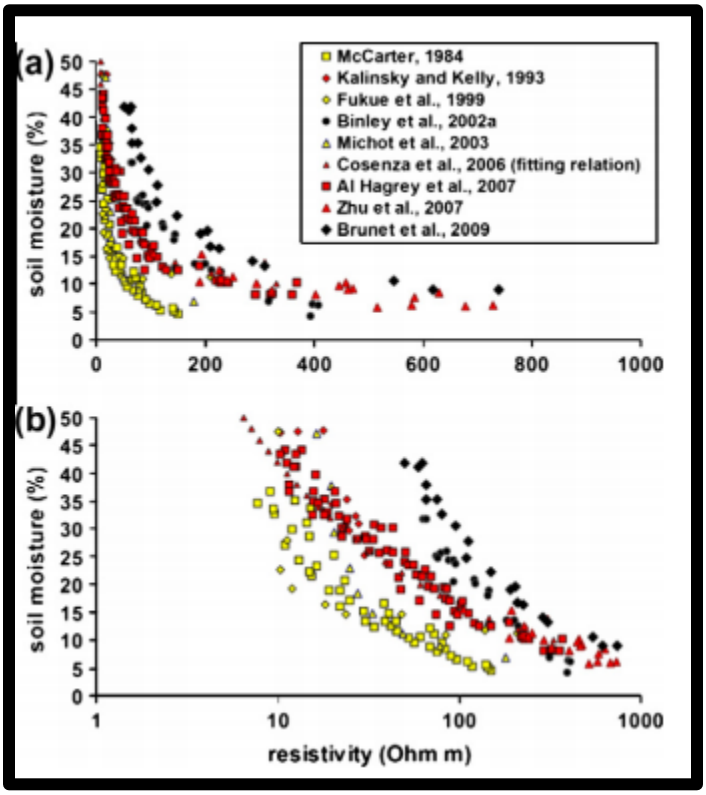

Figure 2-15 Relationship between the electrical resistivity and the volumetric soil moisture

The above semi-logarithmic plot highlights the power law relationship between the two variables. The symbol color represents soil texture, which influences the behavior of the soil (yellow = clay, red = loam, black = sand) (Calamita et al., 2012). For example, studies conducted on sandy soils (e.g. Brunet et al., 2009; Zhu et al., 2007) showed higher resistivity values than those conducted on clay soils (e.g. McCarter, 1984; Fukue et al., 1999) under the same soil moisture conditions.

Due to heterogeneity and the complexity of the hydro-geologic system of soil, it is difficult to determine the moisture profile from a representative subsurface sample. Soil moisture sensors, time domain reflectometry (TDR), neutron probes, gypsum blocks, torsiometers, and gravimetric scaling are commonly-used tools for measuring moisture distribution in subsoils. Some of these methods have certain operational limitations. For example, TDR can determine moisture within ten centimeters of the region under consideration. (Goyal et al., 1996).

The moisture condition of subsurfaces can also be determined by electrical resistivity. Literature shows that resistivity decreases with an increase of soil moisture. Several studie have been conducted to quantify the moisture content of soil by resistivity testing in the laboratory and field. Croney et al. (1951) presented that the measurement was based on three relationships: the suction of the water in the absorbent and the moisture content of the absorbent, moisture content of the absorbent and the resistance of the gauge, and the suction of water in the soil and the moisture content of the soil. Plaster of Paris and high alumina cement were used as absorbent materials. This experiment showed that electrical resistance gauges could be used to determine the soil suction and soil moisture; however, because of the disturbance of the soil, their reliability as a soil moisture meter was not dependable. According to the study, the calibration of electrical gauges was important to obtaining precise results. The measurements of suction and moisture content of the absorbent were identified as major problems in this method because very small differences in the mixing and curing of the absorbent influence the results significantly.

Kalinski and Kelly (1993) showed, in laboratory testing, how to determine volumetric moisture content from electrical conductivity of soil. The electrical resistivity of soil was measured, using a four-probe circular cell. The experimental results specified

that the ECo/ECw (ratio of soil conductivity and pore water conductivity) increased with the increase of volumetric water content, as illustrated in Figure 2-16. A regression equation was developed to determine the volumetric water content, assuming surface conductivity of 0.24 mho/cm (ECs= 0.24 mho/ cm). It was observed that the predicted volumetric moisture content matched well with the measured one.

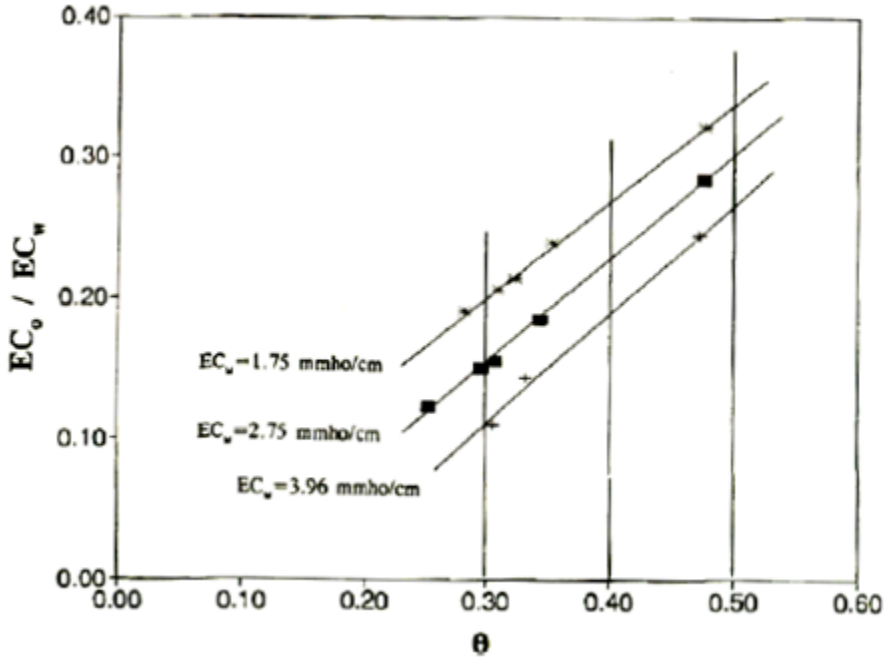

Figure 2-16 Relationship between ratio of bulk soil and pore water conductivity with volumetric moisture content (Kalinsky and Kelly 1993)

Ozcep et al. (2009) conducted a study to determine the relationship of soil resistivity and water content in Istanbul and Golcuk, Turkey. Electrical resistivity was measured, using vertical electrical sounding (VES), in 210 points of two sites. A soil test boring was also conducted for the collection of the samples. The soil resistivity and moisture content ranged from 1 to 50 Ohm and 20% to 60%, respectively. Two exponential equations, correlating moisture content with resistivity, were developed for Istanbul and the Golcuk area, as presented below:

$$W = 51.074\, e^{-0.0199R}, R^2 = 0.76(for\ Istanbul)$$

$$W = 47.579\, e^{-0.0158R}, R^2 = 0.75(for\ Golcuk)$$

Schwartz et al. (2008) conducted a study to quantify field-scale moisture content, using the 2D electrical resistivity imaging (ERI) method at the Virginia Tech Kentland experimental farm, Montgomery County, Virginia. ERI and time domain reflectometry (TDR) were used at the same time to obtain resistivity and moisture content. The 1D resistivity profile was determined from 2D ERI, using EarthImager software. The coefficients of Archie's law were numerically adjusted for the quantification of the moisture content from 1D resistivity. The proposed model utilized extractable cations to represent the role of pore water conductivity in developing Archie's law. It was seen that the model provided valuable results for determining meter-scale moisture heterogeneities compared to small-scale variations. In addition, Brunet et al. (2010) performed research to obtain the water deficit from electrical resistivity tomography (ERT) in Southern Cevennes, France. During February 2006 and December 2007, more than 10 ERTs were performed on the study area, and volumetric water contents were measured using TDR. Archie's law was calibrated in the laboratory to quantify the moisture content and water deficit from ERT. Based on the laboratory test results, the cementation (m) and saturation coefficient (n) were determined as 1.25 and 1.65, respectively. The in-situ soil moisture content and water deficit were calculated from the calibrated Archie's law at 25^0C temperature. The authors specified that the interpretation of water content or water deficit from resistivity was sensitive to temperature, water solution resistivity, porosity, and the inversion algorithm of resistivity tests. The ERT profiles and comparison of predicted and observed water content at different depths are presented in Figure 2-17 and Figure 2-18. The solid lines in Figure 2-18 indicate the ERT-predicted moisture contents.

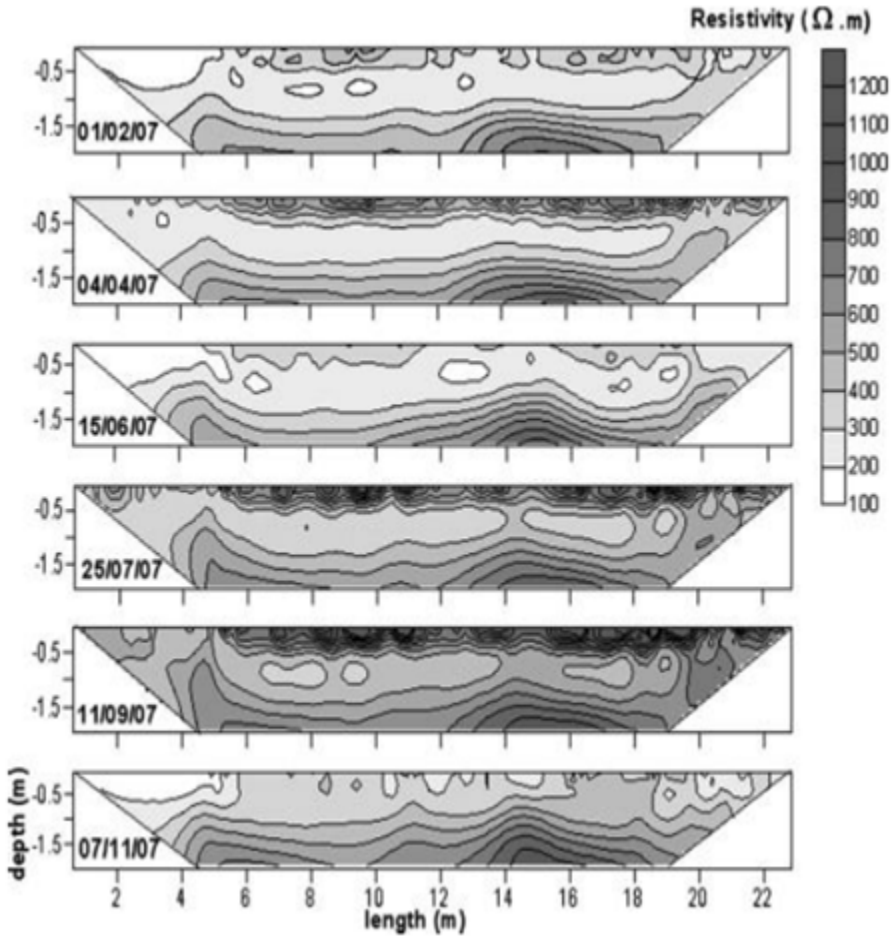

Figure 2-17 ERT during the year of 2007 (Brunet et al., 2010)

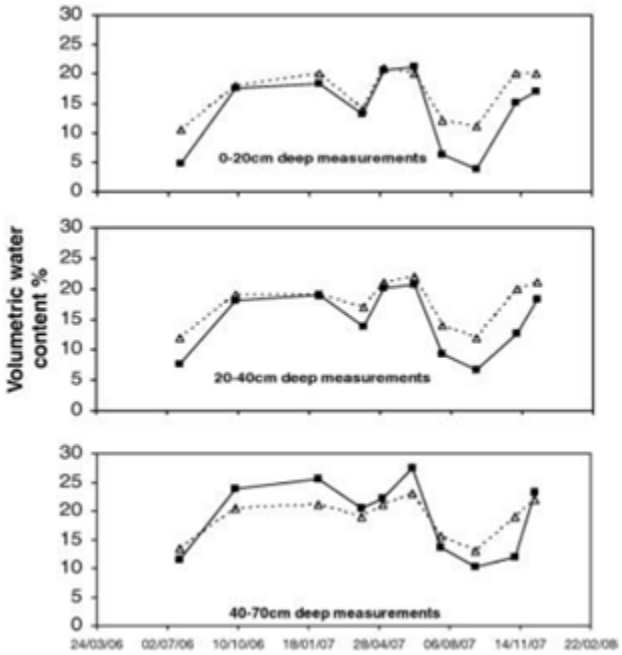

Figure 2-18 Comparison of ERT and TDR predicted water content at depths (a) 0-20 cm, (b) 20-40 cm, and (c) 40-70 cm (Brunet et al., 2010)

Soil Density and Degree of Saturation

Soil bulk density is the quantity of air and solid elements in a given volume of soil. It decreases when the amount of air in the soil increases; i.e., when the air-filled porosity increases, the electrical resistivity increases by numerous orders of magnitude. As a result, electrical resistivity can be used to detect crack patterns in a soil when it becomes dry. In that scenario, the electrical resistivity of the soil without cracks is about 30-50 ohm-m, while the electrical resistivity of the cracked soil of the same texture can reach several hundred ohm-ms. Electrical resistivity can also be used to distinguish any increase of porosity due to cracking under drying, formation of tubular pores by the biological activity, or creation of voids by ploughing or tillage operations.

The bulk density can increase under some cultural processes, due to soil compaction, when the electrical resistivity increases several ohm-m. For example, for a

loamy clay soil at 0.3 m^3/m^3 water content, the electrical resistivity is 40 ohm-m for a bulk density of 1.39 Mg m^3 and is 30 ohm-m for the same soil after compaction (bulk density of 1.59 Mg m-3) (Besson et al., 2004).

Density is an important geotechnical property which relates volume with mass of soil. Bulk density of soil can be defined as the ratio of weight of soil to the total volume. It can be defined by the phase diagram (Figure 2-19) of soil. The expression is

$$\gamma = \frac{W}{Vt}$$

where, W=Weight of soil mass and Vt= Total volume. Bulk density is closely related to degree of saturation. It is defined by the ratio of volume of water to the volume of void. It can be given by

$$Sr = \frac{Vv}{Vw}$$

Where, Vw= Volume of water, Vv= Volume of void

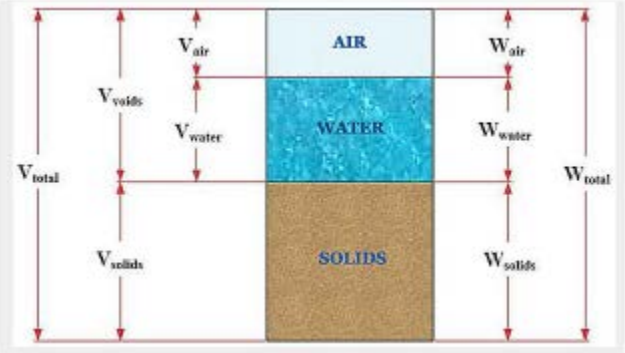

Figure 2-19 Phase diagram of soil

Studies have shown that soil resistivity is affected by changes in bulk density and degree of saturation. When the air volume in the pore space of the soil decreases, the bulk density and degree of saturation increases. Dissolved ions from the pore water adsorb on the solid surface and influence the formation of a double layer of fine-grained soil. That is why an increase of degree of saturation causes a proportional decrease of

soil resistivity. However, this relationship is only effective above a critical value of degree of saturation, which corresponds to minimum amount of water required to uphold a continuous film of water in soil. A sudden increase of soil resistivity occurs below the critical degree of saturation (Bryson, 2005). Furthermore, bulk density increases contact between individual particles. A decrease in pore space and closer contacts between the particles allow easy conduction of current. Rinaldi and Cuestas (2002) showed that the relationship curve of conductivity and degree of saturation was concave upward. The effect of degree of saturation on conductivity at different electrolyte concentrations is presented in Figure 2-20.

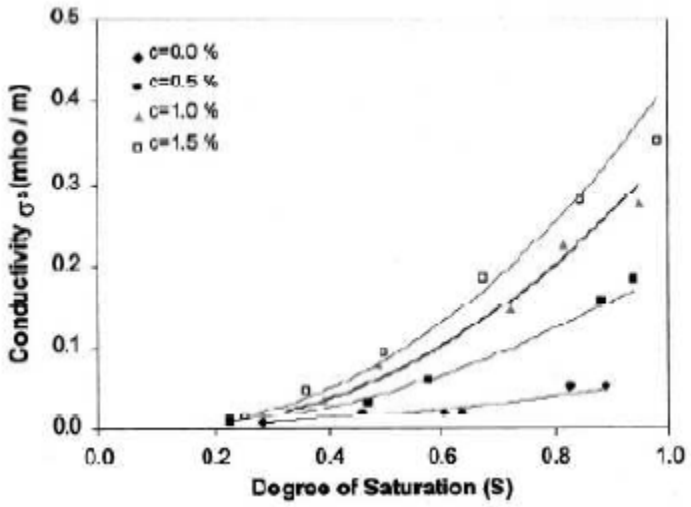

Figure 2-20 Effect of degree of saturation on conductivity at different electrolyte concentrations

Rinaldi and Cuestas (2002) conducted a laboratory investigation to assess the relationship between electrical conductivity and compaction. Soil samples were sieved with a No. 40 sieve and compacted at 18% moisture content. Compaction was performed in a rectangular mixing pan, using the Standard Proctor method. After compaction, conductivity was measured, using a four-probe electrode device. Based on the

experimental results, an iso-conductivity contour was obtained, as illustrated in Figure 2-21.

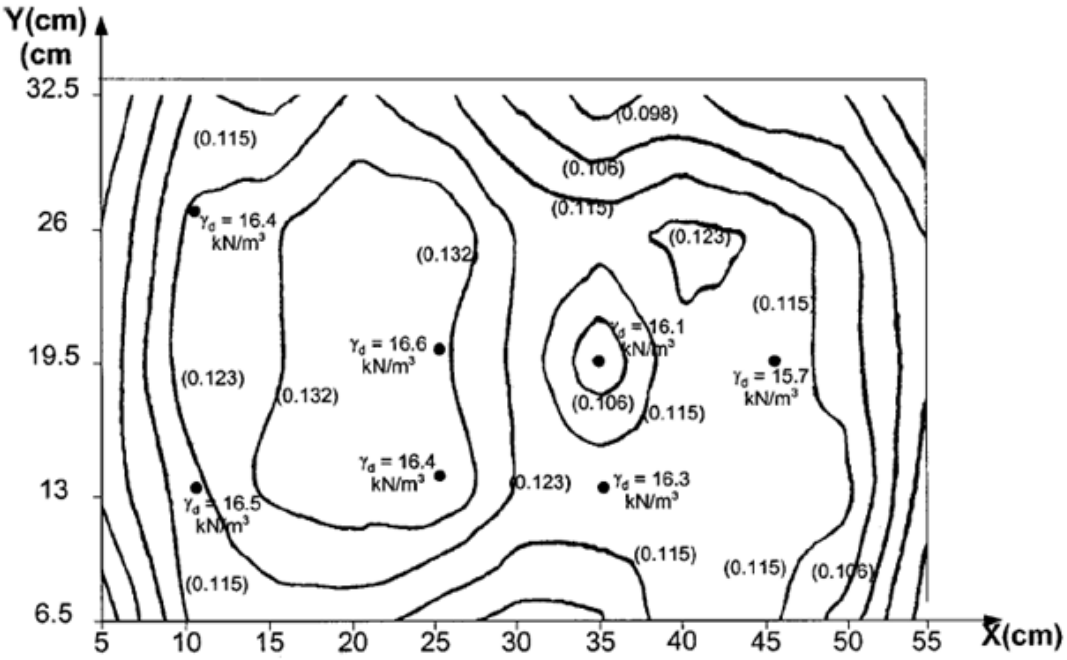

Figure 2-21 Iso conductivity contour of compacted sample (Parentheses show electrical conductivity in mho/m.) (Rinaldi and Cuestas, 2002)

According to Figure 2-21, the conductivity at the middle portion was higher than that of the right hand side and border, leading Rinaldi and Cuestas to conclude that the variation of conductivity was due to the variations of soil unit weight. The unit weight was higher on the left side and lower on the right side and border due to the low stiffness of the wall of the mixing pan.

McCarter (1984) performed a study to evaluate the effects of air void ratio in soil resistivity on Cheshire and London clay. A significant decrease in soil resistivity was observed for the increase of degree of compaction or degree of saturation. The study results emphasized that the compaction condition is an important factor in resistivity variations.

Abu Hassanein et al. (1996) performed a comprehensive study on the effects of molding water content and compacting efforts on soil resistivity. The soil samples were compacted, using three different compaction methods: a) Standard, b) Modified and c) Reduced Proctor. It was observed that the resistivity was high when soil was compacted at dry optimum, and low when compacted at wet optimum. Moreover, resistivity was sensitive of molding water content below optimum condition. At wet of optimum, resistivity was almost independent of molding water content. The authors presented that this relationship might be useful in assessing the compaction condition of soil. The observed test results from the study are presented in Figure 2-22.

The disparity of resistivity with molding water content can occur due to structural changes in the soil through compaction. At low compaction effort and dry of optimum water content, clay clods are tough to remold. The interclod pores are also comparatively large, the pores are filled with dielectric air, the diffused double layers are not fully developed, and the interparticle contacts are poor at this condition. Clods of clay can be easily remolded at wet of optimum and with high compaction effort, which leads to an increase in saturation. An improved particle-to-particle contact and formation of bridges between particles advance the electrical conductivity of the soil (Abu Hassanein et al. 1996).

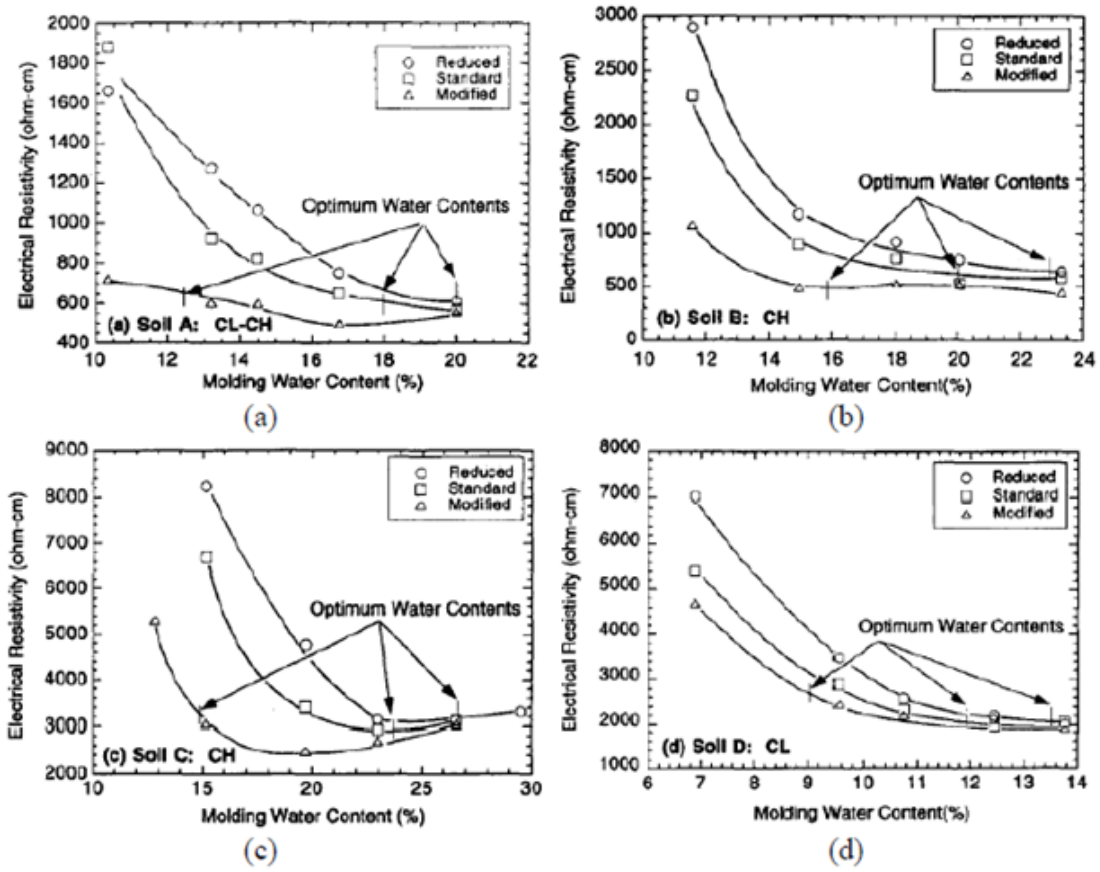

Figure 2-22 Relationship between electrical resistivity, molding water content, and compaction effort for different soils (Abu Hassanein et al., 1996)

Soil Temperature

Electrical resistivity decreases with increasing temperatures because of the agitation of ions. With an increase of one degree of temperature Celsius, electrical conductivity increases 2.02% (Campbell, 1948).Temperature variation is basically scaled in to two segments, variations throughout the year or daily variations.over a year like day and season in field scale. Most of the studies make the assumption that temperatures remain constant over the day; however, in annual scale (season), the effect of temperature cannot be avoided. Abu Hassanein et al., (1996) presented a study on the

effect of temperature on three different soils. They observed that above 0^0C, the relationship between electrical resistivity and soil was approximately exponential, as shown in Figure 2-23.

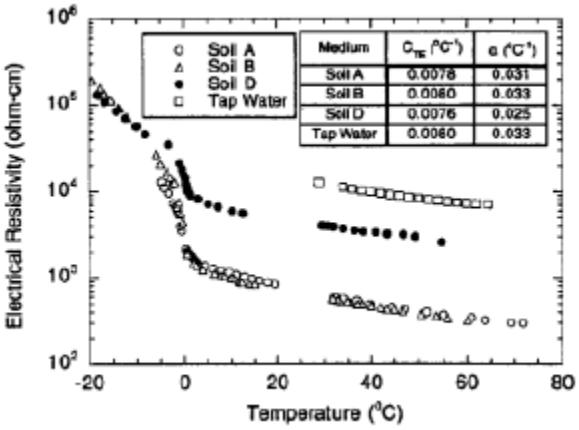

Figure 2-23 Relationship between electrical resistivity and temperature (Abu Hassanein et al., 1996)

Their studies also showed that soil resistivity is also affected by the operating frequency. The application of an electric field in clay soil causes ions to be released from the double layer at high frequency, which increases the overall conductivity of the soil. This occurrence is known as double-layer relaxation. In most soils with frequencies below 100 kHz, conductivity becomes independent of frequency.

Electrode polarization can occur at low frequency also. The exchange and accumulation of ions near the electrode cannot occur when polarization occurs. Ion accumulation causes the formation of double layers adjacent to the electrodes, causing the electrodes to have reduced conductivity.The effect of polarization is significant for electrodes made of gold, nickel, and copper (Rinaldi and Cuestas, 2002). A typical curve of conductivity is presented in Figure 2-24.

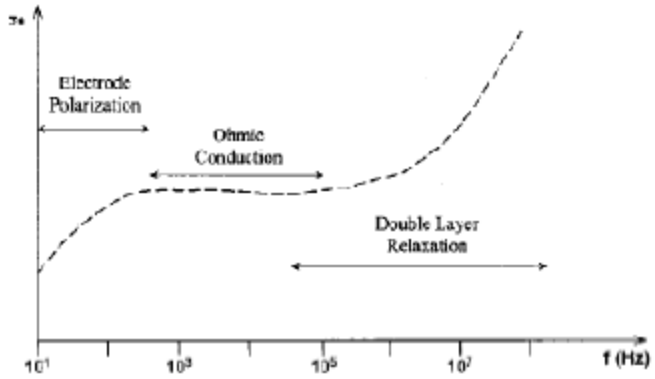

Figure 2-24 Conductivity of clay soil at different frequencies (Rinaldi and Cuestas, 2002)

Agitation of ions increases with temperature, as the viscosity of the fluid decreases. Therefore electrical resistivity decreases with an increase in temperature. Comparisons of electrical resistivity, therefore, require a standardized temperature correction. Campbell et al. (1948) showed, by means of comprehensive laboratory experiment, that conductivity increased by 2.02% per °C between 15 and 35 °C for saline and alkaline soils.

Corrections can be calculated to express the electrical conductivity at the standardized temperature of 25 °C as follows:

$$\alpha 1 = \alpha_{25°C}[1 + \alpha(T - 25°C)]$$

where σ_t is the conductivity at the experiment temperature, $\sigma_{25°}$ the conductivity at 25 °C, and α is the correction factor equal to 2.02%.

Campbell's equation was validated by Colman and Hendrix (1949), using 13 soils with a wide range of textures. These results matched the formula proposed by Campbell and the temperature effect chart provided by Schlumberg (1989). The temperature of soil varies with the temporal scales of days and seasons during a year. In the absence of a temperature correction, assumptions are made about temperature stability, mostly because measurements are done every day at the same time over a short period of time

(Bottraud et al., 1984). These assumptions do not work, however, for the annual scale in field scale electrical resistivity measurements. The greatest resistivity values are usually recorded from September to November in the northern hemisphere, while the smallest resistivity values are recorded from June to July. Aaltonen (2001) reported that coarse-grained materials present a wider range of seasonal resistivity variations than clayey soil. Thus, a knowledge of the seasonal variations of the temperature and their effect on electrical resistivity is essential to avoid misinterpretation of field measurements when comparing resistivity acquisition at the same place but on different dates.

Soil Index properties

Clay mineral characterization is necessary for engineering and physico-chemical behavior identification of fine-grained soils. In addition, design of stabilizers also requires a specific determination of clay minerals (Chittoori and Puppala, 2011). Casagrande utilized Atterberg limits to determine the qualitative mineralogical content of soils. Mitchell and Soga (2005) presented information on the range of activities in clay minerals, and provided information about the dominant mineral in a soil sample. A chart was developed for the identification of dominant minerals. It provides a mean for preliminary assessment of minerals, which can be useful from an engineering point of view. The typical ranges of LL, PI, and the activities of different minerals are presented in Table 2-5.

Table 2-5 Typical ranges of LL, PL, and activity of minerals (Mitchell and Soga, 2005)

Mineral	Liquid limits	Plastic limits	Activity
Montmorillonite	100-900	50-100	1-7
Illite	60-120	35-60	0.5-1
Kaolinite	30-110	25-400	0.5

Note: Activity= PI/%<2μm

Cation Exchange Capacity and Specific Surface Area

Adsorbed cations contribute significantly to the electrical resistivity of medium and fine-grained soils. Literature shows that the physico-chemical properties such as adsorbed ions, pore water conductivity, and surface charge are correlated with cation exchange capacity (CEC) of the soils (Friedman, 2005; Tabbagh and Cozenza, 2007; Schwartz et al. 2008). Kibria and Hossain (2012) presented a study on the electrical resistivity responses of high plastic clays at varied moisture contents and unit weights. In the study, the authors indicated that there is a substantial effect of electrical conductivity in fine-grained soil and that a large amount of moisture is needed for soils with a high specific area for formation of water film. So, below saturation, the electrical resistivity of soils was found to be high.

In electrical resistivity of medium and fine-grained soils, the contributions of adsorbed cations are noteworthy. It is evident from the literature that the physico-chemical properties such as adsorbed ions, pore water conductivity, and surface charges are related to the cation exchange capacity (CEC) of the soils (Friedman, 2005; Tabbagh and Cozenza, 2007; Schwartz et al. 2008).

Kibria and Hossain (2012) presented a study on the electrical resistivity responses of high plastic clays at varied moisture contents and unit weights. The authors presented that the effect of a specific surface area was substantial on the electrical conductivity of fine-grained soils. According to the study, soils with a high specific surface area require a large amount of moisture for the formation of water film. Thus, below saturation, soils with high SSA had high electrical resistivity.

Liquid limits (LL) and plastic limits (PL) of soils are also influenced by surface activity, so these index properties are also correlated with electrical resistivity. Bryson

(2005) indicated that LL and PI were related to electrical conductivity, according to the power function, as presented below:

$$LL = (BQ)^{\beta 1}\alpha 1$$

$$PI = (BQ)^{\beta 2}\alpha 2$$

where, BQ= conductivity in siemens/m, LL and PI are in decimals. The coefficient α and β are the function of clay mineralogy.

The effects of clay mineralogy on electrical resistivity and the index properties of soil are also mentioned in the study of Abu Hassanein et al. (1996). Soil with high smectite content showed increased LL, PI, and electrical conductivity.

Soil Texture and Soil Composition

The nature of the soil particles that constitute the soil influences the electrical resistivity, and the electrical resistivity of soil primarily depends on the displacement of ions. Nevertheless, in some conditions, and especially when the soil contains clay, the surface conduction cannot be neglected and the apparent soil electrical resistivity is influenced by the clay content. The electrical resistivity of clay ranges from ~2 to ~100 ohm-m, whereas the electrical resistivity of sand is usually higher than 1000 ohm (Samouëlian et al., 2005). Organic matter is said to be an influence on the electrical resistivity, but the literature is less focused on that subject.

For greater storage capacity, finer-grained materials, like silts and clayey silts, are typically used for monolithic barriers and the top layer of a capillary barrier. Sandy soils are typically used for the bottom layer of the capillary barrier to provide a contrast to the unsaturated hydraulic properties between the two layers. Many ET covers are constructed of soils that include clay loam, silty loam, silty sand, clays, and sandy loam.

Clay Content

Shevinin et al. (2007) conducted a study for the estimation of clay content in soil, using electrical resistivity and taking the electrochemical process of soil micro pores into account. The experimental tests were accomplished on brine-saturated soil samples, where the concentration of NaCl ranged from 0.6 to 100 gm/L. According to the authors, at salinity concentration of 0.6 to100 gm/L, soil properties like clay content, CEC, and porosity can be obtained from resistivity measurements. The method was compared with the sand-clay mixtures, and an overall error of 20% was found. The method was tried for some sites in Mexico for determination of the clay content, CEC, and porosity, and it was found that a boundary resistivity value differentiated between clean and oil-contaminated soils. Thus the model could identify the oil-contaminated zone.

An evaluation of variations of electrical resistivity with Atterberg limits was also done by Abu Hassanein et al. (1996). The specimens were compacted at optimum moisture contents and dry unit weights, using the Standard Proctor method. The study showed that with higher LL and PI, the resistivity value was lower, as shown in Figure 2-25. Soils with 47% coarse fraction showed high resistivity. The increase of LL and PI was explained, using the mineralogy of the samples. Clay samples with smectite content (high LL and PI) were more active and exhibited higher surface conductivity.

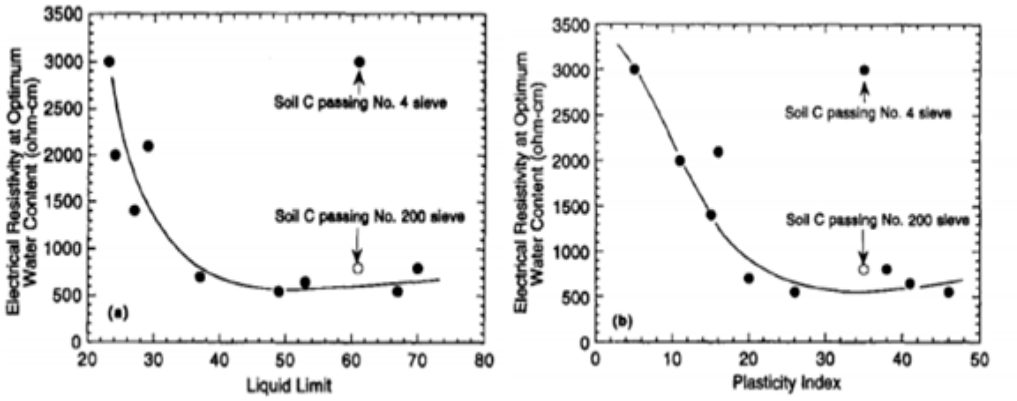

Figure 2-25 Relationship between electrical resistivity and Atterberg limits at optimum water content (Abu Hassanein et al. 1996)

Clay fraction also indicates the surface charge of a soil specimen. An increase of clay fraction increases the surface activity and affinity to water, meaning that electrical resistivity fluctuates with the clay fraction. According to Shah and Singh (2011), the cementation and fitting parameters of Archie's law are also functions of clay fraction.

Hydraulic Conductivity

Hydraulic conductivity depends on the porosity, structure, saturation, and tortuosity of soil. Due to dependence of electrical resistivity on these parameters, researchers have often correlated hydraulic conductivity with electrical resistivity (Bryson, 2005). A study was performed by Sadek (1993) to explore the possibility of using electrical conductivity as an alternative to hydraulic conductivity in compacted clay liners. The author developed extensive research including: a) detailed evaluation of the influential parameters affecting electrical and hydraulic conductivity, b) development of a theoretical model to integrate pore water conductivity and surface conductance, and c) design of new equipment to study the electro-kinetic properties. Study results showed that the sensitivity of electrical conductivity was not enough to measure hydraulic conductivity. A sample with dispersed structure and low hydraulic conductivity had

electrical conductivity similar to the sample with flocculated structure and high hydraulic conductivity. A better correlation was indicated by the authors which used a “Cluster model” to incorporate surface conductance and internal pore geometry, but quantification of the internal geometry is required for this correlation. Even though the study could not prove that electrical conductivity is a reliable indicator of hydraulic conductivity, it provided useful insight into the electrical properties of soils.

Arulanandan (1968) discussed the electrical conductivity of saturated kaolinite, illite, and montmorillonite clay in the 50-108 cycle/sec frequency range. The study observed a direct proportional relationship of electrical conductivity frequency which did not depend upon particle size for the first dispersion. The microscopic permeability coefficients were evaluated based on the electrical properties, and the correlation of coefficients of Darcy’s law, with electrical properties like conductivity of AC and DC ranges and the ratio of phenomena logic transport coefficient, was indicated. A schematic of the study results is presented in Figure 2-27.

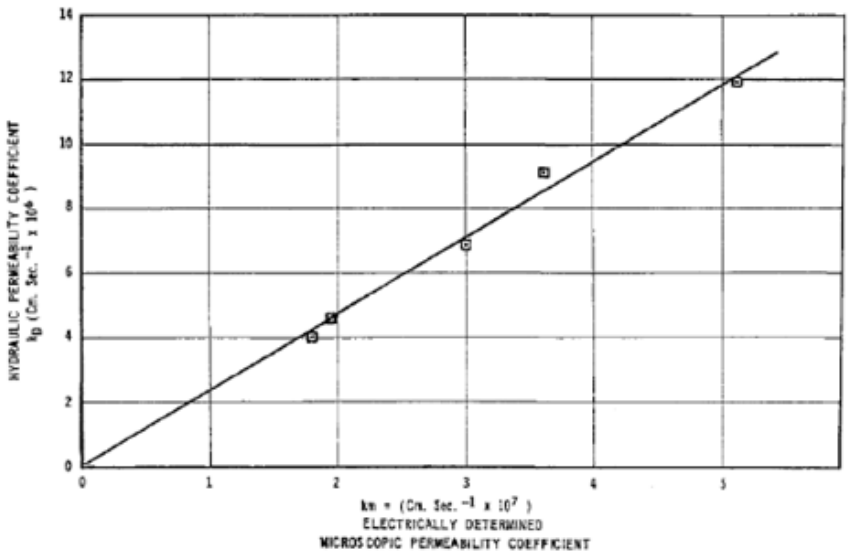

Figure 2-26 Correlation between microscopic and hydraulic permeability coefficients during consolidation (Arulanandan, 1968)

Soil pH and Nutrient Availability

The acidity or alkalinity of any particular soil is designated by pH. Soil corrosivity increases and lower resistivity occurs with extremely high alkanity, but it is not affected by mild alkanity. In soils, the electrical conduction is mainly related to the displacement of ions. Therefore, the composition of the soil solution (i.e. the composition of the fluid inside the porous network of the soil) can alter the apparent electrical resistivity of the soil. Generally, the electrical resistivity data related to the soil solution is discussed in conductivity, the reverse of resistivity. The relationship between the soil's apparent conductivity and the conductivity of the soil solution has been analyzed in several studies by laboratory experiments (Coleman et al., 2004). It was demonstrated that, for a soil solution concentration higher than 40 mM, a linear relationship exists between the electrical conductivity of the soil solution and the apparent electrical conductivity of the soil. This threshold is quite high for soils and corresponds to salt soils or sodic soils.

However, Murad 2016 concluded that with high acid pH value in soil and with courser particles such as gravel, sand, etc., electrical resistivity will be higher.

Plant and Plant roots

Electrical resistivity methods have been widely used for the last 40 years in many fields: groundwater investigation, soil and water pollution, engineering applications for subsurface surveys, etc. Many factors can influence the electrical resistivity of a media and thus influence the ERT measurements. Among those factors, it is known that plant roots affect bulk electrical resistivity; however, this impact is not yet well understood.

Soil compaction has been determined by electrical resistivity tomography (ERT) in plant and soil science (Besson et al., 2004), water content and flow in soil and plants (Hagrey and Michaelsen, 2002), and soil cracks (Samouelian et al., 2003). Alterations in soil electrical resistivity have been observed in plant root zones (Panissod et al., 2001). There are some attributions to roots (Hagrey et al., 2004), and correspondence of large tree roots has been found for resistive soil volumes (Amato et al., 2008). Amato et al. (2008) accurately mapped root biomass in 2D in an alder stand, showing that resistivity imaging for the non-destructive characterization of the spatial structure of root data can deliver a tool for the spatial optimization of measurements.Quantitative relationships between root biomass trees are evident from literature (Loperte et al., 2006; Lazzari et al., 2008). Amato et al. (2008) showed a strong quantitative relationship between soil electrical resistivity and root biomass in trees, to the point that the roots masked the effects of other soil features. Nevertheless, it is difficult to discern the effect of roots from the background noise at low root biomass density. According to literature, quantitative relationships are not available for herbaceous plants. Amato et al. (2008) observed the strong effect of root biomass for woody species above 40 m. The authors hypothesized that at lower values of resistivity, the response of resistivity to roots might be too weak to

be clearly discriminated from that of other soil properties. Electrical resistivity was also applied to the study of structure, moisture, and flow in soils and plants (Loperte et al. 2006, al Hagrey 2007). Soil electric anomalies that may be related to roots have been found under plants by resistivity tomography (Panissod et al. 2001, al Hagrey et al. 2004). Amato et al., 2008 developed a regression model depicting root mass density (RMD) and electrical resistivity. Figure 2-26 shows a highly significant positive correlation ($P < 0.01$, n=97). The regression model, which was selected on the basis of minimization of the sum of square residuals, was a logistic curve cut at RMD = 0. To verify the model when applied to Dataset II, the regression equation obtained from Dataset I yielded RMD_c values that were highly correlated ($P < 0.01$, $n = 67$) with RMD_m values. Among the soil parameters measured along the transect (Table 1), only volumetric soil water content yielded a significant correlation with ($P < 0.01$) but with low r^2 (0.326).

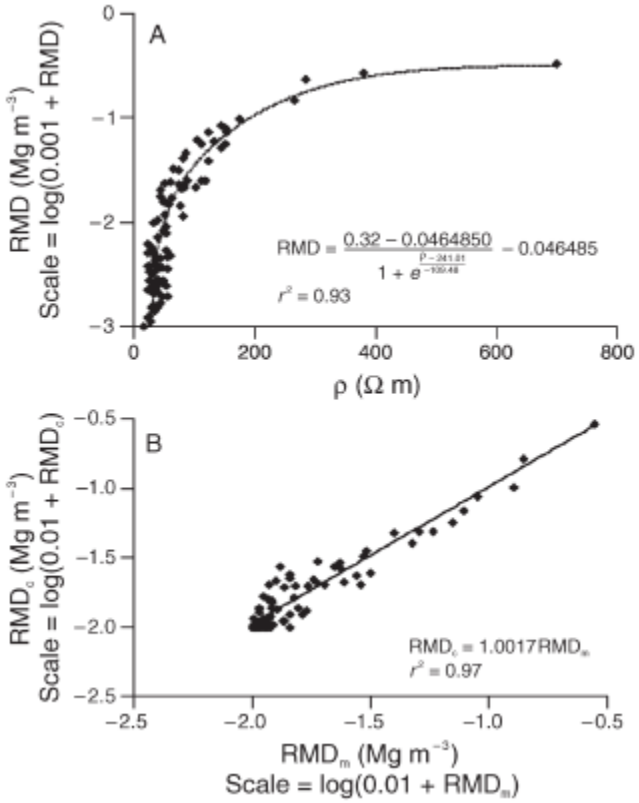

Figure 2-27 (a) Root dry mass per unit soil volume (RMD) as a function of electrical resistivity (ρ). (b) RMD calculated with the logistic regression model (RMD_c) versus measured RMD (RMD_m) (Amato et al., 2008)

ELECTRICAL RESISTIVITY MEASUREMENT

Laboratory Measurement Systems

Electrical resistivity can be measured in the laboratory by using a direct current (DC) or an alternative current (AC). For an alternate current system, a range of frequency from low Hz to microwave can be used to characterize different material types. However, for DC, the method includes the association of Ohm's law, where the drop in potential difference is measured while applying an electric current. Depending on the type of

configuration to be used, the resistivity tests in the laboratory can be performed with a two-or-four electrode system.

ASTM G187-05 describes the standard method for two-electrode electrical resistivity measurements, and Figure 2-28 shows the setup used.

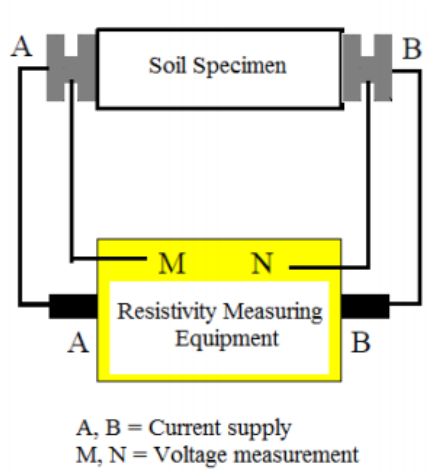

Figure 2-28 Two-electrode electrical resistivity measurement system

The setup consists of a two-electrode soil box, current source, resistance-measuring equipment, and electrical connections. This method uses only two electrodes for applying the currents and measuring the potential difference. It is important to construct the two-electrode soil box, using insulated material to avoid a short circuit. Corrosion-resistant metal can be used for the two end plates, for measuring the current flow and voltage. It is recommended that the resistivity measurement be corrected at 15.5 deg. C temperature, according to following equation provided by the ASTM G187-05 standard:

$$\rho_{15.5} = \frac{(24.5 + T)}{40} \rho_T$$

here, ρ15.5 = resistivity corrected at 15.5 deg. C, ρT= measured resistivity at medium temperature, T = temperature during experiment.

Studies conducted by Santamarina et al., 2001 and Kibria 2014 discussed the probable sources of error in these kinds of measurements. The flow of the current in soil is mostly ionic, and the conduction phenomenon in the electrode and the cable is carried out by the electron flow. This might result in an accumulation of charge in the soil-metal interface, also known as polarization. Furthermore, the air gap in the soil-metal interface may cause a chemical reaction and non-uniform electric field, which might make the resistivity results less accurate.

The four-electrode system is an alternative lab measurement system. The current is applied to the soil specimen from both ends, and the potential drop is measured between any two points in the soil specimen. Figure 2-29 shows the experimental setup for a four-electrode system. This method is more preferable than the two-electrode system, as the potential drop is measured far away from the charge transfer location and results in minimization of the polarization. Also, as the current and potential electrodes are separate, there is less potential for the electrodes to be subjected to a chemical reaction.

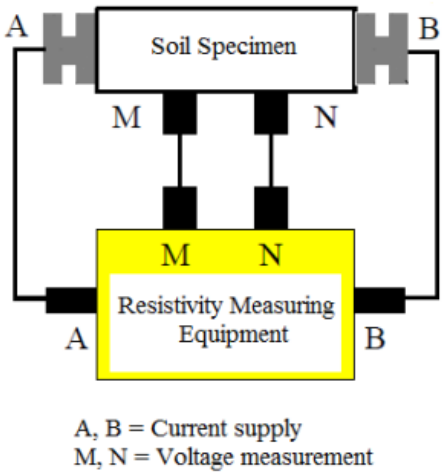

Figure 2-29 Four-electrode electrical resistivity measurement system

Field Measurement Systems

Electrical resistivity measurements have been used in the investigation of sub-surface geology since the early 20th century. However, this method has become very widespread in recent years with the improvement of test methods and data processing. Presently, geo-electrical measurements are a useful instrument in geophysics, soil science, hydro-geological studies, environmental, and geotechnical engineering (Aizebeokhai, 2010; Hossain et al. 2010). A current (I) is injected through the current electrode in the isotropic homogenous half-space of earth (Figure 2-30). The electric potential decreases in reverse with the increase of distance from the current source. The current distribution follows an external radial direction through shell area of $2\pi r^2$, vertical to equipotential lines. The potential for one electrode can be mentioned as:

$$\acute{\emptyset} = \frac{\rho\, I}{2\,\pi\, r}$$

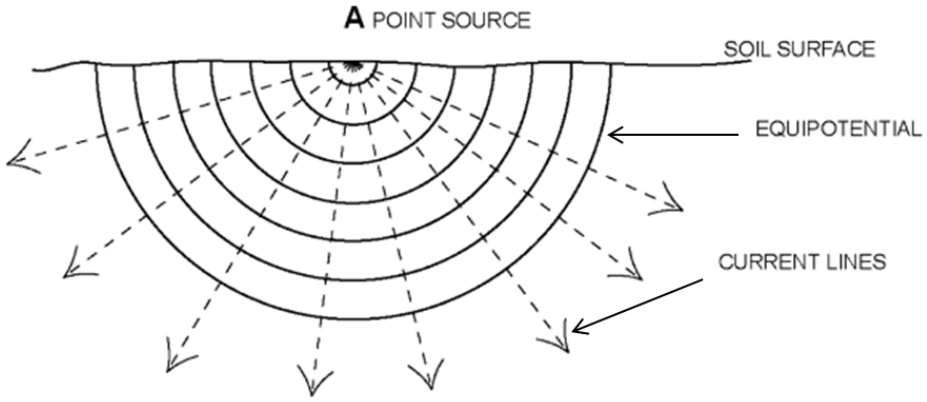

Figure 2-30 During field investigations, four electrodes are typically positioned at arbitrary locations. For the four-electrode system, the resistivity is measured by the following equation:

$$\acute{\emptyset} = \frac{\rho\, I}{2\,\pi}\,(\frac{1}{r_1} - \frac{1}{r_2} - \frac{1}{r_3} + \frac{1}{r_4})$$

The equation shown is applicable to real field investigations where the medium is anisotropic and inhomogeneous. The apparent resistivity is calculated from measured current and potential, using the modified equation shown below:

$$\rho_a = \frac{k\,\Delta\acute{\emptyset}}{I}$$

where, k is a geometric factor that depends on the arrangement of the four electrodes and can be expressed as:

$$k = \frac{2\,\pi}{\frac{1}{r_{c1p1}} - \frac{1}{r_{c2p2}} - \frac{1}{r_{c3p3}} + \frac{1}{r_{c4p4}}}$$

Apparent resistivity is defined as the electrical resistivity of a homogenous subsurface medium that delivers the exact resistance in the same electrode configuration. Apparent resistivity gives the qualitative estimation of the electrical parameters of the medium (Meheni et al., 1996). It provides the weighted average of the resistivity of the medium under the electrodes' configuration. The measurement obtained depends on the array system, and inversion modelling is carried out to obtain the true resistivity from the apparent resistivity (Loke, 2001; Aizebeokhai, 2010).

Electrode Configuration

For field resistivity, a number of different electrode configurations is available to record the field data. The suitability of each configuration depends on the specific geological condition, with fluctuating anomaly resolution. Conventional electrode arrays used for field investigations are Wenner (Wenner-alpha), Schlumberger, dipole-dipole, pole-pole, and pole-dipole. Other alternatives to the conventional Wenner array available are Wenner-beta, Wenner-gamma, and Wenner-Schlumberger arrays (Dahlin and Zhou, 2004; and Loke et al., 2001). Figure 2-31 shows the illustrations for all different types of

arrays. The Wenner-Schlumberger array is a fusion of Wenner-alpha and Schlumberger arrays (Pazdirek and Blaha, 1996). This is a digitized version of the Schlumberger array that permits the use of automated multi-electrode systems with fixed electrode spacing. The Wenner-beta array is a dipole-dipole array, with the value of n factor being 1. For the Wenner-gamma array, the current and potential electrodes are enclosed together.

Comparison of Different Array Methods

Conventional methods such as Wenner and Schlumberger arrays are comparatively more sensitive in terms of vertical variations in the subsurface resistivity under the center of the array. However, they are less sensitive in the horizontal direction. These arrays provide a reasonable depth of investigation in the field with strong signal strength, which depends on the geometric factor used to calculate the apparent resistivity. The relationship between the factor and strength of the signal is inversely proportional. The limitation of these arrays is the reduced horizontal coverage with increased electrode spacing. For a noisy site, the Wenner array is preferred, as it provides high signal strength; however, it is not a good choice for 3D structures. The pole-dipole array is a disproportionate array system which has asymmetrical apparent resistivity anomalies for proportioned structures in the pseudo section which may alter the inversion model. Horizontal range is better in this array, and it is also less vulnerable to noise than the pole-pole array. It is sensitive to vertical structures, and the strength of the signal for the pole-dipole array is lower for than Wenner and Schlumberger arrays. The pole-pole array contains one electrode for potential, with the second current and potential electrodes at infinite distances. Their limitations are the difficulty in obtaining ideal locations for the electrodes and their susceptibility to noise, which degrades the image quality. It has the highest horizontal coverage, but due to smeared image in inversion model, it has the most-reduced resolution (Loke, 2001). For small electrode spacing and

horizontal coverage, the pole-pole array is ideal. The dipole-dipole array is not ideal for mapping horizontal structures, but it is the most suitable array for 3D structures (Dahlin & Zhou, 2004). It is less sensitive to vertical variations, but very sensitive to horizontal directions; therefore, it is preferred for mapping vertical structures. The depth of investigation of the array relies on both the current electrode spacing and the distance between the two dipoles, and is typically shallower than the Wenner array. However, the dipole-dipole array has better horizontal data coverage than the Wenner array. The major disadvantage of this array is the decrease in signal strength with increasing distance between the dipole pair (Okpoli, 2013). It is characterized by low electromagnetic coupling, which makes it a very efficient method for field surveys (Loke, 2001).

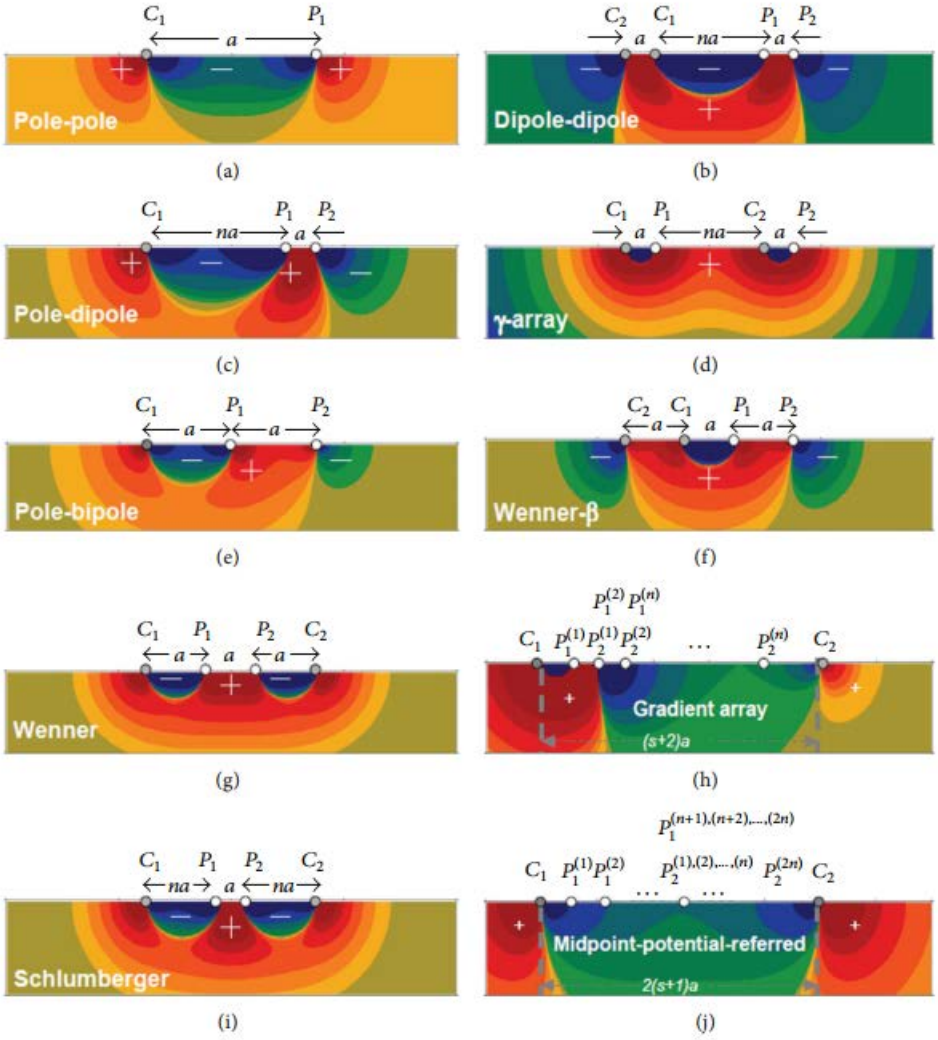

Figure 2-31 Sensitivity and resolution diagrams of electrode configurations. (a) Pole-pole, (b) dipole-dipole, (c) pole-dipole, (d) Gamma-array, (e) pole-bipole, (f) Wenner- Beta, (g) Wenner, (h) gradient array, (i) Schlumberger, and (j) midpoint-potential-referred (Dahlin & Zhou, 2004).

Dimensions of Resistivity Survey

One-dimensional resistivity surveys are performed using vertical electrical sounding (VES). In this type of survey, the spacing between the electrodes is increased

to acquire resistivity in the deeper sections; however, the center of the electrodes remains constant during the test. The soil resistivity obtained provides the resistivity in the vertical direction only, without taking the horizontal direction into account (Loke, 2001). The VES interprets data by assuming several horizontal layers (Pozdnyakova, 1999). Complex resistivity results with horizontal variations require 2D and 3D survey display results.

Two-dimensional resistivity surveys are multi-electrode arrays in two dimensions that provide a continuous display of the subsurface. Electrodes for current and potential measurements are placed at a fixed distance along a line and moved progressively along the soil surface. Each line or each step takes one measurement. Figure 2-32 illustrates the setup used in the field. The measured apparent resistivity is used to develop a 2D pseudo section. Thereafter, a 2D continuous image of the subsurface is obtained by performing inversion modelling on the measured apparent resistivity (Samouelian at al. 2005).

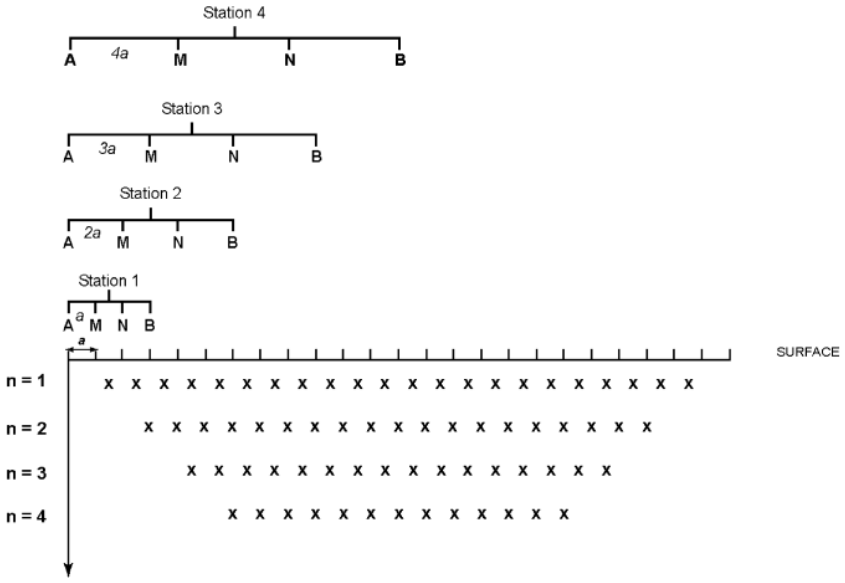

Figure 2-32 2D resistivity measurement (Samoulien et al. 2005)

Three-dimensional resistivity surveys are used to obtain robust information about the subsurface in three dimensions. Two methods are used to measure the 3D resistivity profile of the subsurface. The first method is called Quasi #D method, where a three-dimensional electronic picture is reconstructed using parallel pseudo sections of a two-dimensional network (Zhou et al., 2001). The second method is performed by measuring the resistivity in both X and Y directions to obtain an actual 3D resistivity profile of the subsurface (Arjwech, 2011).

Resistivity Data Interpretation

A mathematical inversion of the apparent resistivity is required to obtain quantitative resistivity information. The inversion converts the volumetric apparent resistivity to obtain inverted resistivity data that represents the resistivity at the effective depth of investigation, as opposed to the pseudo-depth.

For vertical electrical sounding (one-dimensional), the data is plotted on a graph (curves) which expresses the disparity of the apparent resistivity with the increasing electrode spacing. These curves show the variations of the resistivity along the depth in a qualitative way. In relatively simple cases the depth of the layer can be estimated by comparing the field data with theoretical apparent resistivity curves. This method provides a coarse interpretation in the absence of computer facilities, or permits derivation of an approximate model that is compulsory as a starting point for the iterative modelling schemes. If the ground is not one-dimensional, the two-or-three-dimensional data treatment requires the numerical modelling inversion procedure. Numerous numerical solutions have been developed, including finite-difference approximation (Dey and Morrison, 1979; Oldenburg and Li, 1994) and moment–method modelling, applied first to electromagnetic surveys. The inversion process is non-linear type, and the resolution

essentially starts with a deduction model whose parameters are rationalized, using a linearized iterative-type adjustment procedure, shown in Figure 2-33.

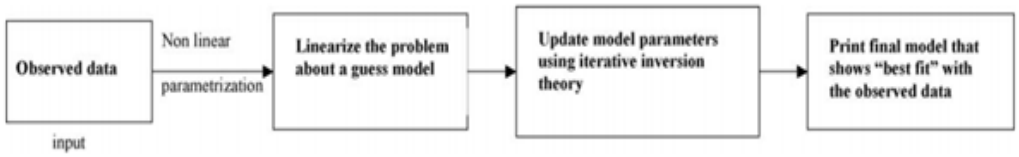

Figure 2-33 Schematic of iterative inversion modelling (Sharma, 1997)

During inversion of resistivity measurements, a model is determined that can provide a similar response to the actual values. The model consists of a set of parameters, which are the physical quantities estimated from the observed data (Loke, 2001). For subsurface resistivity distribution, forward modeling can be used to provide theoretical values of apparent resistivity. Typically, finite difference and finite element modeling are used to calculate the theoretical apparent resistivity. Eventually, inversion methods produce a subsurface model whose responses match with the measured quantities under certain conditions. A detail of mathematical procedures for inversion modeling is presented in study of Loke (2001) and review of Arjwech (2011).

Chapter 3

FIELD-SCALE QUANTIFICATION OF SOIL MOISTURE USING ELECTRICAL RESISTIVITY IN EVAPOTRANSPIRATION COVER SYSTEM

Hossain, M.I.[1], Hossain, M.S.[2]

[1] Graduate Research Assistant, Department of Civil Engineering, University of Texas at Arlington, 417 Yates Street, NH 119, Arlington, TX 76019, United States. E-mail: ishtiaque0704094@gmail.com

[2] Professor, Department of Civil Engineering, University of Texas at Arlington, 416 Yates Street, NH 119, Arlington, TX 76019, United States. E-mail: hossain@uta.edu

ABSTRACT

Evapotranspiration (ET) cover systems are becoming popular as an alternative means of waste containment. Monitoring soil moisture in ET covers is necessary for assessing the performance of the final cover system. Current methods to assess soil moisture provide only discrete information and are unable to provide an accurate spatial or depthwise variation. Electrical resistivity imaging (ERI) is an alternative method for evaluating soil moisture. A substantial number of studies have been conducted in both the laboratory and field to correlate soil moisture and electrical resistivity; however, very few studies have correlated these parameters for the ET cover system. Additionally, there have been no significant studies on soil moisture sensors and ERI relations, and no study has been conducted to acknowledge the difference that the presence of a plant root systems makes in soil conditions. Therefore, the objective of this study is to perform correlation and regression analyses over a simultaneously collected data set of electrical resistivity and soil moisture measurements obtained from an ET cover lysimeter. The ERI measurements were carried out using an ERI instrument from the Advanced Geoscience

Institute, and soil moisture was measured using 5TM sensors. Six different lysimeters were under investigation for two years. The data was acquired from different depths to acknowledge the differences in soil conditions due to soil temperatures and plant root systems. The statistical analysis was performed by separating the data set into different groups for different lysimeters, for different depths, and for different soil conditions. The rresults indicated good correlation between soil resistivity and soil moisture, and two separate sets of model parameters were proposed. The compacted clay model had an R^2 value of 0.92, and the vegetated clay model had an R^2 of 0.87. Further model validation showed that the error of percentage was within 10% for the developed models. Compared to other soil moisture instrumentations, the ERI method provides information for a greater extent of area, is less expensive, and is more convenient to carry out in the field. Therefore, this technique can be considered as a suitable alternative for qualitative and quantitative estimation of soil moisture in an ET cover system.

INTRODUCTION

An evapotranspiration (ET) cover is an alternative earthen final cover system for waste containment (Hauser, 2008). ET cover systems are becoming popular as a final cover alternative because their design allows them to act very similar to nature (Benson et al., 2002). The comparative high cost of installing conventional covers and the unpredictability of long-term conventional cover performance have made the alternative cover systems more attractive (Licht et al., 2001). The primary purpose of an ET cover is to store the infiltrated water from rainfall in the cover soil and transpire the water through plants during drier periods of time (Barnswell and Dwyer 2011; Benson et al., 2002). Therefore, the performance of an ET cover largely depends on the water storage capability of the cover soil. Although ET covers are becoming more common for full-scale use, research regarding their effectiveness in removing water from the cover soil is

limited (Madalinski et al., 2003). Hence, the invention of field-scale lysimeters. Lysimeters consist of a large pan, typically constructed of a geomembrane and installed beneath the cover in test sections, with provisions for measuring the runoff and percolation (Benson et al., 1995, 2001, Malusis and Benson, 2006). They monitor the field performance of ET covers by directly measuring the water flowing through the bottom of the cover in the field. They may also be equipped with soil water monitoring sensors and are commonly used as a secondary or indirect monitoring tool to verify the effectiveness of the lysimeters in terms of moisture storage and percolation (Malusis and Benson, 2006). The monitoring and maintenance of the ET cover system in an efficient way is essential to preserving the integrity and effectiveness of the cover system for long-term use. Drainage lysimeters and soil instrumentations are the methods most commonly used for performance monitoring (USEPA, 2011).

Moisture monitoring tools such as a capacitance sensor, thermal dissipation unit, psychrometer, tensiometer, or time domain reflectrometry are available and have been employed as non-destructive techniques for testing ET covers (USEPA, 2011). Currently available non-destructive methods might be used to monitor the soil water storage for discrete locations and at different depths, providing information about the availability of soil moisture. The measured soil moisture is then evaluated to estimate the changes over time in vertical and horizontal gradients. However, discrete measurements of soil moisture in cover soil may not be suitable for assessing the overall performance of the covers (Schnabel et al., 2012). In addition, installing sensors in the cover soil is expensive, and they are not suitable for long-term moisture monitoring due to their short warranty (Rock et al., 2012). Therefore, an alternative method is required to overcome the limitations of currently available moisture monitoring devices. One such method is electrical resistivity imaging (ERI), which is an established non-destructive method for

subsurface investigation (Liang et al., 2007; Nijland et al., 2010; Schnabel et al., 2012). Studies conducted by Abu Hassanein et al., 1996, and Kibria, et al., 2014 showed a significant correlation between soil moisture content and electrical resistivity in different types of soils in laboratory investigations. In addition, several other researchers such as Bourennane et al., 2012; Nijland et al., 2010; Schnabel et al., 2012; Kibria and Hossain 2015; and Calamita et al., 2012 performed field investigations to correlate the electrical resistivity and soil moisture for different types of soil. Detection of soil moisture in these field studies was carried out by conventional methods, such as gravimetric moisture measurements from the soil core (Bourennane et al., 2012; Nijland et al. 2010; Schnabel et al., 2012; Kibria and Hossain 2015) and time domain reflectometry (TDR) (Calamita et al., 2012, Schwartz et al., 2008). It should be noted that no comprehensive field studies have been conducted to correlate the soil moisture obtained from a sensor (dielectric) with the ERI results. Furthermore, very few studies have been conducted on the application of ERI to the ET cover system. The use of ERI to estimate the volumetric moisture content over the entire cross section of the lysimeter provides a spatial variation of moisture in the lysimeters. The advantage of using ERI is that it is possible to obtain the soil moisture of a wide region rather than for a discrete point, as with the soil moisture sensor. ERI is able to visualize and quantify the entire cover soil moisture, which might go undetected by other point-based soil moisture measuring systems.

In addition to soil moisture content, field studies have shown that several other factors, such as soil temperature (Campbell et al., 1948; Friedman, 2005), soil density (Seladji et al., 2010), and the presence of plant roots (Paglis, 2013; Jayawickreme et al., 2008) significantly influence soil electrical resistivity results. Campbell et al., 1948 reported that ion agitation increases with increased soil temperature, resulting in lower resistivity. Abu Hassanein et al., 1996 stated that increased soil compaction or increased

soil density results in higher resistivity. The change in soil density in ET cover soil can be attributed to the presence of plants, as was reported by Hossain et al., 2017. The presence of plant roots in the ET cover soil causes higher suction in vegetated soil, facilitating evapotranspiration. Cracks form around plant roots under vegetated areas, causing lower penetration resistance (Ng and Zhan, 2007). Furthermore, anomalies in soil resistivity found in vegetated ground may be attributed to the root systems, as shown by (Hagrey, 2007, Amato et al., 2008).

Several studies have been conducted on the relationship between soil moisture and soil resistivity. In most cases, the relationships are non-linear. McCarter, 1984 presented a non-linear law on laboratory-based results conducted on clay soil. In addition, Kalinski and Kelly, 1993 proposed a second-order polynomial equation, and Zhu et al., 2007 and Kibria, 2012 showed an exponential relationship between soil moisture and soil resistivity. In spite of these developed relationships, laboratory-based models are very limited in the field (Michot et al., 2003). A significant number of studies have reported an exponential relationship between soil moisture and soil resistivity. (Pozdnyakova, 1999; Zhu et al., 2007; Ozcep et al., 2009). However, limited moisture ranges have also shown linear models between these soil moisture and electrical resistivitytwo parameters (Goyal et al., 1996; Michot et al., 2003). In brief, literature shows that non-linear models, such as power law or exponential relationships, are the most popular, but statistical analysis is required to conclude which model is statistically significant for a limited range of variation between variables (Pozdnyakova, 1999).

The objective of this study was to perform correlation and regression analyses over a simultaneously collected data set of soil electrical resistivity and soil moisture measurements obtained from ET cover lysimeters. Six different lysimeters were constructed and installed in the City of Denton, TX landfill to provide a non-destructive,

extensive, and inexpensive method for estimating soil moisture for ET cover monitoring. Spatially and depthwise variable data, using electrical conduction phenomenon of soil, was employed to provide data on moisture variations and detect the heterogeneity of the subsurface.

MATERIAL AND METHODS

Study Area

The field scale measurements for this study were carried out at the City of Denton Municipal Solid Waste Landfill in Denton, Texas, USA, which is located on the southeast side of Denton, Texas. Figure 3-1 shows the location of the ET lysimeters and illustrates the field installation setup. Six pan lysimeters with dimensions of 40 feet by 40 feet were constructed in Cell 1 of the landfill. The lysimeters were referred to as 1, 2, 3, 4, 5, and 6.

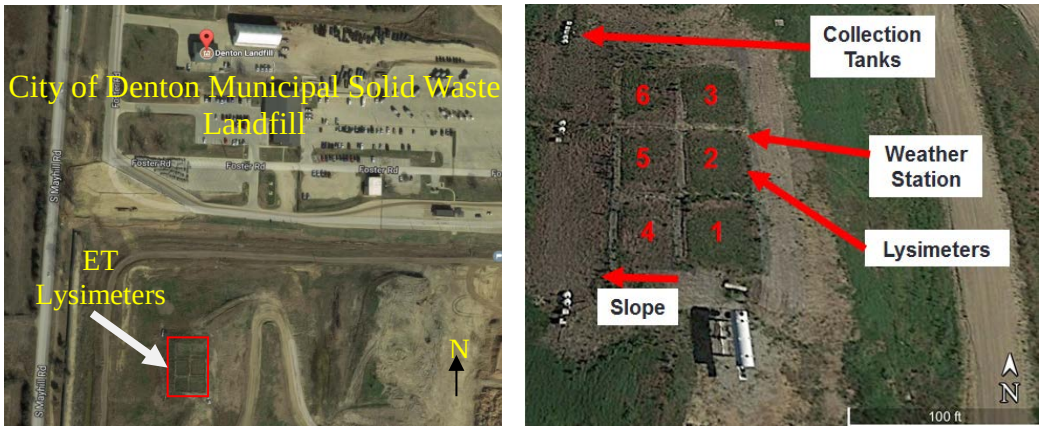

Figure 3-1 Location of ET lysimeters (on left) and field installation setup (on right).

The locations of the lysimeters were suitable for regular monitoring, as they were installed at the top of the intermediate cover in Cell 1, where lysimeters 1, 2 and 3 with 2% slope and lysimeter 4, 5 and 6 with 25% slope were installed. The lysimeters were designed in accordance with the Environmental Protection Agency's Alternative Cover Assessment Program (ACAP) guidelines, with a buffer area of 3 meters around the

lysimeter parameter to provide an area for vegetation and soil investigation, which will consequently also reduce the effect of boundary (Albright et al., 2002).

Lysimeter Construction and Field Instrumentation

Construction of lysimeters began on June 17th, 2014 and ended on November 1st, 2014. Figures 3-2 (a) to 3-2 (i) illustrate the steps involved in the construction, which began with the construction of a 4 foot embankment, using local soil. The embankments were then excavated to accommodate the subgrade material for the lysimeters. After the subgrade was compacted, a 60 mil geomembrane layer was placed on the subgrade and along the side walls. Twelve geomembrane boots in total were placed in the lysimeters where each lysimeter had two boots; one for percolation and one for runoff water collection. Compacted clay was placed up to 3 feet, with 8-inch lifts in all of the lysimeters.

Sheep foot rollers were used and density tests were conducted at each lift, using a nuclear density gauge, to achieve a 95% maximum dry density condition. One foot of topsoil was placed on top of the compacted clay to ensure initial vegetation growth in the lysimeters. Three different types of plants were planted in the six lysimeters (one type plant was planted in two lysimeters). Native vegetation mixes were used to ensure sustainable vegetation performance throughout the different seasons of the year. Several soil samples were collected from different depths of the lysimeter to conduct the cover soil characterization in terms of liquid limit, % clay, unit weight and specific gravity. Figure 3-3 shows the experimental results. In table 3-1 the soil characteristics were summarized to show range of soil parameters for the cover soil used in all the lysimeters. As the cover soil were obtained from the same source, all the lysimeters had soil characteristics in the same range with liquid limit within the range of 46-60%, percentage of clay within 43-53%, specific gravity within 2.64-2.69 and dry unit weight within 102 to 105 pcf. Table 3-2 illustrates the vegetation mix details used in the lysimeters.

Upon completion of the lysimeters, a total of 48 5TM soil moisture & temperature sensors (manufactured by Decagon Devices of USA) were installed in the six pan lysimeters at various depths. Table 3-3 shows the details of the moisture and temperature sensor installation. The sensors' data was collected from the data loggers placed at the site.

Figure 3-2 Steps of Lysimeter Construction (a) Embankment construction, (b) Embankment excavation, (c) Geomembrane placement (d) Percolation collection system installation, (e) Geo-composite drain placement, (f) Compacted clay placement, (g) Topsoil placement, (h) Vegetation and erosion mat placement, (i) ET cover lysimeter after completion

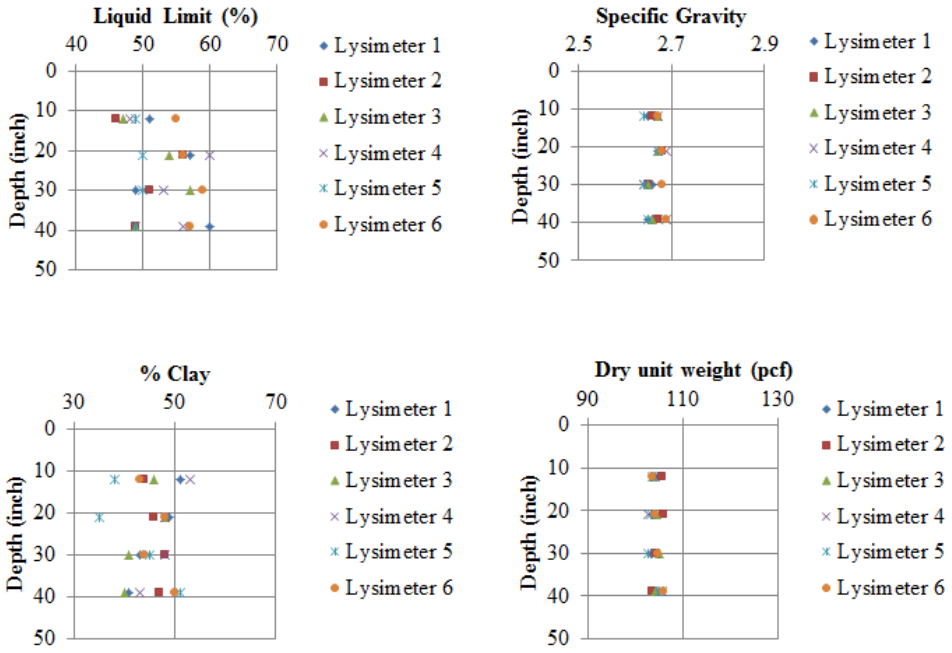

Figure 3-3 ET cover soil properties for different lysimeters at different depths

Table 3-1 ET cover soil characterization summary

Liquid limit (%)	46-60
Dry unit weight (pcf)	102.57-105.52
Specific gravity	2.64-2.69
% clay	43-53
USCS classification	CH-CL

Table 3-2 Vegetation mixes used in the ET lysimeters

Lysimeter	**Vegetation Details**
1 and 4	Mix of Native Trail, Perennial Wildflower Mix, and Caliche
2 and 5	Mix of Upland Switchgrass, Perennial Wildflower Mix, and Caliche
3 and 6	Common Bermuda Grass

Table 3-3 Moisture and temperature sensors installed in the ET cover soil

	Depth (inch)
Installed Moisture and Temperature Sensors in each ET Cover lysimeters (1, 2, 3, 4, 5 and 6)	12
	21
	30
	39

Data collection

From January 2015 to December 2016, the ET lysimeters were monitored monthly, using ERI and soil moisture sensors. For this study, 2D dipole-dipole resistivity imaging was used along the ET cover site. The dipole-dipole array was used because it provides low electromagnetic coupling and high sensitivity in a horizontal direction, which is efficient in field surveys (Loke, 2000; Kibria, 2014). Electrodes were located at fixed positions along the 81 foot length of the lysimeters, with 3 foot spacing and 28 electrodes in each line. The idea was to obtain the soil resistivity from two lysimeters, by doing one test. Therefore, one lysimeter in the flat section (2% slope) and another lysimeter in the slope section (25% slope) were investigated by a single resistivity line. Figure 3-4 shows the locations of the soil moisture sensors and the ERI profile along the lysimeters for a single investigation in January 2015 (Appendix-A shows all the profiles).

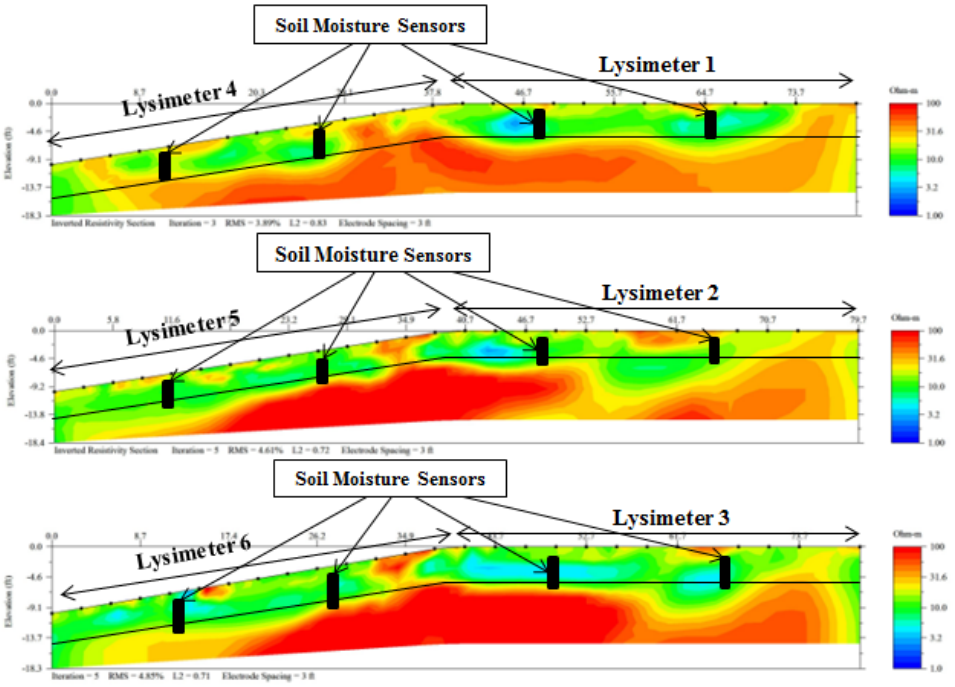

Figure 3-4 ERI profile along the lysimeters showing moisture sensor locations

Resistivity equipment manufactured by Advanced Geosciences Institute (AGI) was used for the resistivity tests in the field. The equipment has a programmable eight-channel option, which assisted in conducting the tests in a shorter time. Furthermore, the dipole-dipole array was used for the tests to obtain better resolution and achieve more accurate quantitative results. Earth Imager 2D software package (version 2.4.2) (AGI, 2008) was utilized to process the collected raw resistivity data. The imaging software uses a forward modeling subroutine to calculate the apparent resistivity values. The apparent resistivity then uses an iterative resistivity inversion algorithm to convert the apparent resistivity values into inverted resistivity values. After an initial inversion, relative data misfit, limited to 20%, was tested for all of the ERI profiles. (In most cases, the misfits did not cross 10%) Smooth inversion modelling, terrain correction with damped mesh transform, average chargeability starting model, and a horizontal-vertical ratio of 0.2 were used for the data analysis. A maximum of four iterations were performed, and the RMS error reduction was kept within 5%. The forward modelling was carried out using the finite element method with Cholesky decomposition as the forward equation solver, with two mesh divisions, a thickness incremental factor of 1.1, and a depth factor of 0.7. Non-linear least squares optimization was performed, and a resistivity log was obtained along the soil moisture locations to extract quantitative values.

For the field investigation, electrodes were placed within a foot from the moisture sensors in the ET cover soil, thus providing resistivity at different locations and at different depths. The calculated resistivity values were corrected for soil temperature. According to Campbell et al., 1948, the activity of the ions present in the soil varies with changes in temperature; therefore, resistivity measurements should be compared at a standardized temperature. On the investigated timescale, electrical resistivity of soil may also vary due to temperature. Friedman (2005) found the effect to be about 2% per 1 °C.

Depending upon the moisture and temperature sensors installed in the cover soil, the temperature data can be divided into three ranges. For this research, the soil temperature range was from 10.1^{o}C to 12.1^{o}C during the winter season (from January to May). During the summer season (from June to October), the soil temperature range was from 14^{o}C to 35.9^{o}C, after which it decreased to 9.5^{o}C to 18^{o}C. The variable temperature range in the field suggests that the resistivity results require temperature correction to represent the results uniformly throughout the year. The temperature data obtained from the sensors was used to perform the temperature correction of the resistivity value obtained from field testing. Therefore, the measured resistivity was corrected at 25°C temperature by using the following equation (3-1) (Samouelian et al., 2005):

$$\rho = \rho T * (1 + \alpha * (T - 25°C) \quad (3\text{-}1)$$

Where, T = temperature (°C), ρT = electrical resistivity measured at temperature T, ρ is electrical resistivity at the reference temperature of 25 °C, α = correction factor (0.0202).

The soil moisture and temperature sensors installed at different depths of the lysimeters employed an oscillator with a 70 MHz frequency to measure the dielectric permittivity. The accuracy level of ± 0.03 m^3/m^3 was based on Topp's equation (Topp et al., 1984). The soil-specific calibration performed in the lab resulted in a similar accuracy level. The 5TM moisture sensor uses a surface-mounted thermistor to measure the soil temperature within a range of - 40 to 60^{o}C, within a resolution of 0.1^{o}C, and at an accuracy level of ± 1^{o}C. Soil moisture and sensor data were collected monthly from the data logger (Em 50 by Decagon Inc., USA) placed on the site, and were analyzed according to the different lysimeters and different depths.

DATA ANALYSIS

The soil moisture sensor data and ERI test results were analyzed using standard univariate summaries. Robust non-parametric statistical components (mean, median, first and third quartile range, and the ratio of inter-quartile range and median) were calculated, as extreme values of the measured components have lower sensitivity, and there are no restrictions on the data distribution of their estimated values.

Correlation analysis

A correlation analysis, including the determination of the parametric Pearson's correlation coefficient, r, was conducted to provide insight into the relationship between the ERI and soil moisture. This particular correlation coefficient measures how closely two sets of data are related. It can be used for variables which are continuous in nature and have a normal distribution and homogeneity of variance over the measured data. Few studies have been conducted using these coefficient correlations to analyze field scale measurements of soil moisture and electrical resistivity of soil. The calculation of Pearson's correlation coefficient enables possible comparisons of previously published studies with current investigations. Confidence intervals were calculated at 95% probability (C.I 95%) to assess the significance of the r values. The previous relationships suggest a negative correlation between the variables, for which the one-tailed t-test was applied. For calculation of upper and lower 95% confidence intervals, a two-tailed t-test was also performed (Jeyaratnam, 1992; Calamita et al., 2012). To establish a more concrete correlation, an addition test on the significance was carried out using the non-parametric Spearman method. As the probability distributions were not normal for the measured data sets, this robust method exhibited the strength of the monotonic relationship presented. The Spearman method was applied only for electrical resistivity

versus soil moisture, as it would have the same value for natural log resistivity tests were performed of resistivity.

Regression analysis

Three different models were chosen (linear, power, and exponential), and regression analysis was carried out to fit the field scale experimental data, as shown in the following equations:

$$R = a + b\theta \quad (3\text{-}2)$$

$$R = a\theta^{b} \quad (3\text{-}3)$$

$$R = e^{a\theta+b} \quad (3\text{-}4)$$

Where R is the electrical resistivity (Ohm-m), θ is the volumetric soil moisture (m^3/m^3), a and b are the two regression model coefficients which are to be estimated. It is noteworthy that Eq. (3-2) is similar in form to Archie's law.

Selection of the suitable model for data fitting was determined by residual analysis in both graphical and numerical forms, and finally by the accuracy of the fitted model. In addition, the root mean square error, RMSE, was calculated between the observed and predicted soil electrical resistivity for quantification of the calibration accuracy between soil electrical resistivity and soil moisture. To further strengthen the analysis, each linear model was subjected to an F test to assess the overall significance of the regression and a t-test to assess the significance, both for linear and non-linear models of the estimated parameters. The application of both of these tests, which are based on the ratio between the variance and the variance between the residuals explained by the regression model, is desired for any statistical regression modelling. The statistical procedures and the tests for this investigation were performed using the RStudio version 1.0.136 (R Development Core Team, 2009), which is open-source statistical software.

RESULTS AND DISCUSSION

In this study, soil electrical resistivity, using field resistivity, and soil moisture content, using soil moisture sensors, were measured in six different ET lysimeters at different depths. To investigate the competency of electrical resistivity in estimating the soil moisture in the ET lysimeters, the data was grouped by lysimeter, depth, and the type of soil condition. Each group was analyzed separately. The lysimeter data included the soil electrical resistivity and soil moisture for a single lysimeter over the period of investigation (from January 2015 to December 2016). Each of the six lysimeters (1, 2, 3, 4, 5 and 6) had its own dataset. The depth wise datasets were compiled by determining the soil electrical resistivity and soil moisture at different depths for each lysimeter and merging the data sets for each depth (39 inches, 30 inches, 21 inches, and 12 inches from the surface). For the 12-inch depth, the data set was separated by year, 2015 and 2016, to represent the condition of non-vegetation and vegetation, respectively. The investigation of soil electrical resistivity and soil moisture performed on the basis of the soil condition was a novel approach. The differences in the soil conditions were analyzed on the basis of vegetated soil (vegetated clay) and non-vegetated soil (non-vegetated compacted clay), with the differences being attributed to the presence of plant roots in the ET cover soil. Plant roots extended 12 inches into the soil by the end of year 2015 and did not extend more than 20 inches into the cover soil during the period of investigation. Therefore, the 12-inch data sets were considered non-vegetated clay from January 2015 to December 2015 and vegetated clay from January 2016 to December 2016. The other depths, of 21 inches, 30 inches, and 39 inches, were considered the compacted clay datasets. It is worth mentioning that the separation of the data set on the basis of soil condition provided a crucial difference in the soil electrical resistivity in both vegetated and non-vegetated conditions. An additional analysis was conducted, using the

combined datasets from all of the lysimeters, to smooth out the small scale variabilities in the data sets for the lysimeters. Correlation and regression analyses were conducted on both linear and non-linear relationships.

Soil Electrical Resistivity Versus Soil Moisture Sensor Measurements

Preliminary analysis of the obtained data sets was conducted by calculating the key statistical descriptors of the resistivity and soil moisture sensor data for the data sets grouped by different lysimeters, different depths, and soil conditions. Table 3-4 (a), (b) and (c) exhibits the summary of the analysis. In Table 3-4 (a) (data grouped by different lysimeters) it can be observed that the soil moisture shows lower variability than the soil resistivity. The range of coefficient of variation (CV) for soil moisture is 0.24 to 0.43 (average CV = 0.29), whereas CV for soil resistivity is from 0.53 to 0.96 (average CV = 0.62). Lysimeter 6 showed the highest variability in resistivity and soil moisture with CV equal to 0.96 and 0.46, respectively. Table 3-4 (b) shows the statistical descriptors for data grouped by different depths, and it is evident that the CV values for the soil moisture did not show any substantial difference, with the CV ranging from 0.2 to 0.31 (average CV = 0.26). However, soil resistivity showed a higher increase in CV when separated by depths. The range of CV increased from 0.60 to 0.92 (average CV = 0.79). To acknowledge the differences in the soil conditions, as previously mentioned in other studies (Entin et al., 2000; Brocca et al., 2007; Amato et al., 2009), the distinctive group of data set by soil condition was considered, as shown in Table 3-4 (c). The CV decreased for soil moisture for both compacted clay and vegetated clay, with values of 0.31 and 0.18. The CV for soil resistivity reduced to 0.89 and 0.72. The non-parametric statistics such as the median, inter quartile range (IQR), and their ratio were also used to support and confirm this variation. The higher variation for the resistivity values can be

attributed to the fact that soil moisture and resistivity are related by an exponential law, as seen from previous studies.

Soil and vegetation characteristics have a substantial influence on soil resistivity, for which depthwise resistivity shows higher variability. However, similar meteorological forces, such as rainfall and evapotranspiration, can cause comparatively smaller variations of soil resistivity within each lysimeter. A similar interpretation can be assumed for soil moisture. Therefore, data grouped by soil conditions considers the difference in soil and vegetation characteristics, which designates the soil electric and condition anomalies (Amato et al. 2008; Lazzari 2008). The correlation analysis shown below describes the variability configuration of the soil moisture and soil resistivity. Limited variability in data sets is expected to provide lower correlation values, and will be discussed in detail in the following section. The probability distribution, using the Pearsons's normality tests, showed that the soil moisture was almost normally distributed, whereas the resistivity values were rightly skewed. However, applying the natural logarithm transformation to the resistivity values reduces the skewness, bringing the resistivity data closer to a normal distribution.

Table 3-4 Summary of descriptive statistical parameters for soil resistivity and soil moisture (a) data grouped by lysimeters (b) data grouped by depth and (c) data grouped by soil condition (SD: standard deviation, CV: coefficient of variation, Min.: minimum, Qu.: quartile, IQR: interquartile range

Site	Mean	SD	CV	Min.	1st Qu.	2nd Qu.	3rd Qu.	Max.	IQR	IQR/Median	No. of Data
(a) Electrical resistivity (Ωm)											
Lysi.1	14.17	7.81	0.55	3.73	8.91	13.22	18.07	50.9	9.15	0.69	114
Lysi.2	14.99	7.99	0.53	1.78	10.6	12.93	16.45	50.8	5.84	0.45	124
Lysi.3	14.52	9.31	0.64	3.73	8.86	13.23	18.23	71.6	9.37	0.71	109
Lysi.4	25.58	14.3	0.56	3.65	14.87	22.19	33.66	67.0	18.8	0.85	77
Lysi.5	16.70	8.92	0.53	5.72	10.98	15.23	18.88	55.7	7.90	0.52	78
Lysi.6	30.17	29.2	0.96	1.76	13.21	21.47	36.87	144.	23.6	1.10	92
Soil moisture content (%)											
Lysi.1	33.96	8.27	0.24	11.4	29.8	34.70	39.02	51.1	9.21	0.26	114
Lysi.2	32.45	8.98	0.27	10.4	26.55	31.44	38.02	65.8	11.4	0.36	124
Lysi.3	33.98	8.4	0.25	8.38	29.68	34.59	39.39	51.1	9.70	0.28	109
Lysi.4	25.75	9.26	0.36	9.75	19.44	25.58	31.82	55.3	12.3	0.48	77
Lysi.5	30.81	7.52	0.24	12.5	26.54	30.39	35.99	47.3	9.45	0.31	78
Lysi.6	26.61	11.4	0.43	0.51	20.14	28.29	33.46	60.1	13.3	0.47	92
(b) Electrical resistivity (Ωm)											
Depth											
39 in.	16.58	14.43	0.87	1.76	8.96	12.87	18.4	118.	9.48	0.74	117
30 in.	16.91	16.0	0.94	4.22	9.42	12.73	18.71	143	9.29	0.73	145
21 in.	20.14	17.23	0.86	4.1	10.9	15.95	22.36	144	11.3	0.71	135
12 in.(2015)	20.42	12.25	0.60	5.68	14.2	18.3	26.8	51.9	12.6	0.68	67
12 in.(2016)	20.88	14.99	0.72	1.78	13.41	17.2	25.44	128.	12.0	0.69	130
Soil moisture content (%)											
39 in.	30.00	9.44	0.31	1.83	24.86	30.66	35.41	60.1	10.5	0.34	117
30 in.	29.64	8.58	0.29	0.69	25.24	30.82	35.22	47.9	9.97	0.32	145
21 in.	26.39	8.62	0.33	0.50	20.48	26.78	31.96	45.6	11.4	0.43	135

Table 3-4 (continued)

12 in.(2015)	36.8	7.36	0.2	24.4	30.5	37.4	9.9	52.0	9.93	0.26	67
12 in. (2016)	38.55	7.13	0.18	21.8	33.89	38.93	43.10	65.8	9.22	0.24	130
(c) Electrical resistivity (Ωm)											
Com. Clay	17.91	16.04	0.89	1.76	10.11	13.72	20.32	144.	10.2	0.74	464
Veg. Clay	20.88	14.99	0.72	1.78	13.41	17.20	25.44	128.	12.0	0.70	130
Soil moisture content (%)											
Com. Clay	28.65	8.98	0.31	0.50	22.99	29.56	34.53	60.1	11.5	0.39	464
Veg. Clay	38.55	7.13	0.18	21.8	33.89	38.93	43.10	65.8	9.22	0.24	130

Correlation Analysis Between Soil Moisture and ERI

Figure 3-5 shows all of the data points collected for the soil resistivity and soil moisture measurements, in all the lysimeters, throughout the investigation period from January 2015 to December 2016. Figure 3-5 (a) shows the resistivity versus soil moisture and Figure 3-5 (b) shows the natural logarithmic resistivity versus soil moisture. A correlation analysis was performed to establish a general relationship between the datasets (Table 3-5).

Initially, the Pearson's correlation coefficient was estimated to show the relationships, if any, between the data sets. All 594 data points subjected to Pearson's correlation coefficient, r, resulted in an estimated value equal to 0.67 (absolute value of r has been used). However, when the resistivity value was transformed, using the natural logarithm, the coefficient increased to 0.784. This implies that the relationship between soil resistivity and soil moisture is more suitable in a non-linear form. Correlation analysis for the different lysimeters showed similar coefficients, ranging from 0.657 to 0.754 with a mean of 0.694. However, the natural logarithm applied to the resistivity data substantially increased the coefficient with a range of 0.649 to 0.796 and a mean of 0.740. Interesting results were observed when depthwise data was analyzed. The r value increased when the datasets were analyzed depthwise. The average r value for the depthwise dataset increased to a range of 0.752 to 0.823, with a mean of 0.781. In addition, with the application of the natural logarithm, the r value further increased to a range of 0.758 to 0.970 with a mean of 0.891, thus suggesting a strong correlation between soil resistivity and soil moisture at different depths.

Figures 3-5 and 3-6 illustrates the measured soil resistivity and soil moisture data grouped by lysimeter and depth, respectively. The segregated clusters of data for different lysimeters represent the variability of measured data at various depths. This implies that the variability of a soil condition due to vegetation characteristics, soil compaction levels, and soil temperatures has a significant effect on the correlation. Plant roots or root masses cause the soil compaction level to reduce (Hossain et al., 2017), which in turn varies the resistivity data at different depths. Therefore, when the depthwise data is analyzed (Figure 3-5), it can be seen that the measured data shows similar trends for depths of 39 inches, 30 inches, 21 inches, and 12 inches (2015), whereas the power law coefficient for the resistivity and soil moisture is higher at 12-inch depth, and similar moisture content resistivity is higher compared to all other depths. Another important consideration for this difference in data sets for different lysimeters and different depths is the established influence of soil temperature on soil resistivity. When depthwise data is considered and depthwise temperature correction is applied, a better correlation is obtained. Calamita et al., 2012 noted the significant effect of soil temperature in his studies. Therefore, the grouping of data sets after soil temperature correction has been a major breakthrough in this study.

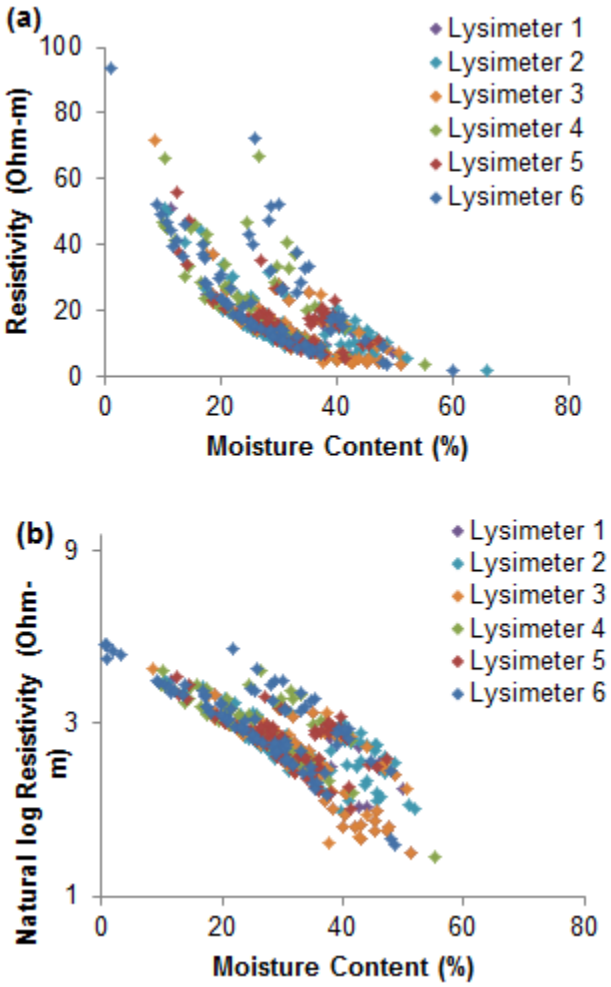

Figure 3-5 Soil resistivity and soil moisture relationship of all the measured data for this investigation (a) Temperature-corrected resistivity vs. soil moisture (b) Temperature-corrected natural log resistivity vs. soil moisture

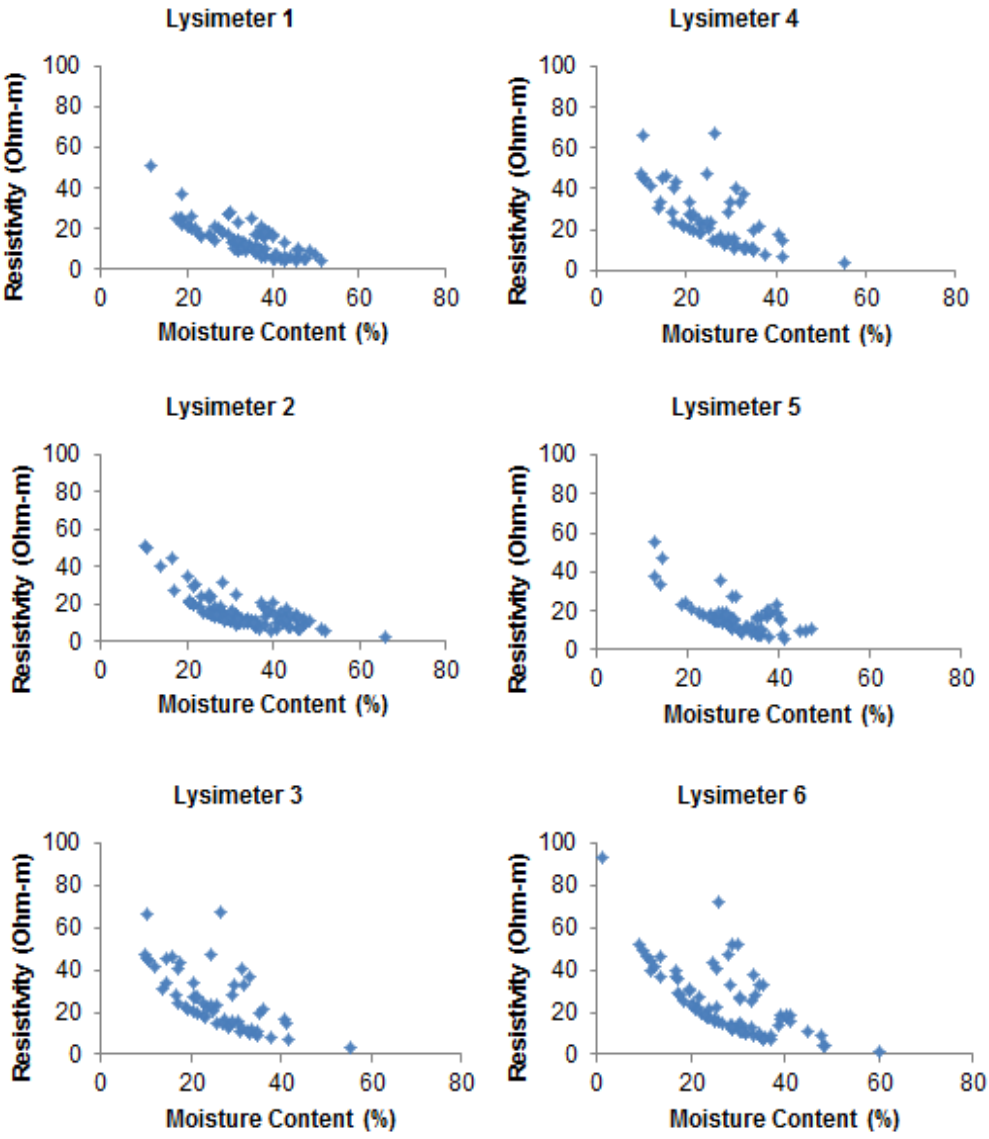

Figure 3-6 Measured soil resistivity and volumetric soil moisture data grouped by lysimeters

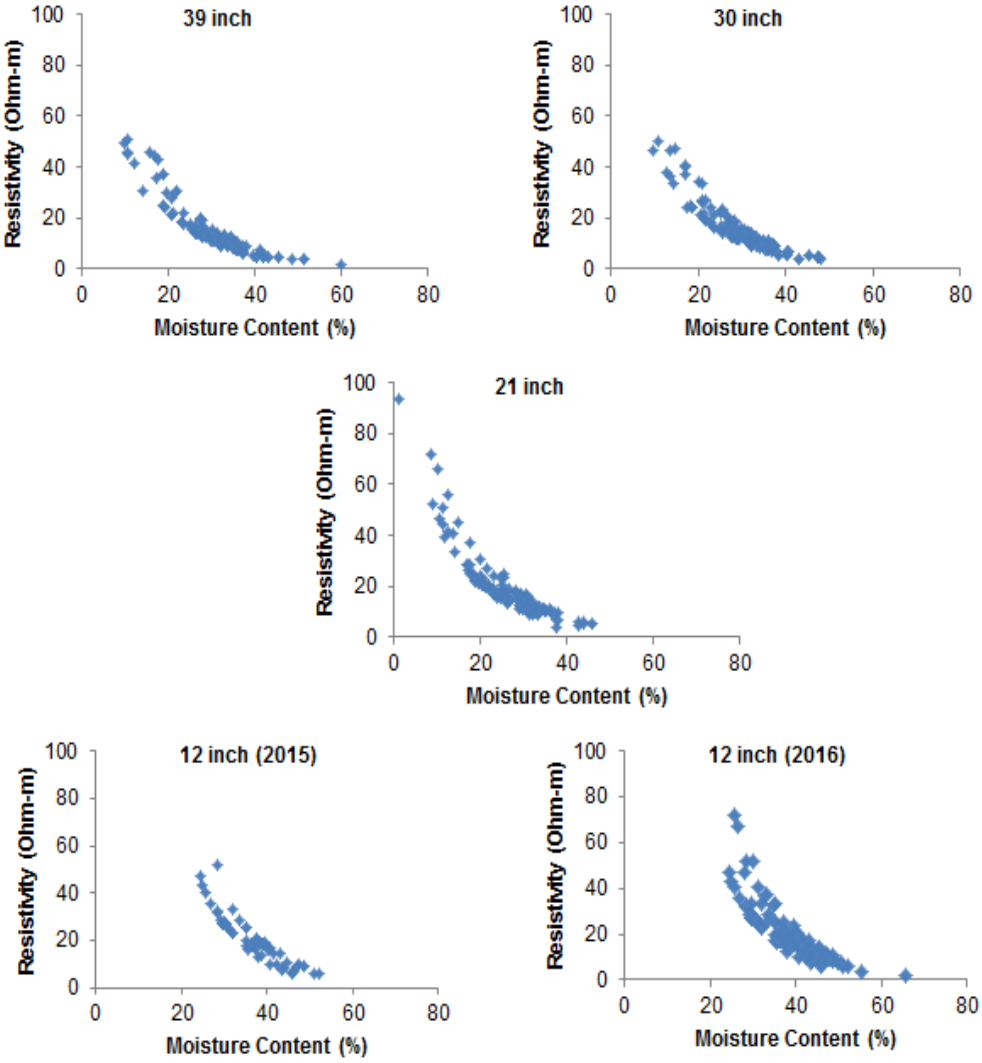

Figure 3-7 Measured soil resistivity and volumetric soil moisture data grouped by different depths

Table 3-5 Correlation analysis between soil resistivity and volumetric soil moisture for different data sets measured in this investigation (r*: Spearman correlation coefficient, r: Pearson's correlation coefficient, C.I. 95%: 95% confidence interval, # of points: sample size)

	Sampling Type	Resistivity			Ln Resistivity		# of Points
		r*	r	C.I. 95%	r	C.I. 95%	
All Lysimeters at all depths	All data points	-0.725	-0.670	-0.715 to -0.620	-0.784	-0.815 to -0.748	594
Lysimeter	Lysi.1	-0.733	-0.754	-0.830 to -0.651	-0.770	-0.841 to -0.672	114
	Lysi.2	-0.687	-0.673	-0.767 to -0.576	-0.753	-0.820 to -0.665	124
	Lysi.3	-0.714	-0.723	-0.807 to -0.611	-0.753	-0.828 to -0.651	109
	Lysi.4	-0.716	-0.664	-0.788 to -0.488	-0.759	-0.851 to -0.621	77
	Lysi.5	-0.513	-0.657	-0.774 to -0.497	-0.649	-0.769 to -0.486	78
	Lysi.6	-0.725	-0.694	-0.789 to -0.566	-0.796	-0.862 to -0.703	92
Depth	39 in.	-0.967	-0.823	-0.874 to -0.754	-0.970	-0.979 to -0.958	117
	30 in.	-0.955	-0.789	-0.844 to -0.719	-0.962	-0.973 to -0.948	145
	21 in.	-0.909	-0.752	-0.817 to -0.668	-0.758	-0.818 to -0.669	135
	12 in.(2015)	-0.926	-0.854	-0.878 to -0.758	-0.888	-0.936 to -0.697	67
	12 in.(2016)	-0.924	-0.762	-0.826 to -0.678	-0.933	-0.952 to -0.906	130
Soil Condition	Com. Clay	-0.957	-0.802	-0.835 to -0.764	-0.964	-0.970 to -0.956	464
	Veg. Clay	-0.924	-0.762	-0.826 to -0.678	-0.933	-0.952 to -0.906	130

A comparison of the data obtained from the lysimeters and the depthwise data reveals that the depthwise data shows lower variability due to higher sets of data used. In addition, when separated by soil condition, the variability further reduces with r values of 0.964 and 0.933 and confidence intervals of 0.97 to 0.956 and 0.952 to 0.906 for compacted clay and vegetated clay, respectively. Pearson's coefficient provides information on the linear relationship between the two variables. As seen from the analysis, natural logarithm transformation provides better correlation for measured data separated by soil conditions. The correlations obtained are slightly better than previous field scale studies by Calamita et al., 2012. The lysimeters were situated within an area of 900 m^2 and were built with cover soil from same location. Thus, the number of factors influencing the correlation were limited to the presence of vegetation, which relates to the soil compaction level and the soil temperature. Further analysis was carried out by estimating a sturdier test coefficient, using the Spearman method (Table 3-5). The Spearman method measures the strength of the linear relationship between the paired data, which further supports the correlation calculated by using the Pearson's coefficient. The r* calculated for different groups revealed that the depthwise data is strongly correlated by a negative monotonic relationship.

Regression Model Development for Soil Moisture and ERI

A regression model was fitted to assess the accuracy of the measured soil resistivity and soil moisture data. Considering models suggested by previous studies (Zhou et al., 2001; Zhu et al., 2007; Brunet et al., 2009; and Kibria, 2014), an exponential relationship was fitted to the different groups of data sets (Table 3-6). Regression analysis of all of the data resulted in a model with coefficient of determination, R^2 value of 0.61. However, separating the data sets into different groups yielded better fitted models. The fitted models did not produce strong models for the group of lysimeters, which had

an R^2 value ranging from 0.42 to 0.63. In addition, the RMSE values were closer to 0.5 for natural logarithm resistivity value, ranging from 0.342 to 0.483. This implies that the model was unable to effectively estimate the field scale moisture. Further model fittings, using the depth wise group data, showed promising results. The R^2 value for depth wise data increased to a range of 0.87 to 0.94, and the RMSE values decreased to a range of 0.162 to 0.211. Moreover, as the depth wise data implies, for the depths of 39 inches, 30 inches, 21 inches, and 12 inches (2015), where the soil conditions were similar (no vegetation), the fitted models yielded similar coefficients (a and b) and RMSE. Therefore, grouping the data sets for these depths on the basis of soil condition produces a general model for soil resistivity and soil moisture with an R^2 value of 0.92 and RMSE value of 0.168. At a depth of 12 inches (2016), the vegetated clay soil generated a fitted model with a R^2 value of 0.87 and RMSE value of 0.211.

Figure 3-8 shows the relationship between soil resistivity and soil moisture, depending on the soil condition of compacted clay and vegetated clay. The fitted model for compacted clay are shown in table 3-7.

Based on the analysis, it can be concluded that the depth wise assessment of soil resistivity and soil moisture models is better in terms of estimating soil moisture in the field. When separated by soil conditions, the models provided a more accurate assessment, showing that the effect of vegetation is significant when considering these kinds of field scale models. Laboratory results may yield stronger models, as factors influencing the measured data in the field are not under controlled conditions (Pozdnyakova, 1999).

Table 3-6 Regression analysis between soil resistivity and volumetric soil moisture for different data sets measured in this investigation (SE: standard errors, C.I. 95%: 95% confidence interval of regression parameters, RMSE: root mean square error, R^2: coefficient of determination, SD (MC): standard deviations of soil moisture measurements, SD R: standard deviation of resistivity measurements, N: # of samples)

Site	a	SE (a)	b	SE (b)	a (C.I. 95%)	b (C.I. 95%)	RMSE (ln Ohm-m)	R^2	SD (MC)	SD (R)	N
All Lysimeters at all depths											
All data points	-0.051	0.002	4.30	0.058	-0.055 to -0.048	4.19 to 4.42	0.387	0.61	15.83	9.56	594
Lysimeters											
Lysi.1	-0.051	0.005	4.25	0.155	-0.06 to -0.042	3.94 to 4.55	0.349	0.59	8.27	7.81	94
Lysi.2	-0.039	0.003	3.85	0.103	-0.045 to -0.033	3.65 to 4.05	0.302	0.56	8.98	7.99	124
Lysi.3	-0.052	0.005	4.28	0.163	-0.062 to -0.043	3.96 to 4.61	0.382	0.57	8.4	9.31	96
Lysi.4	-0.049	0.006	4.34	0.155	-0.06 to -0.037	4.03 to 4.64	0.383	0.58	9.26	14.3	57
Lysi.5	-0.039	0.006	3.91	0.179	-0.05 to -0.028	3.56 to 4.27	0.342	0.42	7.52	8.92	68
Lysi.6	-0.056	0.005	4.56	0.134	-0.065 to -0.047	4.30 to 4.83	0.483	0.63	11.4	29.2	87
Depth											
39 in.	-0.069	0.0016	4.642	0.050	-0.072 to -0.066	4.54 to 4.74	0.162	0.94	9.44	14.43	117
30 in.	-0.068	0.0016	4.627	0.049	-0.071 to -0.065	4.52 to 4.725	0.165	0.92	8.58	16.0	145
21 in.	-0.065	0.0017	4.527	0.049	-0.069 to -0.062	4.43 to 4.622	0.173	0.91	8.62	17.23	135
12 in.(2015)	-0.067	0.0016	4.632	0.051	-0.068 to -0.064	4.45 to 4.644	0.164	0.88	7.36	12.25	67
12 in.(2016)	-0.077	0.0026	5.837	0.103	-0.082 to -0.072	5.63 to 6.04	0.211	0.87	7.11	14.99	130
Soil Condition											
Com. Clay	-0.067	0.0009	4.593	0.0283	-0.069 to -0.066	4.54 to 4.65	0.168	0.92	8.98	16.04	396
Veg. Clay	-0.077	0.0026	5.837	0.103	-0.082 to -0.072	5.63 to 6.04	0.211	0.87	7.13	14.99	130

Table 3-7 Developed Model for different soil condition

Model	Soil Condition
$R = e^{-0.067\theta+4.593}$	Non-vegetated Clay
$R = e^{-0.077\theta+5.837}$.	Vegetated Clay
Where, R is electrical resistivity (Ohm-m) and θ is the volumetric moisture content (%)	

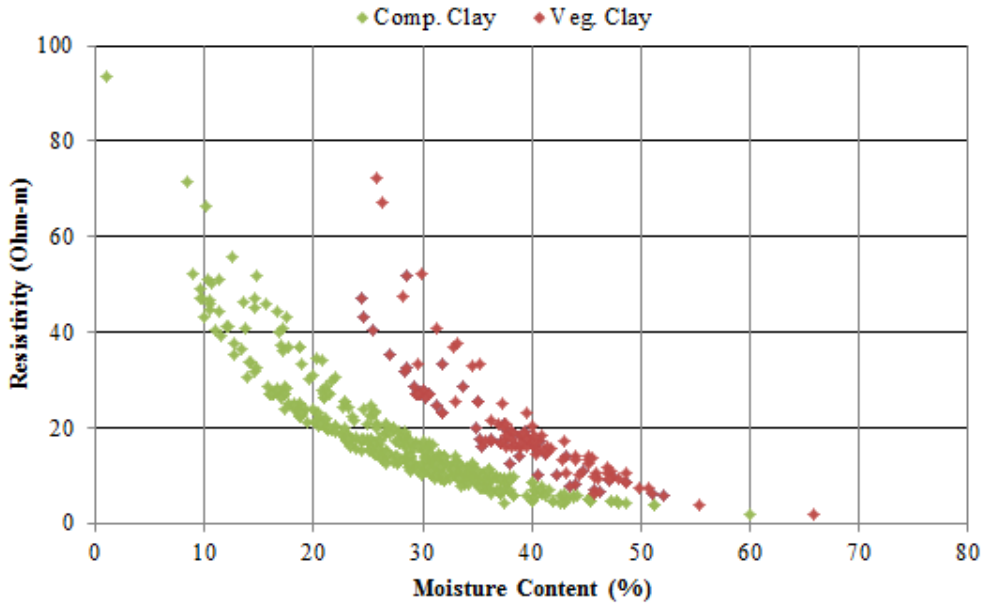

Figure 3-8 Relationship between Soil Resistivity and Volumetric Soil Moisture for Compacted clay and vegetated clay

Comparison with Established Model and Proposed Modified Model

Moisture content is one of the major properties of soil that can be detected by ERI. This is because, along with other factors, soil resistivity changes with the presence of moisture (Kibria and Hossain, 2015). Kibria, 2014 developed a two parameter MLR

model based on laboratory investigation and the current models proposed are compared with the established model in the following section.

The two-parameter model was R^-0.75 = -0.13063 + 0.00304* S_r + 0.00387* CEC, where R is the soil resistivity in Ohm-m, S_r is the degree of saturation in %, and CEC is the cation exchange capacity in cmol+/kg. The degree of saturation obtained from the field study was plotted with the results with the equation developed by Kibria, 2014. Figure 3-9 (a) shows the comparison between non-vegetated clay and the two parameter model. The bands in the graph represent the 20% error margin. The variation was found to be a maximum of 20%. However, more than 80% data were within 10% error band. It needs to be mentioned that the equation proposed by Kibria, 2014 was obtained by laboratory investigation on different types of compacted clay. Figure 3-9 (b) shows the comparison of the two-parameter model with the field scale model for vegetated clay. It can be observed that there was a shift in the line for the vegetated clay model. With an R^2 value of 0.8864, the two-parameter model shifted by a multiplication factor of 1.4236, and an additional factor of -70.17 that can predict the degree of saturation. Due to the presence of plant roots, the shift in the model is understandable, as the two-parameter model did not consider the effects of plant roots. Therefore, a correction factor added to the established equation enables the estimation of the degree of saturation in vegetated cover soil.

Table 3-8 Established and proposed model for non-vegetated and vegetated cover soil respectively.

Established model for non-vegetated clay	**Modified model for vegetated clay**
Sr = (14.35204*CEC^-1.5 + R^-0.25 - 0.43398)/0.00309	Sr = [(14.35204*CEC^-1.5 + R^-0.25 - 0.43398)/0.004398]+70.17
where, R = electrical resistivity (Ohm m), Sr = degree of saturation (%), CEC = cation exchange capacity (cmol+/kg).	

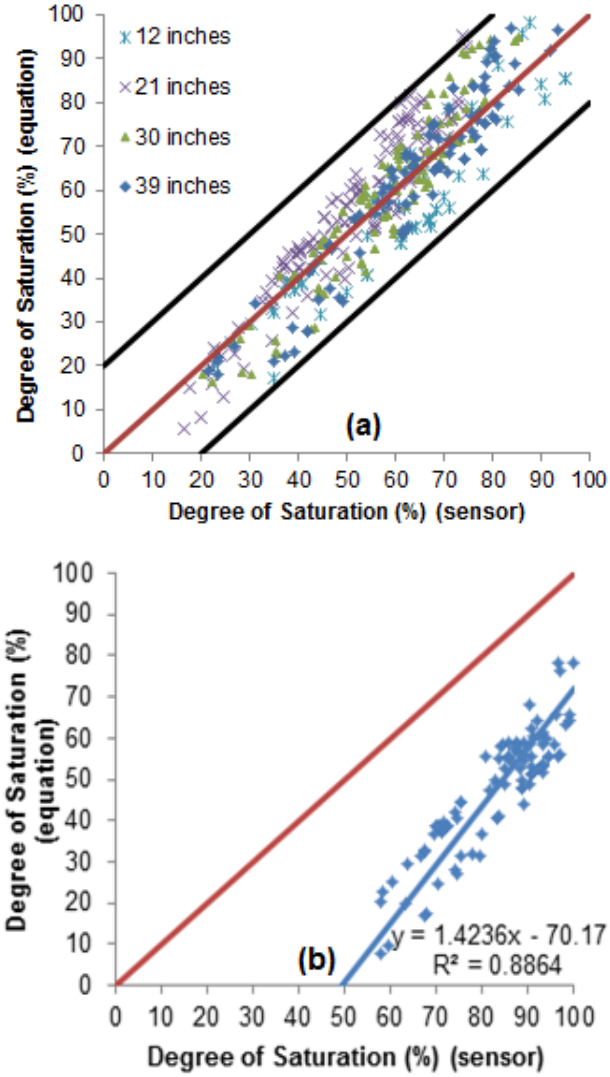

Figure 3-9 Comparison of present study with two-parameter model (a) non-vegetated clay, (b) vegetated clay

SUMMARY AND CONCLUSION

In this study, the competence of soil resistivity for soil moisture estimation was tested at different scales. The soil moisture sensors were installed and the soil resistivity

measurements were conducted in six ET cover lysimeters, and the data was grouped by lysimeters, different depths, and different soil conditions (compacted clay and vegetated clay). Based on the results of the analysis, the following conclusions can be drawn:

(1) Significantly higher variability was observed in electrical resistivity measurements compared to the soil moisture sensors measurements in all of the grouped data.

(2) The spatial variability in the ERI data for the lysimeters was lower than the ERI data analyzes by depth..

(3) The linear relationship between soil moisture and soil resistivity was found to be considerably weaker, with an average coefficient of 0.694 for different lysimeters and an average of 0.781 for different depths. However, higher and steadier correlations were obtained when a natural logarithmic transformation was applied. The coefficient increased significantly and had a mean of 0.740 for different lysimeters and an average of 0.891 for different depths.

(4) Data grouped by soil condition resulted in higher coefficients, with a value of 0.964 for compacted clay and 0.933 for vegetated clay.

(5) A regression analysis established the relationship between soil resistivity and soil moisture, with the coefficient of determination value averaging 0.56 for the lysimeters and 0.91 for different depths. The relationship was more pronounced for depthwise data, and when the data grouped by soil condition was analyzed, the R^2 was equal to 0.92 for compacted clay and 0.87 for vegetated clay.

(6) Considering the overall analysis of data grouped by soil condition provides two field scale models most appropriate for ET cover lysimeters, where for non-vegetated clay the fitted model is $R = e^{-0.067\theta+4.593}$ and for vegetated clay the fitted model is

$R = e^{-0.068\theta+4.627}$. The results are in good accordance with previous studies which support the use of these models in ET cover lysimeters under similar field conditions.

(7) Inclusion of factor such as different soil conditions was a novel approach in this investigation and resulted in better field scale correlations.

(8) Comparison with established two parameter model showed promising result for the non-vegetated clay. About 80% data were within 10% error band. However, for vegetated clay modified model was proposed as a shift in the model value was observed for vegetated clay.

In conclusion, this study was a unique approach to determine soil moisture in evapotranspiration cover. Development of two separate models for vegetated and non-vegetated clay showed there is a considerable difference in soil resistivity depending on the soil condition. Further verification with established model generated good correlation for non-vegetated clay and a correction factor was added to the established model to generate a modified model for vegetated clay. Future studies are required to account for the factors that are influencing the soil resistivity in two different soil conditions.

Chapter 4

EVALUATION OF FACTORS INFLUENCING ELECTRICAL RESISTIVITY IN EVAPOTRANSPIRATION COVER SOIL

Hossain, M.I.[1], Hossain, M.S.[2]

[1]Graduate Research Assistant, Department of Civil Engineering, University of Texas at Arlington, 417 Yates Street, NH 119, Arlington, TX 76019, email: mdishtiaque.hossain@mavs.uta.edu

[2]Professor, Department of Civil Engineering, The University of Texas at Arlington, 416 Yates Street, NH 119, Arlington, TX 76019, e-mail: hossain@uta.edu

ABSTRACT

Alternative landfill final cover systems, or evapotranspiration (ET) covers, use the water balance technique to remove infiltrated water from the cover soil. The principle function of the ET cover is to store the infiltrated water until it is transpired by plants into the atmosphere, thus minimizing percolation. Hence, the determination of soil moisture in ET cover soil is important for assessing the performance of the cover. The ET covers can be separated by depth into two segments: vegetated and non-vegetated clay. Statistical analysis and regression model development were conducted by Hossain and Hossain, 2017[a] to estimate the soil moisture of ET cover soil, using electrical resistivity imaging (ERI). Two separate models were developed: one for vegetated and one for non-vegetated cover soil. This demonstrates the significant difference between conventional landfill covers and ET covers. Several researchers previously studied the ERI and soil moisture relationship for compacted clay. However, this study is unique for vegetated clay. As a non-destructive and inexpensive method, ERI is very efficient for determining the amount of soil moisture in both vegetated and non-vegetated soils. However, the generation of two different models requires understanding of the factors that influence the

ERI in the two different soil conditions. The ERI technique has not been previously applied to ET covers; therefore, closer investigation was necessary. Due to the presence of plant root systems, physical and chemical properties of cover soil might be affected, which could, in turn, influence the ERI results. Therefore, the objective of this study was to investigate the factors that influence ERI and are different for the two types of landfill cover soil: vegetated and non-vegetated.

For this investigation, a control section of vegetated and non-vegetated landfill cover, along with six vegetated lysimeter sections, were constructed in the City of Denton landfill in Denton, Texas. Field scale testing of ERI, soil compaction, soil nutrient variability, evapotranspiration, measurement of soil moisture and soil temperature were carried out, along with ambient climate monitoring, to determine how plant roots affect the ERI measurements. Qualitative analysis of data showed the variation of different factors in the field, and the use of ERI showed the comprehensive differences in vegetated and non-vegetated landfill covers. To address the difference in soil condition, the developed model for ERI and soil moisture were further validated in the control section.

INTRODUCTION

Final cover systems are designed and installed in landfills to alleviate any possible long-term risk that the landfilled waste may pose to the environment (USEPA, 2006). Additionally, these covers serve specific purposes, such as minimizing infiltration and further percolation of water into the waste, promoting surface runoff, controlling gas emissions and odors, and preventing erosion (Barnswell and Dwyer, 2010; USEPA, 2006). Conventional landfill covers are constructed with materials having low permeability to minimize downward migration of water through the cover; however, their construction and maintenance are expensive (Hauser, 2009). Evapotranspiration (ET) cover systems are becoming increasingly popular for their capacity to act as an efficient alternative that

satisfies the cover system performance requirements. ET cover systems are a natural and cost-effective alternative to conventional covers. They rely on the ET and the water storage capacity of soil to minimize infiltration into the waste, which allows them to act very similar to nature (Benson et al., 2002).This natural mechanism has a higher probability of a long life than a conventional cover. The primary purpose of an ET cover is to store the infiltrated water from rainfall in the cover soil and transpire the water through plants during drier periods of time (Barnswell and Dwyer, 2011; Benson et al., 2002). Although the actual designs of ET covers tend to be site specific and vary widely between regions, they all utilize locally available soils that have a relatively high water storage capacity and vegetation to increase evapotranspiration (Hakonson, 1997; Hauser et al., 2008; Dwyer, 2003). Lysimeters are typically installed to monitor the field performance of ET covers. They measure the water flowing through the bottom of the cover and may also be equipped with soil water monitoring sensors. They are commonly used as a secondary or indirect monitoring tool to verify the effectiveness of the lysimeters in terms of moisture storage and percolation (Malusis and Benson, 2006). The soil moisture sensors are typically placed at discrete locations and at different depths to provide information about the soil moisture availability.

Efficiently monitoring and maintaining an ET cover system is essential to preserving the integrity and effectiveness of the cover system for long-term use. However, the currently available non-destructive methods, such as moisture sensors, might be used to monitor the soil water storage only for discrete locations, which might overlook the overall performance of the covers (Schnabel et al., 2012). Therefore, alternative geophysical methods, such as electrical resistivity, which are capable of determining soil moisture in ET covers by considering the effect of vegetation, were employed by Hossain and Hossain, 2017[a]. They developed field scale models based on

the relationship between ERI and soil moisture by performing correlation and regression analyses which were capable of estimating cover soil moisture over a wide region. Two separate models were proposed: one distinctly for non-vegetated clay cover soil ($R = e^{(-0.067\theta+4.593)}$, $R^2 = 0.92$) and the other one for vegetated clay cover soil ($R = e^{(-0.077\theta+5.837)}$, $R^2 = 0.87$). The vegetated clay cover was considered to be the section up to which the plant roots extend, and the non-vegetated cover was considered to be the remaining depth of the cover, where no plant roots exist.

The differences in the proposed models were significant; however, no significant studies have been conducted to investigate the factors responsible for variation of ERI in the ET cover system. Several factors might be responsible for this difference. When compared to conventional cover systems, ET covers are newer, with inherent uncertainties associated with their performance. Laboratory investigations and a conventional bottom clay liner system study showed that ERI might be used to estimate moisture in non-vegetated compacted clay cover soil. However, in an ET cover system, the presence of vegetation might influence the physical and chemical properties of the soil, which may consequently affect the ERI result. (Amato et al., 2008). Plant growth is an important factor in the sustainability of an ET cover, as the infiltrated water is removed by the ET process (Hauser, 2009). Therefore, the ERI method will be studied in the field to assess the influence of physical and chemical variations in different soil conditions on the resistivity values. Since it is able to evaluate the amount of moisture in the cover soil, the ERI method might also be useful on a larger scale, to determine the moisture content in the field, resulting in soil instrumentation systems being superfluous.

The objective of this study was to investigate the effects of the factors that influence the ERI in vegetated and non-vegetated landfill covers. In order to perform this

investigation, a control section consisting of a vegetated and a non-vegetated cover soil were monitored along with six lysimeters in selected locations of the City of Denton landfill. Identification of the factors that influence the ERI in the ET cover system were an important addition to the study and aided in understanding the field scale models that were developed to estimate soil moisture in the cover soil, using ERI.

MATERIALS AND METHODOLOGY

Site Description

The ET lysimeter project selected for this study is situated in the City of Denton Landfill, TX, USA. Figure 4-1 shows the control section installed in the field. The control section study area has cover soil with a depth of 27 inches. The control section has dimensions of 20 feet by 10 feet, which is divided equally into two sections (20 feet by 5 feet each) of vegetated and non-vegetated cover soil. Both the sections had a slope of 2%. The vegetation used in the control section was Bermuda grass, which is a native plant in this region. The control section was also equipped with soil moisture and soil temperature sensors at different depths. Figure 4-1 shows the locations of the moisture and temperature sensors, which were placed at depths of 8 inches, 16 inches, and 24 inches. The sensors were placed in four different locations (B1, B2, V1, and V2), with two location in the vegetated sections (V1 and V2) and two locations in the non-vegetated sections (B1 and B2). Table 4-1 shows the location designations and depths of the sensors placed. To perform ERI tests along the fixed locations, electrodes were permanently placed 8 inches apart in the control section.

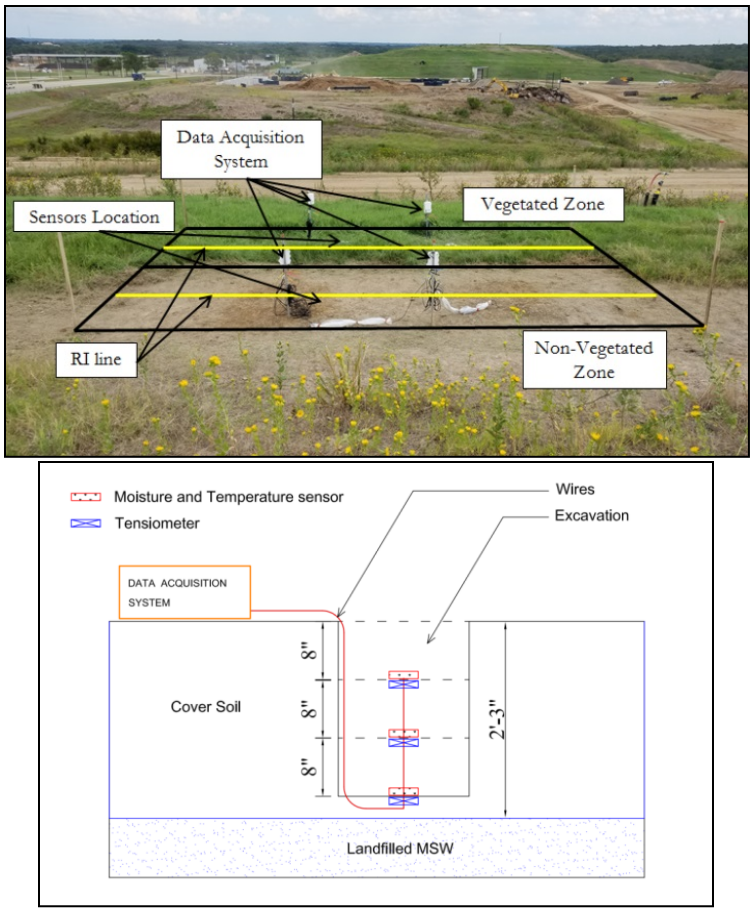

Figure 4-1 Pilot zone section and schematic of sensors placed in the field

Six lysimeters, placed in 3 feet of compacted clay underlying 1 foot of topsoil were monitored, as shown in Figure 4-2. Three of the lysimeters (1, 2, and 3) were placed in flat sections with a slope of 2%, and three (4, 5, and 6) were placed in the slope with 25% gradient. The dimension of each lysimeter was 40 feet by 40 feet. Percolation and runoff water collection tanks were placed along the west side of the lysimeters to determine their hydraulic performance. Details of the construction procedure were discussed by Hossain and Hossain, 2017[a]. A weather station was placed to measure the climatic conditions at the site during the monitoring period.

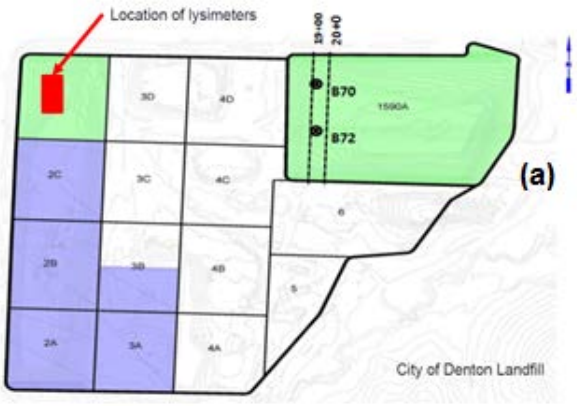

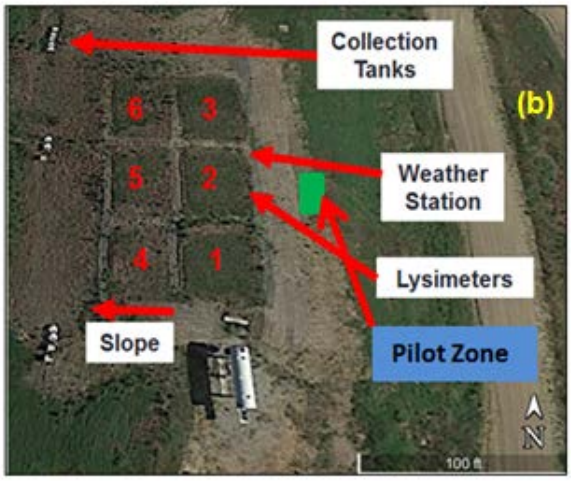

Figure 4-2 (a) Location of ET lysimeters in City of Denton landfill, TX, USA (b) Plan view of the lysimeters and the pilot scale study area.

Table 4-1 Location of moisture sensor placed in the pilot zone

Control Section Location	Designation	Moisture and Temperature sensors placed at depth
Non-vegetated cover soil	B1	8, 16, 24 inches
	B2	8, 16, 24 inches
Vegetated cover soil	V1	8, 16, 24 inches
	V2	8, 16, 24 inches

Field Investigation

Several tests were conducted in the field from May 2016 to April 2017 as part of an extensive field investigation. The year-long investigation revealed the variability of the factors influencing the moisture content and resistivity imaging in the field throughout different seasons. Both physical and chemical properties of soil were considered for investigation. The field tests included: (1) cover soil characterization, (2) soil compaction testing using a soil penetrometer, (3) soil pH monitoring, (4) soil temperature monitoring, (5) collection and analysis of soil moisture sensor data, and (6) electrical resistivity testing. An additional investigation was carried out using an evapotranspiration chamber to compare the amount of excess water that the vegetated and non-vegetated cover soils can transpire.

Cover soil samples were collected from different depths, and geotechnical characterization was carried out between the vegetated and non-vegetated clay cover soil of the control section. A soil penetrometer (Dickey-John compaction tester) was used to measure the soil compaction level in the field (Duiker, 2002). The compaction tester is a diagnostic tool that measures the extent and depth of subsurface compaction. Its use has been mostly confined to agricultural fields, where it is used to measure the compaction (Twum & Nii-Annang, 2015; Arriaga et al., 2011). This was the first time it was employed in landfill cover soil. The tester used in this study was produced under the technical specifications of the American Society of Agricultural Engineers. The penetrometer consists of a circular stainless steel cone, angled at 30 degrees, which is attached to a driving shaft and a pressure gauge. The compaction tester is comprised of two different cones, but for comparatively higher compacted soil in landfill covers, the cone with a base diameter of 0.505 inch is used. The instrument is arranged so that the tip is slightly wider than the driving shaft, thus limiting friction. The driving shaft is

graduated every 3 inches to measure the depth where the compaction is determined. The compaction level is measured from the pressure gauge, termed as cone index, which gives the reading in pounds per square inch. Figure 4-3 shows the compaction tester (a) and its application in the field (b). Table 4-2 summarizes the schedule of compaction testing conducted on the control section.

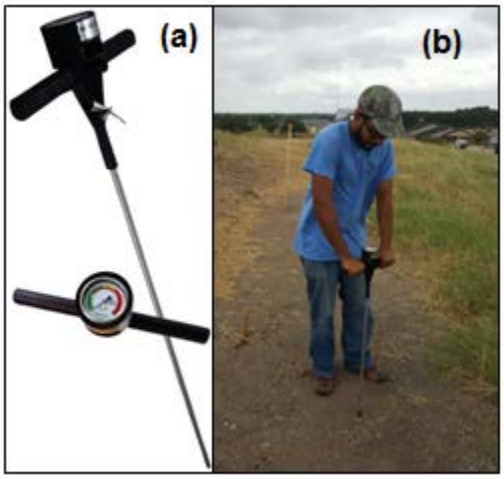

Figure 4-3 (a) Soil compaction tester; (b) Field compaction testing using soil compaction tester

Table 4-2 Summary of soil compaction testing in the control section

Location	Soil Condition	Depth (inch.)	Frequency/depth
B1	Non-vegetated	0, 3, 6, 9, 12, 15, 18, 21, 24	24
B2			26
V1	Vegetated		24
V2			26

In order to investigate the variations of soil pH, a pH probe (Luster Leaf Rapitest 4-way analyzer) was used. Cover soil samples from different depths were collected and laboratory tests were conducted to determine the soil pH according to ASTM D4972. The results were then used to calibrate the pH measurement, using the pH probe.

Soil moisture and temperature sensors (Decagon 5TM probes) installed at the site were monitored on a bi-weekly basis, and the data was collected from the data acquisition system placed on site (Data-logger: Em 50). The soil moisture sensors installed in the cover soil use an oscillator running at 70 MHz to measure the dielectric permittivity of soil to determine the water content (Cobos and Chambers, 2010). The moisture is recorded as volumetric moisture content (m^3/m^3). A thermistor is placed inside the probe, which is in thermal contact with the sensor prongs, thus providing the soil temperature in Fahrenheit. The variations in soil texture and salinity cause the generic mineral calibration of the soil sensors to result in ± 3-4% accuracy for expansive clay (Campbell, 2001). However, Kizito et al., 2008 performed sensor calibration for this specific type of probe for a range of different soil textures, which showed water content from 10% to 60%, with the percentage of error ± 1%. The combined calibration equation proposed in the study suggested that no specific sensor calibration is required.

A Super Sting R8/IP multichannel system (AGI, 2004) was utilized in the landfill cover soil for the field scale ERI testing. The equipment has a programmable eight-channel option, which assists in conducting the tests in a shorter period of time. The dipole-dipole array was used for the tests to obtain better resolution and provide better quantitative results. Earth Imager 2D software (AGI, 2004) was utilized to process the collected test results. It uses a forward modeling subroutine to calculate the apparent resistivity values. To extract the quantitative values of the resistivity results, the apparent resistivity results were inverted, and non-linear least-squares optimization was carried out by the software to generate a desirable profile of the resistivity imaging. The equipment works by delivering an electric current through the soil. The current electrodes deliver the current through the soil, and the potential electrodes determine the potential difference (Muchingami et al., 2013). 2D resistivity imaging was used along the ET cover site. The

resistivity tests were conducted with 8-inch spacing and 28 electrodes that were stretched up to a length of 18 feet. The resistivity line in the cover surface was placed within 6 inches of the sensors, which ensured that the resistivity data was obtained at the exact location of the sensors. The electrodes were located at fixed points throughout the investigation period, and the measurements were acquired at the same locations during each tests. The resistivity imaging was conducted in the field to determine qualitative quantitative values of the resistivity at different locations and at different depths of the cover soil. On the investigative timescale, it was likely that the electrical resistivity of soil would vary due to temperature changes, amounting to about 2% per 1 °C (Friedman, 2005). Therefore, according to (Manzur et. al., 2016), it is necessary to consider a temperature correction, as it affects the numerical value of the resistivity results. The temperature data obtained from the sensors was used to perform the temperature correction of the obtained resistivity value from the tests in the field. Therefore, the measured resistivity was corrected at 25°C, using the following equation (Samouelian et al., 2005):

$$\rho = \rho T * (1 + \alpha(T - 25°C) \quad (1)$$

Where, T = temperature (°C), ρT = electrical resistivity measured at temperature T, ρ is electrical resistivity at the reference temperature of 25 °C, α = correction factor (0.0202).

The measurement of evapotranspiration was performed using a unique instrument known as the evapotranspiration chamber. Portable chambers have been used in earlier studies to measure evapotranspiration (ET) from bare soil and sparsely vegetated plant communities (Stannard 1988; Stannard and Weltz, 2006), from distinct vegetation types within mixed species communities (Stannard, 1988), and from cultivated alfalfa fields (Reicosky et al., 1983). However, this was the first time that this equipment

was used to measure evapotranspiration from landfill cover soil. The ET chambers measure the water vapor exchange between the atmosphere and the earth's surface within a small area (Dugas et al., 1997). This is completed by enclosing a known volume of a plant canopy and/or soil surface, and measuring the increase in the vapor density within the ET chamber (Garcia et al., 2008). The benefits of utilizing a portable ET chamber are: (1) The actual water flux is measured from transpiring vegetation rather than calculated from climatic parameters, (2) Readings can be repeated throughout the day at multiple locations, (3) The instantaneous ET which is obtained requires a brief period of time for the measurement, and (4) It allows a comparison between these rates and other in-place estimation methods for ET (McLeod et al., 2004). Figure 4-4 shows the ET chamber schematic and the setup used in the field. Two ET gauges were placed in the site to measure the amount of evapotranspiration.

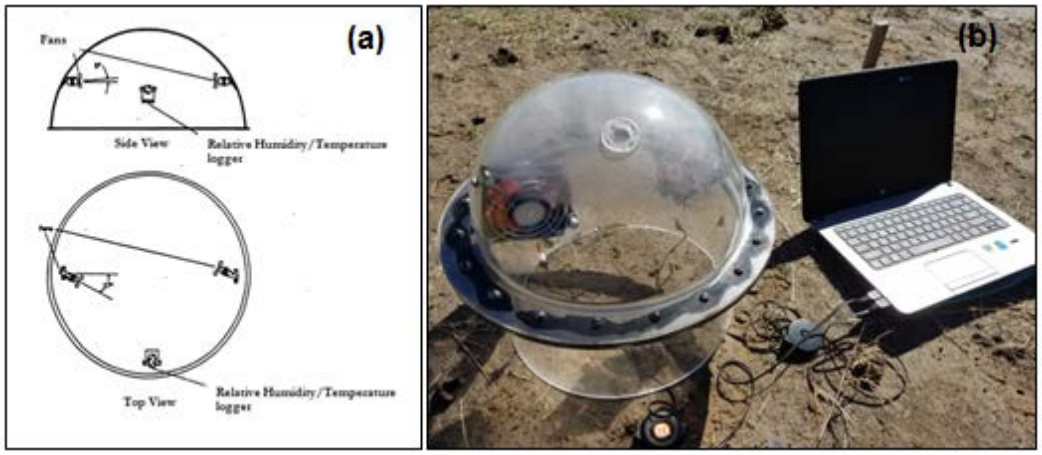

Figure 4-4 (a) ET chamber schematic and (b) the equipment being used in the field

RESULTS AND ANALYSIS

(1) Cover Soil Characterization

Samples of the control section cover soil were collected from different depths of the location to conduct the soil classification and geotechnical characterization. Eight

samples were collected from four different locations. Table 4-3 exhibits the soil characteristics and classification for the pilot section location. The pilot section soils were classified as inorganic high plastic clay (CH) or inorganic low plasticity clay (CL), according to the USCS classification system. The specific gravity varied within a range of 2.65 and 2.68, which is consistent with clay soil. The activities of the soil specimens were within the range of 0.84 to 0.90 which, according to Skempton, 1953, is considered to be active soil. The compaction levels were similar, at 95% relative compaction on the wet side of optimum moisture curve for the pilot section. The dry unit weight of the base layer soil varied from 103.0 pcf to 110.2 pcf. It was noticeable that the non-vegetated (B1 and B2) segments of the pilot section had a higher dry unit weight range (109.8 pcf to 110.2 pcf) than the dry unit weight of the vegetated segments (V1 and V2) of the pilot section (103.0 pcf to 105.6 pcf). The measured liquid limit of the pilot section soil samples were utilized to calculate the cation exchange capacity (CEC) of the soil, using the correlation developed by Yukselen and Kaya, 2006, [CEC=0.2027LL+16.231]. Physical properties of the soil such as Atterberg limits, specific gravity, and CEC were in a similar range for both soil conditions, indicating that the presence of plant roots does not significantly influence the physical properties of the soil. Further investigation was carried out on the collected soil samples from the vegetated control section to determine the root mass density. The collected soil samples were weighed and washed over a 0.2 mm sieve after clay dispersion, using hexametaphosphate (85%) and sodium bicarbonate (15%) at 10% (w/w) dilution (Amato and Pardo 1994). The washed sample was then separated from non-root materials, and the plant roots were weighed after drying, at 70 °C to constant mass. The initial dry mass of the sample was calculated from the fresh mass and its water content. The mass of the dry root was divided by the dry mass of the soil in each sample to obtain the root dry mass per unit soil dry mass in mg/cm^3. The soil

properties observed for both the vegetated and non-vegetated section were in the similar range which indicates that the physical properties of the soil was not affected significantly by the presence of vegetation. Figure 4-5 shows the root mass density obtained at different depths for the summer and winter of 2016. Root mass density (RMD) was higher at 8-inch depth and decreased at deeper depths. During the winter of 2016, the RMD increased at all depths, showing that plant growth had taken place. These results were consistent with the study conducted by Rimi et al., 2012. The RMD density had an overall range of 0.14 to 0.34 mg/cm^3.

Table 4-3 Geotechnical Characterization of Pilot Section Soil Samples

Location	Liquid limit (%)	Plasticity Index (%)	Activity	Specific gravity	Dry unit weight (pcf)	USCS classification	Cation Exchange Capacity (cmol+/kg)
B1-8"	51	26	0.87	2.66	109.8	CH	26.5687
B1-24"	43	21	0.9	2.67	110.2	CL	24.9471
B2-8"	56	32	0.85	2.68	107.6	CH	27.5822
B2-24"	46	24	0.88	2.65	109.8	CL	25.5552
V1-8"	51	30	0.84	2.65	104.6	CH	26.5687
V1-24"	52	27	0.89	2.64	105.6	CH	26.7714
V2-8"	47	28	0.92	2.65	103	CL	25.7579
V2-24"	45	25	0.9	2.66	103.5	CL	25.3525

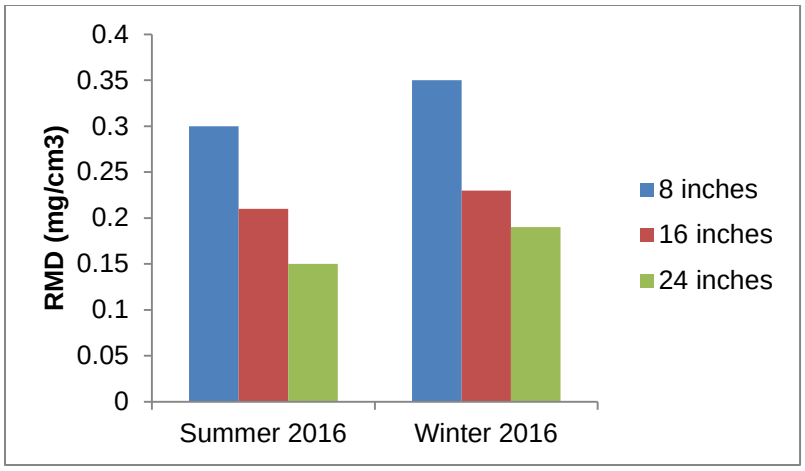

Figure 4-5 Plant root mass density in the vegetated cover soil of the control section

(2) Soil Compaction

Soil density or soil compaction affects the electrical resistivity in the soil (Abu Hassanein et al., 1996), and the root growth of plants in an ET landfill cover soil is dependent upon the compaction condition (Quang, 2012). The following section discusses the investigation of the soil compaction level, using a soil compaction tester or soil penetrometer (Lowery, 2002). The use of a soil penetrometer for detecting the compaction level in the field and performing a root growth study has been quite limited. This investigation was undertaken as an attempt to incorporate the use of a soil penetrometer to detect the effect of vegetation on landfill soil compaction. For an ET cover, it is an important consideration, as soil compaction can easily reduce plant growth by limiting root penetration. In addition, soil compaction can lead to water and soil quality degradation due to increased runoff and soil structure destruction. Soil compaction was investigated for a period of one year, and the variations of soil compaction with depths for non-vegetated and vegetated cover soils are shown in Figure 4-6.

The general trend of soil compaction shows that compaction increases with depth in both vegetated and non-vegetated cover soils. For non-vegetated cover soil, the

range of compaction is from 80 psi to 350 psi; for vegetated cover soil, the compaction level ranges from 20 psi to 350 psi. In this investigation, the non-vegetated cover soil reached 350 psi at 9-inch depth, and the compaction level of the vegetated was 350 psi at a depth of 15 inches. It was evident that the vegetated cover soil had lower compaction levels than the non-vegetated cover soil.

The variations in the compaction levels in the field were measured for one year, after which an average trend line was suggested for both vegetated and non-vegetated cover soils. Figure 4-7 shows the trend lines for the compaction levels of both vegetated and non-vegetated cover soils. The plant roots in the vegetated cover soil reached a depth of 12-16 inches, which explains the comparatively low compaction level in the vegetated cover soil. Vegetated soil has been reported to have more cracks and fissures than non-vegetated land (Ng and Zhan, 2007) because of the growth of roots into the soil, which causes cracks to form.

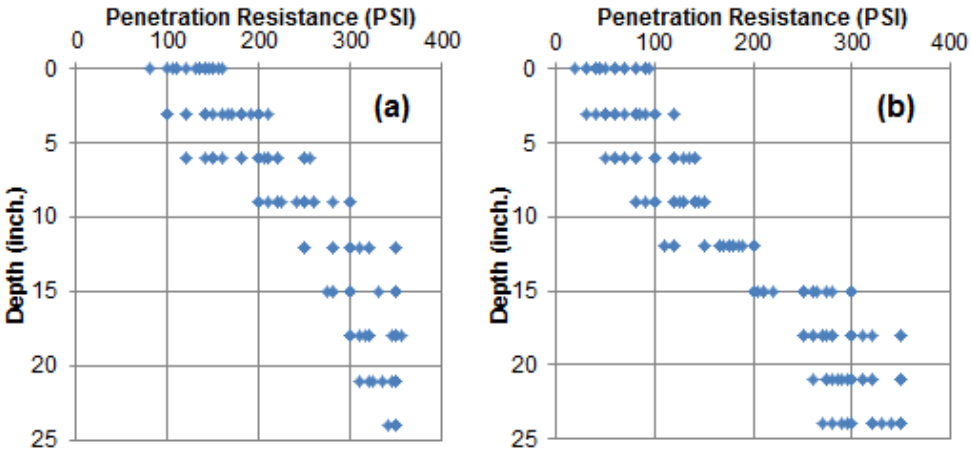

Figure 4-6 Compaction level variations at different depths (a) Non-vegetated cover soil (b) Vegetated cover soil

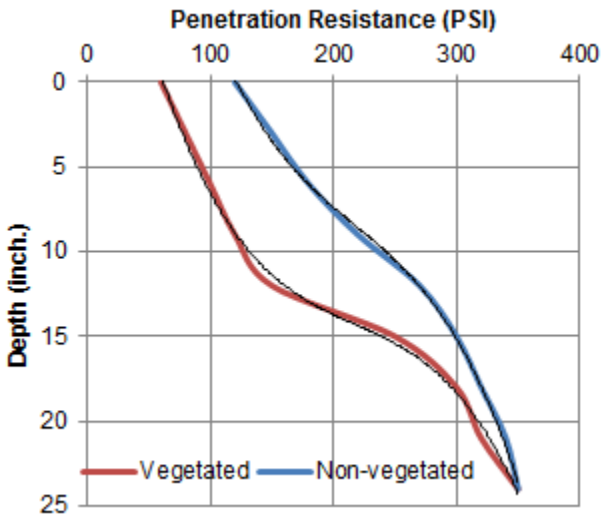

Figure 4-7 Field compaction level profiles for vegetated and non-vegetated landfill cover soils

The root mass in the vegetated ground loosens up the cover soil, causing the soil to have lower bulk density in the root zone. The electrical resistivity is dependent on soil density, and the difference in compaction levels in vegetated and non-vegetated cover soil is a significant factor and influences the ERI results. The lower compaction in the vegetated zone of the cover soil was an unique finding in this study which supports the existence of model with higher exponential for vegetated clay.

Figure 4-8 shows the compaction testing performed in the lysimeters. All the lysimeters exhibited similar trend of compaction level as the vegetated clay cover with an exception of lysimeter 4. This supports the trend suggested in figure 4-7. The difference in lysimeter 4 might have occurred due to inadequate site selection during the testing where the root growth is not significant.

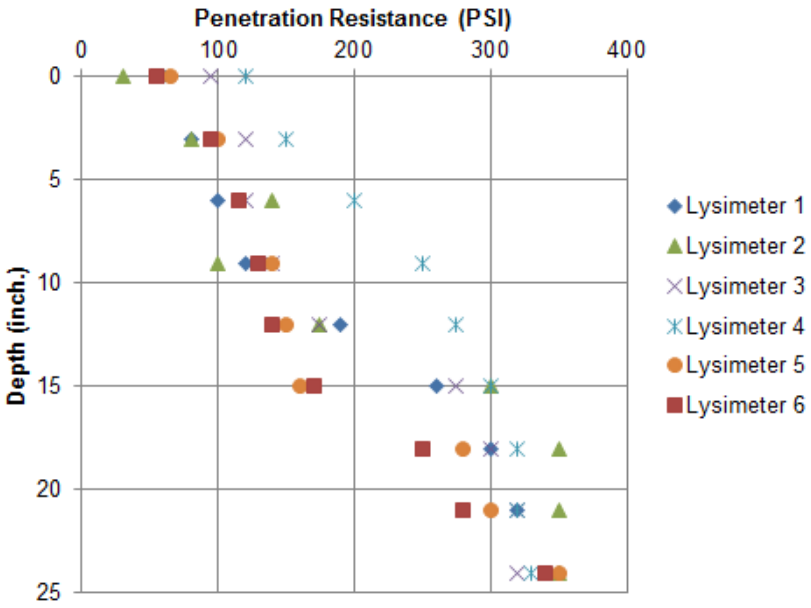

Figure 4-8 Soil compaction level in the lysimeters

(3) Soil pH

Soil pH has been reported to vary with the seasons (Smith, 1996) and is a factor which significantly affects the conductivity of the soil and influences the plant growth rate. According to studies by Mclean, 1982 and Xu et. al., 2006 soil tends to become more acidic with time due to rainwater leaching away basic ions (calcium magnesium, potassium and sodium); the decomposition of organic matter which creates carbon dioxide; and the respiration of roots dissolving in soil water to form a weak organic acid. Therefore, with time and development of the plant roots, it is suggested that soil P^H should decrease. The decrease in soil pH increases conductivity, which correspondingly gives lower resistivity values. Figure 4-9 shows the variations in pH in ET lysimeters (a) and the control section (b). pH values of soils were measured in the field and varied within a range of 6-8 throughout the study period. The major factor influencing the soil pH was the precipitation taking place on-site. It was observed that leaching of ions occurred

after every rainfall event, which caused a drop in the P^H. The change was more prominent in the 2% sloped lysimeters than in the 25% sloped lysimeters because the 2% sloped lysimeters were subjected to higher infiltration of water. As no fertilizer or any other soil nutrient was added during the investigation period, no significant difference in pH was observed. Therefore the effect of salts on resistivity might not be considered a significant factor. In addition, the variation of pH was not significant in the control section which suggests that soil pH has no substantial effect on the electrical resistivity results.

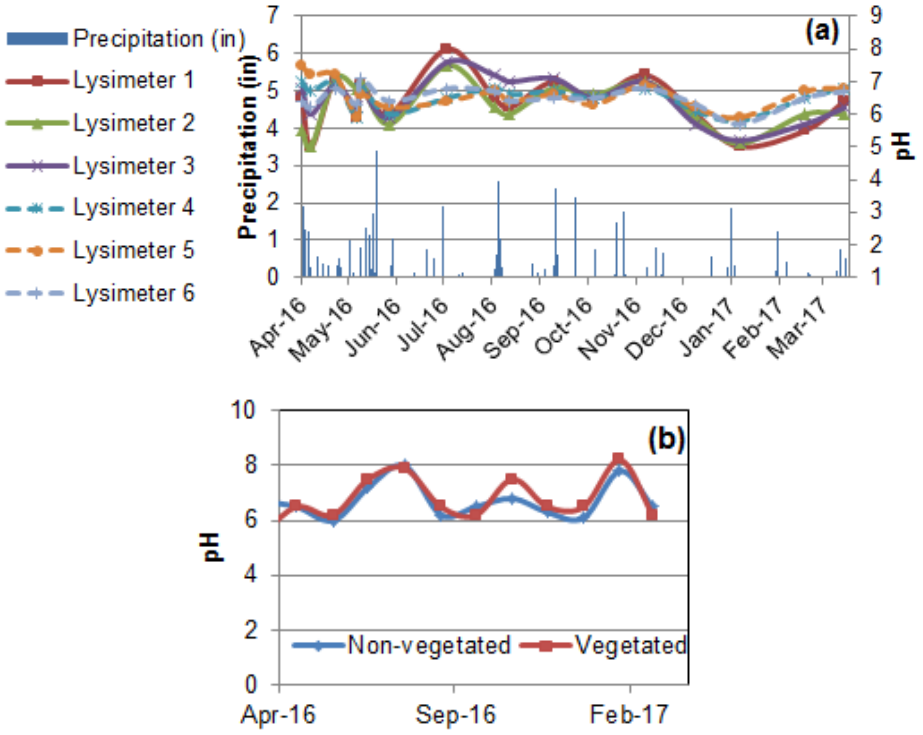

Figure 4-9 Soil pH variations in (a) ET lysimeters and (b) pilot section

(4) Soil Temperature

The soil sensors placed at different depths of the cover soil recorded the soil temperature of the control section. Seasonal variations of the ambient temperature were observed in the soil temperature profile throughout the investigation period (Figure 4-10).

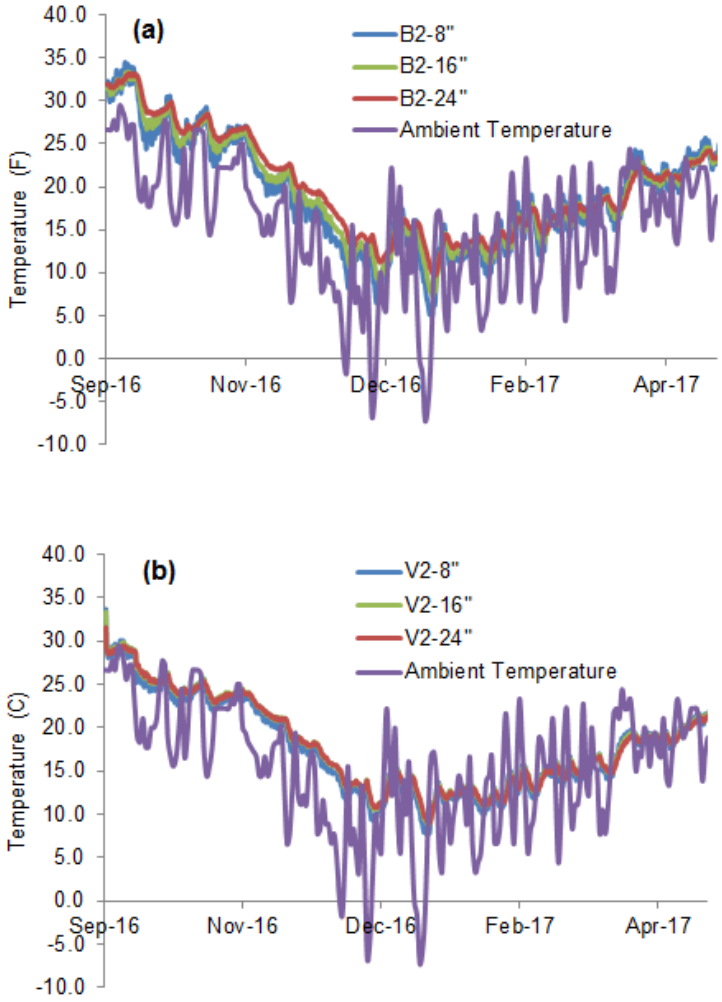

Figure 4-10 Soil temperature variations at different depths of the pilot scale cover soil (a) Non-vegetated (b) Vegetated

The range of temperature for both types of cover soil was similar at various depths. However, the non-vegetated cover had a variation of 5% along the depth, which was lower than the 2% variation of the vegetated cover soil. The soil temperature and the ambient temperature had similar variations throughout the different seasons. The differences in range were not significant, and it can be concluded that temperature correction used for resistivity in non-vegetated cover soil is also suitable for the vegetated

cover soil. In the absence of soil temperature probes, the soil temperature can be estimated using the following equation:

$$T_z = T_m \pm A_s \, exp\left[-\frac{z}{\sqrt{\frac{\alpha p}{\pi}}}\right] + gz$$

where, T_z = temperature in degree Fahrenheit at depth z, A_s = surface temperature amplitude in degree Fahrenheit [0.5 (Max. temperature – Min. temperature)], P = period of time under consideration, T_m = mean temperature of air in degree Fahrenheit, α = thermal diffusivity (ft^2/hr), g = thermal gradient, 1.7 deg. F per 100 ft. depth. The thermal diffusivity of a soil is related to specific heat, thermal conductivity, and dry unit weight of soil, as presented below:

$$\alpha = \frac{k}{\rho c}$$

where, k = thermal conductivity (BTU/ft. hr. deg F), c = specific heat (BTU/lb. deg F), ρ = dry density (lb./ft^3).

The variations of subsurface temperature is a complex phenomenon which depends on factors like ambient air temperature, soil types, soil moisture contents, thickness of layers, snow coverage, ground elevation, slope aspect, wind, etc. (Kibria, 2014). Therefore, temperature determination is required for subsurface investigation of soil using ERI.

(5) Soil Moisture

Soil moisture sensors were placed in the control section study area to understand the variation of moisture content in the field. The sensors were placed at depths of 8 inches, 16 inches, and 24 inches. The depth of the cover soil was 27 inches, for which the sensors provided an overall view of the both vegetated and non-vegetated cover soil. Figure 4-11 shows the moisture sensor data obtained from the pilot section cover soil for a period of 9 months.

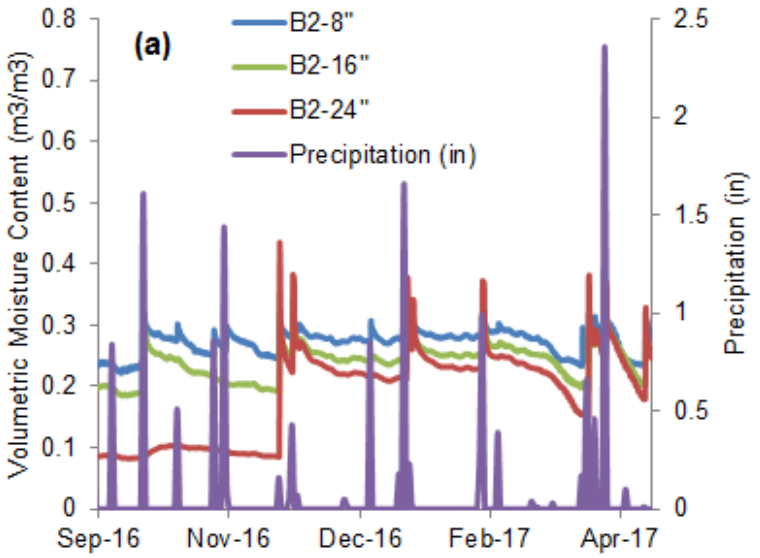

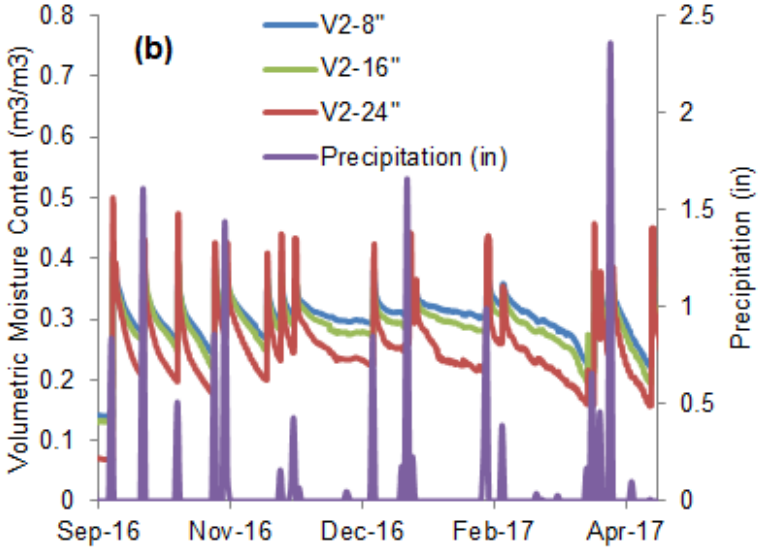

Figure 4-11 Soil moisture variations at different depths of the control section cover soil (a) Non-vegetated (b) Vegetated

In both the non-vegetated and vegetated sections, a rainfall event was followed by a sudden increase in the soil moisture at different depths. Consequently, the

evapotranspiration process caused the soil moisture to decrease with time. The significant difference between the non-vegetated and vegetated section was the rate of sudden increase and decrease of soil moisture with precipitation and soil water intrusion. Another important factor was the lag period that occurs in the 24-inch depth of non-vegetated cover soil. This may be attributed to the vegetated section undergoing higher infiltration of water with a single rainfall event, due to the presence of preferential path generated by the presence of plant roots. The root system provides more channels for the water to infiltrate deeper.

These results were consistent with the test performed by Ng and Zhan, 2007. Transpiration, caused by plants, is responsible for the rapid decrease of soil moisture in vegetated covers and is discussed in detail in the following section. The plant roots in the soil, which extended up to 12-16 inches, captured water quite efficiently by creating a root influence bulb which caused the decrease of soil moisture even at depths of 24 inches. The non-vegetated cover soil also underwent evaporation; however, there was a significant difference between the sections. The lag period of water infiltrating the 24 inch depth explains that, due to higher soil compaction in the non-vegetated soil, it took time for the water to infiltrate the deeper layers. However, less evaporation means that moisture resides in the cover soil for a longer period, which might lead to percolation. Ng and Zhan, 2007 discussed the idea that a grassy area might have deeper, open cracks than bare soil, due to the presence of roots. Therefore, the 24 inches of cover soil in the vegetated section experienced a higher increase in soil moisture than the non-vegetated section. This idea also supports the notion of lower compaction in the vegetated section.

The depthwise variation of soil moisture was further investigated to understand how plants influence moisture after a rainfall event. Figure 4-12 exhibits the depthwise variations of soil moisture in both vegetated and non-vegetated cover soils, over a period

of 21 days, after a single rainfall event. The solid lines depict the vegetated cover soil, and the dotted lines depict the non-vegetated section, The days on which the moisture was measured are color coded. After the first day of rainfall (0 day), the vegetated cover soil had higher moisture content at 24 inches than at 8 inches. However, the moisture content continuously decreased at all depths on days 7, 14, and 21. At the end of 21 days, the moisture content at 8 inches of depth (6.24%) was lower than the initial moisture content. At depth of about 16 inches, the moisture reduced by 12% after 21 days. At 24 inches of depth, a significant moisture reduction was observed, which equaled 20.2 %. The continuous shifts of the moisture profile show how the roots absorb the water with time. However, in the non-vegetated cover soil, the initial moisture at 8 inches of depth was lower than the vegetated cover soil. This was due to the presence of cracks in the vegetated cover. In 7 days, the moisture reduced at all depths; however, no significant change in moisture was observed after 7 days. Moisture reduction at 8 inches after 21 days equaled 5.01%, which was almost equal to the vegetated cover. However, at 24 inches depth, only 9.6% moisture reduction was observed after 21 days. This analysis shows how effectively the vegetative cover soil captures the moisture from the soil and reduces the possibility of percolation with roots growing up to a depth of 12 inches. According to (Ng and Zhan 2007), vegetated ground has higher soil moisture immediately after rainfall at deeper depths due to cracks formed by the plant roots. However, with time, the plant root water uptake causes the soil moisture to vary significantly depending on the weather condition.

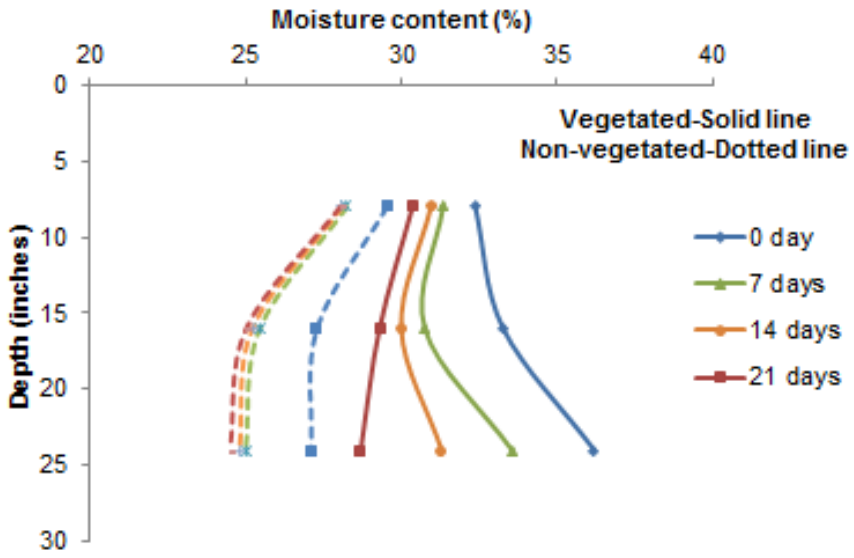

Figure 4-12 Soil moisture variations after a single rainfall event.

(6) Electrical Resistivity Imaging (ERI)

It is important to evaluate the amount of moisture in the cover soil in both vertical and horizontal directions to measure the performance of landfill cover soils (Kibria and Hossain, 2015). It's even more important for an evapotranspiration cover, because it aids in understanding how vegetation draws up the soil moisture and minimizes percolation (Hakonson, 1997). ERI tests were performed in the control section of the study area and Figure 4-13 and Figure 4-14 present the ERI profiles for both the vegetated and non-vegetated sections right after a precipitation event and after 7 days without any precipitation, respectively. Visual analysis revealed a significant difference between the vegetated and non-vegetated sections. The vegetated cover soil was planted with Bermuda grass (scientific name Tetraploids of C. dactylon), which is basically a warm season perennial species. It is a native, locally-suitable plant for ET vegetation in Denton, Texas. The grass grows best with an extended period of high temperatures and moderate rainfall. During the investigation the roots were observed to extend 10-16

inches into the cover soil. The non-vegetated cover soil was completely bare during the whole period. For the 2-D analysis of the ERI results, as shown in Figures 4-13 and 4-14, the electrical resistivity values for all of the tests were kept within the range of 1- 45 ohm-m and the root mean square correction factor was kept within 5%.

During the month of March 2016, the ERI investigation was conducted a day after a precipitation event of 16.256 mm. It can be observed that the vegetated cover soil shows higher resistivity up to 16 inches depth. However beyond that depth the resistivity is low. On the other hand in the non-vegetated cover soil low resistivity is observed in the shallow region up to a depth of almost 24 inch. At deeper depths than 24 inch the resistivity is higher. The difference in this resistivity for two different cover soils can be attributed to the presence of plant roots. As observed from the moisture sensor data with any precipitation event soil moisture increases at all depths of the vegetated cover soil. Based on the soil moisture sensor data resistivity should be lower at all depths of the vegetated cover soil. However, due to presence of plant roots in the vegetated cover soil the compaction level is lower up to a depth of 16 inches. This implicates the higher resistivity in the shallow region of the vegetated cover soil. On the contrary in the non-vegetated cover soil comparatively higher compaction has observed which explains higher resistivity section at deeper depths.

The ERI investigation 7 days after a rainfall event shows a contrasting scenario. Due to the high rate of evapotranspiration in the vegetated cover soil, resistivity is higher all across the section, showing the effectiveness of the plant roots in extracting the cover soil moisture. However, in the non-vegetated cover soil, low rate of evaporation suggests the comparatively low resistivity in the shallow region of the cover and thus supports the idea that the cover soil moisture can further penetrate into the cover soil and thus percolate.

ERI test after 16.256 mm rainfall	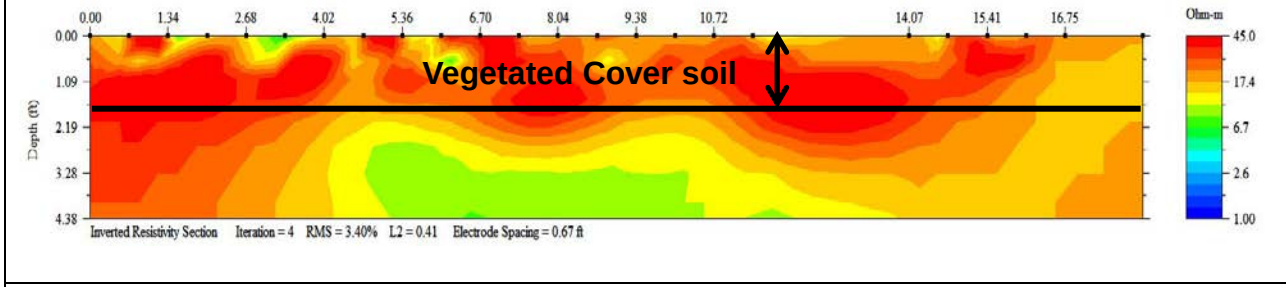 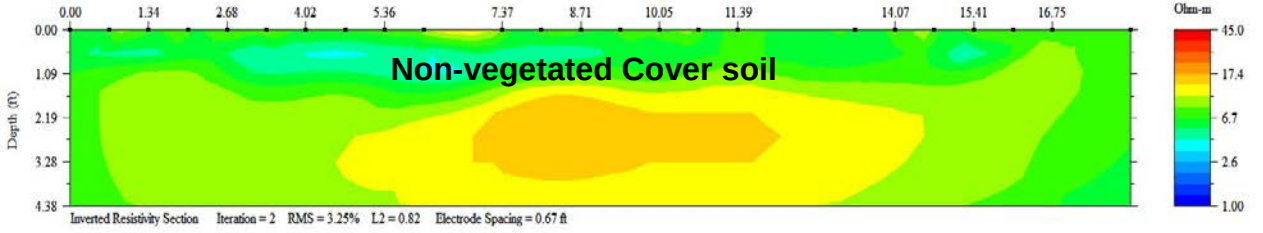

Figure 4-13 ERI profiles of vegetated and non-vegetated cover soil after 16.256 mm precipitation

ERI test after 7 days without any rainfall	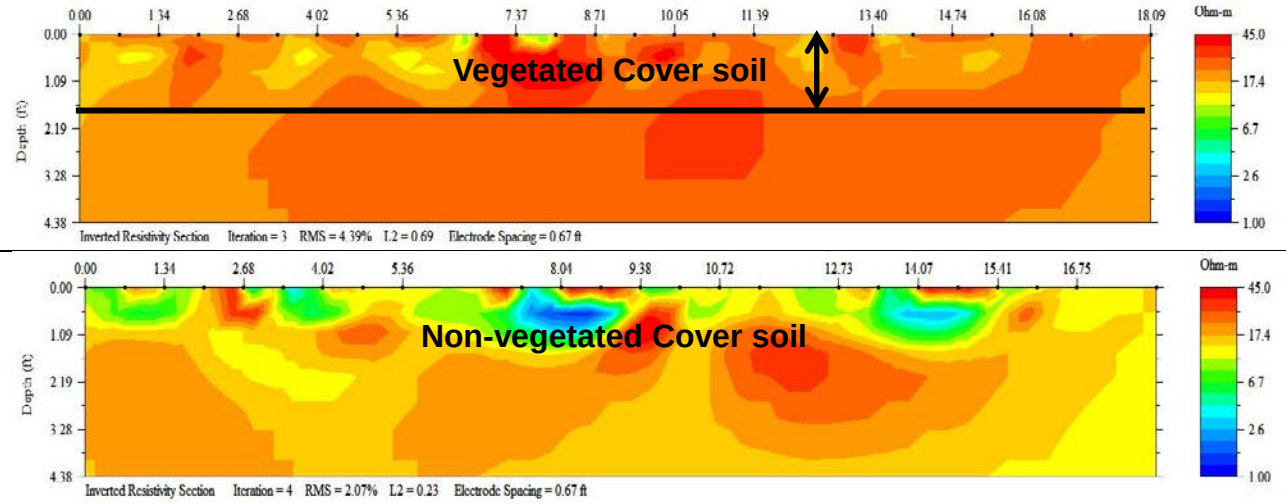

Figure 4-14 ERI profiles of vegetated and non-vegetated cover soil after 7 days without any rainfal

Evapotranspiration

ET chamber tests in the field provided the evapotranspiration rate of the vegetated cover soil and the evaporation rate of the non-vegetated cover soil. Monthly tests were conducted in the pilot section and the lysimeters under different ambient conditions, and the weather data obtained from the weather station was used to analyze the changes in evapotranspiration. ET data was also considered for the time period. The rate of evapotranspiration depends on the amount of vegetation present in the field and the ambient conditions. Figure 4-15 shows the difference between the evapotranspiration rates in the vegetated and non-vegetated cover soils and their variations with differing weather components. Figure 4-15 depicts that during all the tests, the amount of evapotranspiration was higher in the vegetated cover soil than in the non-vegetated cover soil. Crucial factors such as solar radiation, wind speed, and temperature influence the variations in evapotranspiration, and increased solar radiation, wind speed, and temperature increase the rate of evapotranspiration. The combined effects of the climatological factors also affect the evapotranspiration. In this particular site of investigation, factors such as wind speed and solar radiation were observed to be the major ambient factors influencing the evapotranspiration.

The rate of evapotranspiration was measured in all of the ET lysimeters on the same day, and similar trends were observed in all the lysimeters (Figure 4-16). However, the sloped lysimeters, which were placed at 25% gradient along the west side of the landfill, showed higher evapotranspiration than the flat-section lysimeters. Similar results were also observed from the ET gauge readings placed at site. The ET gauge placed in the 2% slope showed a cumulative evapotranspiration of 820 mm over a period of 9 months (from July 2016 to March 2017), whereas the gauge placed in the 25% sloped

lysimeters showed cumulative evapotranspiration of 1023 mm over the same period of time.

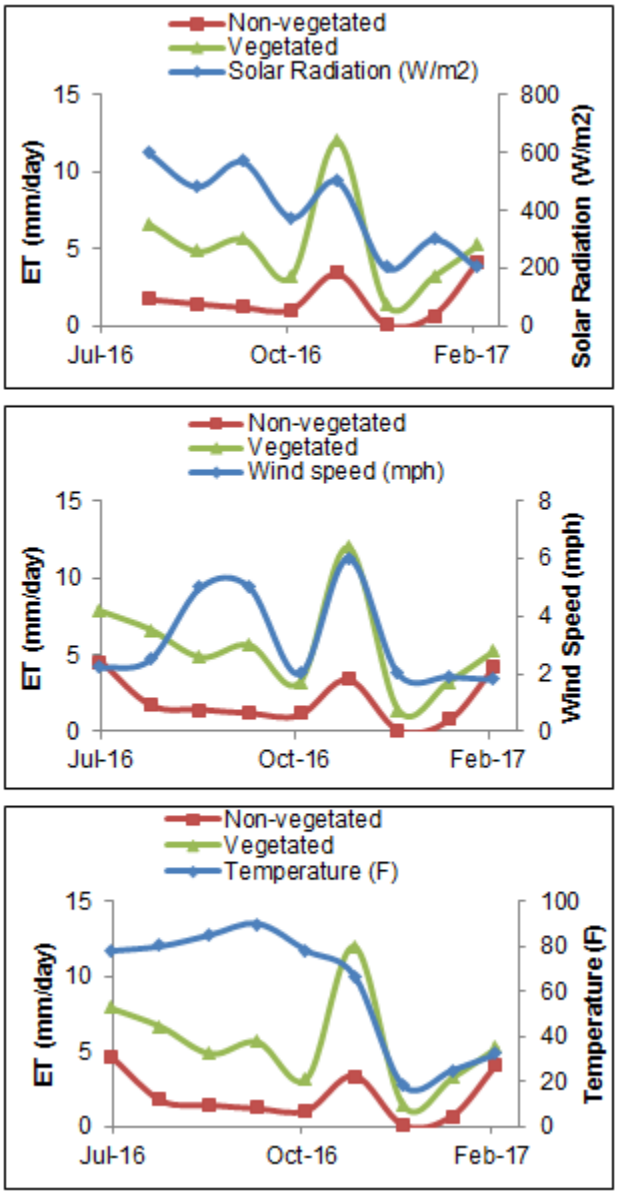

Figure 4-15 Evapotranspiration rate variations in vegetated and non-vegetated cover soil and the weather components which influence process in the field.

This shows that the sloped lysimeters performed well in terms of evapotranspiration. This might be explained by considering the sites. The sloped lysimeters were in the east-west direction, where they were exposed to more solar radiation. Another important observation in the lysimeter is the performance of the Bermuda grass (Lysimeters 3 and 6), which had the highest evapotranspiration of all of the vegetation.

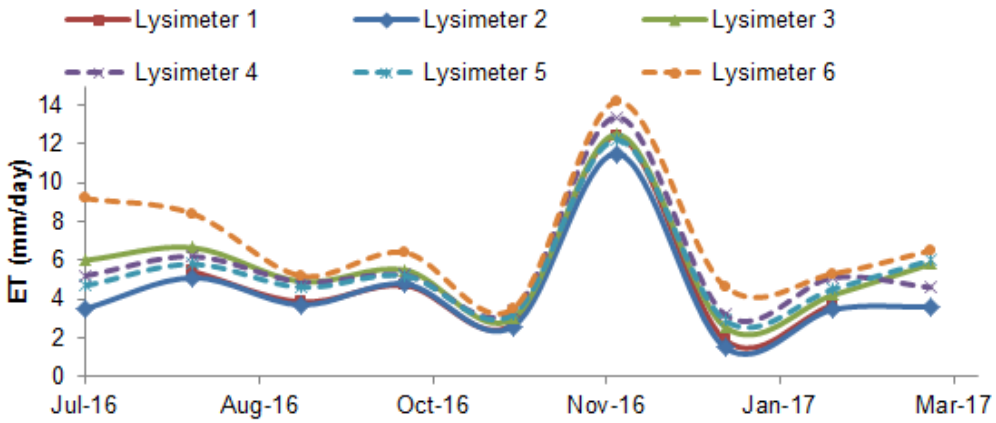

Figure 4-16 Evapotranspiration rate variations in ET lysimeters

The influence of evapotranspiration is observed in the soil moisture content because evapotranspiration reduces water content in the cover soil. This section thus only provides a comparative approach to discussing evapotranspiration in vegetated and non-vegetated landfill covers; however, the rate of evapotranspiration is not directly related with the electrical resistivity value.

ERI and Cover Soil Moisture

Comprehensive analysis of physical and chemical properties of soil revealed that lower penetration resistance which represents low soil compaction is the major factor that separates vegetated and non-vegetated cover soil. The presence of roots causes preferential flow path which in turn lowers the soil compaction. This explains, the field

scale models developed by Hossain and Hossain, 2017[a] for vegetated and non-vegetated clay cover soil. Both the non-vegetated and vegetated cover soils showed an exponential relationship between the soil resistivity and soil moisture. The resistivity decreased with an increase in moisture content. However for same soil moisture, vegetated cover soil showed higher resistivity. It needs to be mentioned that according to the model with soil moisture approximately above 60% the two models generates same resistivity.

For further validation the field scale models (shown in table 4-4) were validated using the control section resistivity and soil moisture sensor data. Table 4-5 illustrates the observed and predicted moisture content. The percentage of error between the model and the sensor data was in the range of 1.29% to 10% which shows that for similar soil characterization, similar meteorological condition, and similar vegetation, the model can predict soil moisture within a range of 10%.

Table 4-4 Developed models for different soil condition

Model	**Soil Condition**
$R = e^{-0.067\theta+4.593}$	Non-vegetated Clay
$R = e^{-0.077\theta+5.837}$.	Vegetated Clay
Where, R is electrical resistivity (Ohm-m) and θ is the volumetric moisture content (%)	

Table 4-5 Model validation in the control section

	Depth (in)	Non-Vegetated Cover Soil				Vegetated Cover Soil			
		Observed Moisture Content (%)	Model	Predicted Moisture Content (%)	Error (%)	Observed Moisture Content (%)	Model	Predicted Moisture Content (%)	Error (%)
Location 1	8	32.11	$R = e^{(-0.067\theta+4.593)}$	34.23	6.60	40.5	$R = e^{(-0.077\theta+5.837)}$	44.55	10.0
	16	25.4		27.95	10.4	38.19		40.6	6.31
	24	32.4		30.59	5.57	32.66	$R = e^{(-0.067\theta+4.593)}$	36.24	10.0
Location 2	8	45.52		46.11	1.29	22.1	$R = e^{(-0.077\theta+5.837)}$	23.11	4.57
	16	36.5		35.88	1.69	22.4		20.8	7.14
	24	22.77		24.23	6.41	34.33	$R = e^{(-0.067\theta+4.593)}$	31.23	9.03

DISCUSSION AND CONCLUSIONS

Alternative landfill covers, such as the evapotranspiration cover, are being increasingly used as a final cover system due to their cost effectiveness and nature - friendly performance. However, comprehensive analyses on how the alternative covers differ from the conventional cover system in terms of field performance have not been performed. This study was an attempt to address the possible factors that might influence the landfill cover soil performance for conventional and evapotranspiration covers. Moisture intrusion in the cover soil is a major concern for landfill cover soil performance, and this study includes non-destructive processes like electrical resistivity imaging to analyze the moisture intrusion in the cover soil. In addition, several other field tests,

including soil sensor data, were utilized to provide a comparative study and a means to estimating the landfill cover soil moisture, using the electrical resistivity method.

Based on the comparative study of surface and subsurface investigation of the vegetated and non-vegetated landfill cover systems, the following conclusions are drawn.

1. Cover soil characterization of both vegetated and non-vegetated cover soil shows that the physical properties for both the section are similar. The presence of vegetation does not show any influence on the cover soil.

2. Vegetated cover soil initiates a lower compaction level of the cover soil, due to the presence of roots. The low compaction level in the vegetated soil extends up to the root length. The presence of cracks lowers the soil density, leads to higher resistivity, and is a major factor in controlling the soil resistivity and moisture content relationship.

3. Soil P^H tends to vary all throughout the season; however, the range of variation is within 6.5 to 7.5 in the topsoil of the cover system. P^H variations in deeper depths are negligible, and soil resistivity values may not be affected by this parameter. The variation was more defined in the side slope lysimeters compared to the top section lysimeters., where the rate of higher infiltration in flat lysimeters led to comparatively higher variations in soil P^H.

4. Soil temperatures along the depth in both vegetated and non-vegetated sections were in a similar range. The ambient temperature had similar variability with the soil temperature, though it was in a higher range than the soil temperature.

5. Moisture sensor data showed continuous variability in soil moisture in the vegetated cover soil relating it to precipitation and the drying period. This suggests that lower compaction and the presence of vertical fissures due to plant roots increase the moisture content at all depths of the vegetated cover soil after each rainfall event.

However, the roots absorb the water quite rapidly and are more effective in drying up the cover soil than the non-vegetated cover soil..

6. Soil resistivity is an efficient parameter that differentiates the vegetated cover soil from the non-vegetated cover soil. Soil resistivity shows higher resistivity in vegetated cover soil at all times. The moisture absorption by plant roots is the major factor for this result. After each rainfall event higher resistivity in shallow region of the vegetated cover soil shows the lower compaction effect compared to the non-vegetated cover soil. However, with time the vegetated cover soil achieves higher resistivity due to higher evapotranspiration rate.

7. The vegetated landfill cover is responsible for a higher rate of evapotranspiration at all times. However, in this particular semi-arid region of Texas, a year-long study determined that ambient temperature is the major key factor in evapotranspiration. In addition lysimeters with steeper slopes (25% gradient) are susceptible to higher rates of evapotranspiration due to the wind effect.

8. Two separate field scale models, one for non-vegetated and one for vegetated clay, were validated using the field scale models developed by Hossain and Hossain, 2017[a]. The field model could predict the soil moisture, using only the electrical resistivity value. The variation in prediction was limited within 10%. This proves that the significant difference in compaction between vegetated and non-vegetated clay cover soil is responsible for two separate models.

Chapter 5

NON-DESTRUCTIVE APPROACH TO ESTIMATING SOIL WATER STORAGE AND PERCOLATION IN EVAPOTRANSPIRATION COVER SYSTEM

Hossain, M.I.[1], Hossain, M.S.[2]

[1]Graduate Research Assistant, Department of Civil Engineering, University of Texas at Arlington, 417 Yates Street, NH 119, Arlington, TX 76019, email: mdishtiaque.hossain@mavs.uta.edu

[2]Professor, Department of Civil Engineering, The University of Texas at Arlington, 416 Yates Street, NH 119, Arlington, TX 76019, e-mail: hossain@uta.edu

ABSTRACT

Evapotranspiration (ET) covers are becoming a popular alternative to conventional covers as final cover systems for landfills. The performance of an ET cover primarily depends on the moisture storage capacity of the cover soil and the transpiration of the infiltrated water through the plants. Small-scale field lysimeters are constructed in landfills, with provisions for measuring the runoff and percolation of the test sections. However, lysimeters also exhibit limitations such as no flow boundary and capillary effect which might reduce their effectiveness in the field. In addition, indirect methods have been used in the past to assess the performance of ET cover systems, but they are point-based, expensive, and time consuming. Therefore, a more efficient system is needed. One such non-destructive and inexpensive method is electrical resistivity imaging (ERI), which may be used as an effective tool for estimating the variation in moisture storage and hence percolation of the ET cover systems.

The objective of the current study is to use a novel approach to evaluating the soil water storage and percolation of the ET cover by using the ERI method. Six lysimeter

cells were constructed and equipped with moisture sensors at different depths at the City of Denton, Texas landfill. ERI tests were carried out and soil moisture sensor data was collected monthly. The changes in excess soil moisture at the base layer of the lysimeters showed a direct correlation with the rate of percolation (r squared = 0.9324), enabling the prediction of the rate of percolation. The field scale ERI results were correlated with the field scale soil moisture sensor data for cover soil (r squared = 0.9236). The correlation predicted the soil moisture in the base layer at field scale and estimated the percolation, even in a semi-arid area such as Texas.

INTRODUCTION

Evapotranspiration (ET) covers are an alternative earthen cover system for waste containment (Hauser, 2008). They are becoming popular as a final cover alternative because their design allows them to act very similar to nature (Benson et al., 2002). The comparative high cost of installing a conventional cover and the unpredictability of its long-term performance has made these alternative cover systems very attractive (Licht et al., 2001). The primary purpose of an ET cover is to store the infiltrated water from rainfall in the cover soil and transpire the water through plants during drier periods of time (Barnswell and Dwyer, 2011; Benson et al., 2002). Therefore, the performance of an ET cover largely depends on the water storage capability of the cover soil. Although ET covers are becoming more common for full-scale use, information pertaining to their effectiveness in removing water from the cover soil is limited (Madalinski et al., 2003). In this research, lysimeters were used to mitigate this problem in the field. Lysimeters consist of a large pan, typically constructed of a geomembrane, installed beneath the cover to measure the runoff and percolation (Benson et al., 1995; Malusis and Benson, 2006). Lysimeters also present limitations such as no flow boundary, capillary effect,

lateral diversion and leakage (Benson et al., 2001). However, this method is most commonly used as a form of direct measurement of runoff and percolation.

Indirect estimation of percolation for ET cover systems might be carried out using different types of soil instrumentations (USEPA, 2011), but the accuracy of monitoring the cover soil moisture of ET covers has been of concern for different researchers. Benson et al., 2001, concluded that methods to measure percolation such as trend analysis of soil moisture sensors, tracers, and water balance have higher levels of discrepancy than the lysimetry method. However, the changes in the base layer (bottom layer of lysimeter) moisture content or the moisture storage has shown qualitative and quantitative effects on the percolation rate of the ET cover system (Schnabel et al., 2012). An increase in moisture beyond the field capacity in the base layer has shown promising results for the rate of percolation in ET cover systems. Madalinski et al., 2003 suggested that when the cover has high water, it is approaching the storage capacity, thereby increasing the possibility of percolation. The percolation rate is the basic monitoring criteria for any ET cover system (Albright et al., 2010). This suggests the importance of estimating the percolation rate, using the moisture content of the base layer. Current soil moisture monitoring methods can provide moisture content only at discrete locations (USEPA, 2011), but large-scale monitoring of ET cover systems using soil instrumentation is not feasible (Benson et al., 2001). Therefore, alternative methods such as electrical resistivity tests have been conducted and field scale relationships were proposed by Hossain and Hossain, 2017[a].

Hence, the objective of the current study was to evaluate the soil water storage changes and percolation of the ET cover, using the ERI method. In order to conduct the study, six lysimeters were installed in the City of Denton, TX landfill, and ERI investigation, percolation, and runoff measurements were conducted. This study also

focused on the correlation between the changes in the base layer of the lysimeters and the rate of percolation measured by the lysimeter system, which would enable the measurement of the percolation rate of lysimeters only by measuring the soil moisture content of the base layer of the lysimeters. The ET cover lysimeters installed were built in accordance with the EPA's Alternative Cover Assessment Program (ACAP) (Albright et al., 2004).

It should be noted that there has been no significant study in the past to use ERI in ET cover systems to replace the moisture sensors as a method for monitoring changes in water storage which leads to percolation. This unique approach of using ERI in ET cover system will be able to visualize and quantify the entire base layer moisture which might go undetected by other point-based soil moisture measuring systems. Estimation of soil moisture using ERI at the base layer can be employed in the field to estimate the percolation rate of ET cover systems. Large ET cover systems may contain regions of heterogeneity which might be assessed by the cross-sectional image of the lysimeters, using ERI. Hence, the present study uses the ERI data to estimate the excess moisture in the base layer soil of the ET cover system, thus providing an estimate of the percolation rate of the lysimeters. The establishment of ERI as a monitoring tool for ET covers will be effective for estimating soil water storage and percolation in ET cover systems located in semi-arid regions, such as Texas.

MATERIAL AND METHODS

Site Description

The ET cover project selected for this study is situated in the City of Denton Landfill, TX, USA. Six 40' x 40' lysimeters, with 3 feet of compacted clay underlying 1 foot of topsoil were placed in Cell 1 of the landfill, as shown in Figure 5-1. The detailed construction sequence was not considered in this study, but was discussed in a study by

Hossain and Hossain 2017[a]. Three lysimeters (1, 2, and 3) were placed in flat sections with a slope of 2%, and three (4, 5, and 6) were placed in the slope with 25% gradient. Percolation and runoff water collection tanks were placed along the west side of the lysimeters to determine the hydraulic performance of the lysimeters. A weather station was placed to measure the climatic conditions at the site during the monitoring period.

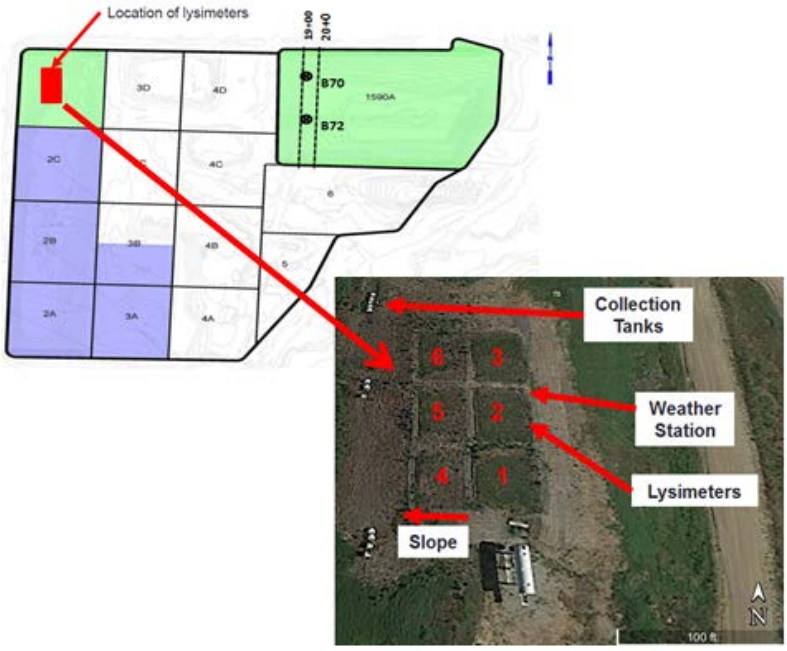

Figure 5-1 Location of the ET cover project in the City of Denton Landfill, TX

ET Cover Soil Characterization

The cover soil characterization was carried out for the ET cover soil at different lifts of compaction; however, only the base layer soil characterization is discussed in the next section. Table 5-1 exhibits the soil characteristics and classification for the base layer of the ET lysimeters. The base layer soils were classified as high plastic clay (CH) or low plasticity clay (CL), according to USCS classification. The specific gravity varied within a range of 2.65 and 2.69, which is consistent with clay soil. The activity of the soil

specimens were within the range of 0.74 to 0.94, which according to Skempton, 1953 is considered active soil. The compaction levels were similar at 95% relative compaction on the wet side of the optimum moisture curve. The dry unit weight of the base layer soil varied from 103.5 pcf to 105.8 pcf. The measured liquid limit of the base layer soil was utilized to calculate the cation exchange capacity (CEC) of the soil, using the correlation developed by Yukselen and Kaya, 2006, [CEC=0.2027LL+16.231].

Table 5-1 Geotechnical Characterization of ET Lysimeter Base Layer Soil

Lysimeters	Liquid limit (%)	Plasticity Index (%)	Activity	Specific gravity	Dry unit weight (pcf)	USCS classification	Cation Exchange Capacity (cmol+/kg)
1	60	24	0.97	2.65	104.8	CL	28.393
2	49	25	0.75	2.67	103.5	CL	26.163
3	49	31	0.74	2.66	104.2	CH	26.163
4	56	31	0.80	2.69	105.5	CH	27.582
5	49	30	0.76	2.65	104.5	CL	26.163
6	57	27	0.93	2.69	105.8	CH	27.785

Sensor Nests

Soil moisture sensors were installed at different depths of the compacted cover soil, including the base layer of the lysimeters. Figure 5-2 shows the locations of the sensors. Moisture and temperature sensors were placed in each lysimeter at different depths of the cells (12, 21, 30, and 39 inches). The sensor placed at 39 inches was considered to provide the base layer moisture content of the lysimeters. The data from the sensors was collected from the data loggers placed at the site.

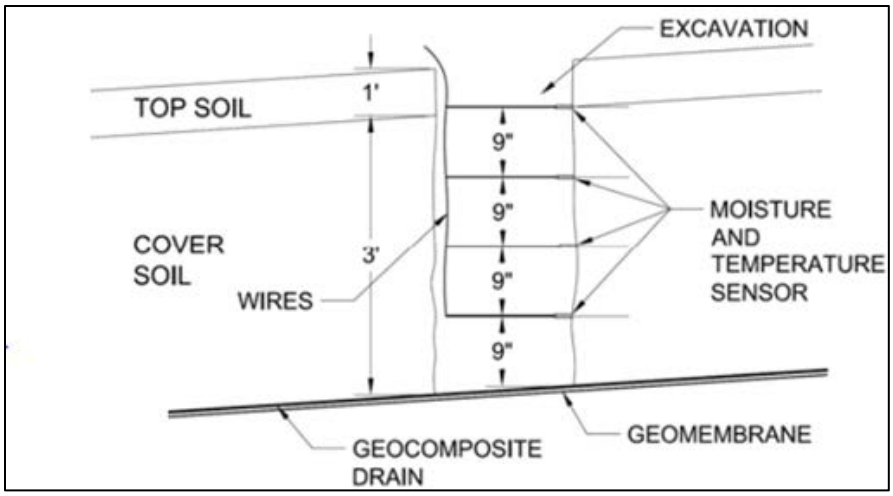

Figure 5-2 Location of moisture sensors in the cover soil

Electrical Resistivity Tests in the Field

The electrical resistivity monitoring of the ET cover site was conducted on a monthly basis from January 2015 to December 2016. Figure 5-3 shows the resistivity line placed at 3 foot spacing to monitor and extract the resistivity data from the ET cover soil. For this study, 2D resistivity imaging was used along the ET cover site. The resistivity tests were conducted with 3 foot spacing and 28 electrodes stretched up to a length of 81 feet, which covered the length of two lysimeters: one in the flat section (2% slope) and another in the slope section (25 % slope). Therefore, a single resistivity line was adequate to extract data from two cells at one time. The location of the resistivity line was placed within 1 foot of the sensors, which ensured that the resistivity data was obtained at the exact locations of the sensors. The electrodes were located at fixed points, and monthly measurements were acquired at the same locations each month. Equipment manufactured by Advanced Geosciences Institute (AGI) was used for the resistivity tests in the field. The equipment has a programmable eight-channel option which assisted in conducting the tests in shorter time. Dipole-dipole array was used for the tests, to obtain better resolution and provide more accurate quantitative results. EarthImager 2D

software (version 2.4.0) (AGI, 2004) was utilized to process the collected test results. The resistivity imaging was conducted in the field to determine quantitative values of the resistivity at different locations and at different depths of the ET cover soil. According to (Manzur et. al., 2016) it is necessary to consider temperature correction, as it affects the numerical values of the resistivity results. The temperature data obtained from the sensors was used to perform the temperature correction of the obtained resistivity value from the tests in the field.

Therefore, the measured resistivity was corrected at 25°C temperature, using the following equation (Samouelian et al., 2005):

$$\rho = \rho T * (1 + \alpha(T\text{-}25°C) \quad (1)$$

Where, T = temperature (°C), ρT = electrical resistivity measured at temperature T, ρ is electrical resistivity at the reference temperature of 25 °C, α = correction factor (0.0202).

Figure 5-3 Electrical resistivity imaging along the lysimeters

RESULTS AND DISCUSSION

Monitoring ET Lysimeters

The percolation of water through the cover soil was directly measured by the percolation tanks placed at the bottom of the slope; however, indirect measurement of moisture content was performed to use the sensors as a secondary monitoring tool. According to Schnabel et. al., (2012), immediately after the observed increase in base layer moisture content, the lysimeters should begin to percolate water from the base.

According to the Texas Commission of Environmental Quality (TCEQ) regulations (TCEQ, 2012), an alternative cover system should meet the criteria to achieve equivalent infiltration, hence minimize percolation. Therefore the primary goal of this study was to accurately measure the percolation of the lysimeters, using a non-destructive method, and compare it with the direct measured value. The lysimeter tanks collected the runoff and percolated water, and the cumulative runoff and percolation was reported by DeVries, 2016. The cumulative rainfall for the years 2015 and 2016 was 53.23 inches and 42.83 inches, respectively, which was measured by the weather station placed on the site. The rate of runoff and percolation were estimated, and Figure 5-4 shows the rate of runoff for the six different lysimeters.

The runoff rate varied from 527 mm/year to 1088 mm/year in 2015. However, in 2016, with growth of vegetation in the lysimeters, the runoff rate decreased in all of the lysimeters. The range of the runoff rate in the year 2016 was 330 to 779 mm/year. Runoff accounted for 39.0% to 80.5% of the precipitation in 2015 and decreased to 34.6 to 71.6% in 2016. Lower precipitation in year 2016 also led to lower runoff in year 2016. The variation of runoff rate was mainly determined by the vegetation condition in each of the lysimeters. It is expected that continuous monitoring of the ET lysimeters for another growing season will reveal further decreased runoff in the site.

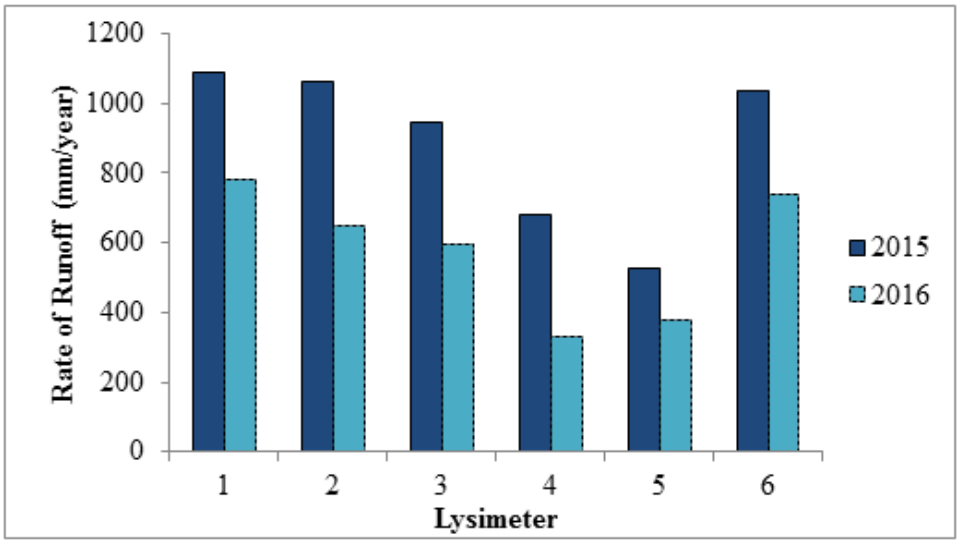

Figure 5-4 Measured rate of runoff of the lysimeters for two-year period

The change in the runoff rate indicates that the cover soil water storage should change due to the growth of plants and the extension of plant roots into the soil. Lysimeters 1 and 2, installed in the 2% slope, had had higher runoff rates than the lysimeters in the 25% slope (4, 5 and 6). This might be explained by the fact that vegetation growth in the 2% sloped lysimeters was comparatively lower than the vegetation density in the 25% sloped lysimeters (DeVries, 2016). Albright et al., 2004 suggested that the relatively small size of the lysimeters, compared to the typical landfill cover, may have caused the lack of a slope effect. The percentage change in surface runoff was within a range of 28% to 51% from year 2015 to 2016.

Direct measurement of percolation from the lysimeters was transformed into a yearly rate, as shown by Figure 5-5. The rate of percolation for the year 2015 varied from 26.42 mm to 67.52 mm, and in the following year the range decreased to 29.163 mm to 54.75 mm. The lysimeter percolation for the initial stage after construction (from October 2014 to December 2014) was neglected, as the moisture obtained during the

construction period might have affected the percolation value. This might also be considered suitable from a regulatory point of view.

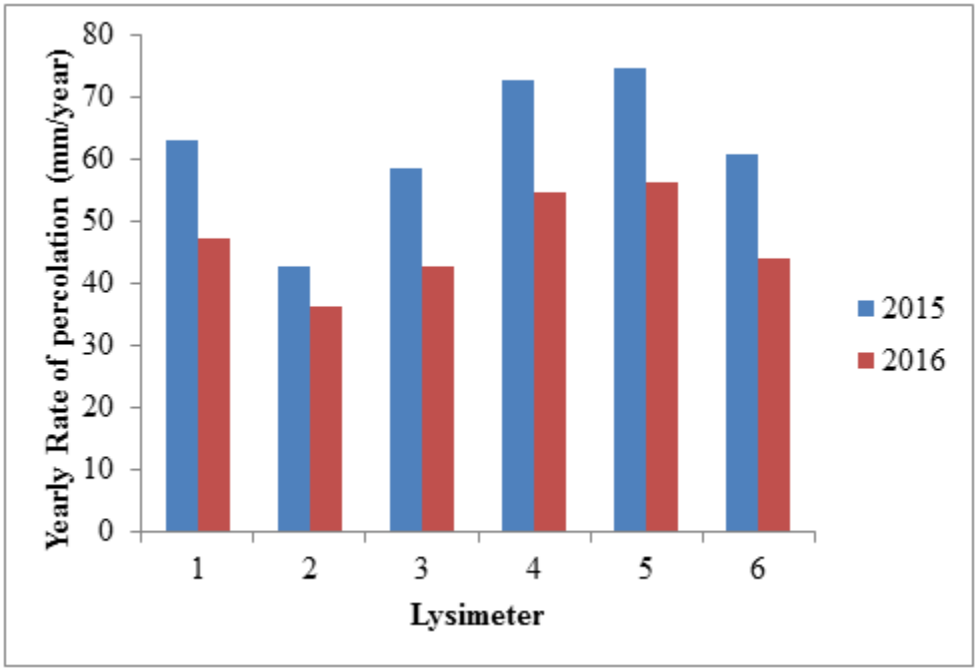

Figure 5-5 Measured percolation rates for two-year period of the lysimeters

Percolation accounted for 3.16% to 5.52% of the precipitation for the year 2015 and 3.34% to 5.18% for the year 2016. The rates of percolation decreased for all of the lysimeters in the year 2016, and it is expected that the rate of percolation will further decrease with increased root depth into the cover soil. The effect of the plant roots storing moisture was not prominent during first year of the study, as the root growth was not sufficient to store the water. The 3 feet of compacted clay cover with 1 foot layer of ET soil experienced root growth of approximately 12 inches at the end of year 2016, which was not considered significant. The compacted clay cover moisture storage and the soil water storage were the only functions resisting the percolation of the cover. The highest decrease in rate of percolation was observed in lysimeters 3 and 6, where the percentage of decrease was 27.2% and 27.5%, respectively. Both of these lysimeters

were planted with Bermuda grass, which indicates that this particular plant was more efficient at removing water from the cover soil than other planted vegetation. The ET gauge data (Figure 6.9) shows that the 25%-sloped lysimeters had higher evapotranspiration. This observation was also observed in the percolation data, where the percentage decrease in percolation was higher in all of the sloped (25%) lysimeters compared to the flat (2%) ones. This is why lysimeter 6 had a higher decrease in rate of percolation than lysimeter 3.

Moisture Distribution Using ERI to Predict Moisture flow in the Lysimeters

This section describes the analysis of the direction of moisture flow in the lysimeter cells by analyzing the moisture distribution. Resistivity tests were performed to determine the direction of the water flow in the lysimeter cover soil section I (Figure 5-10). Previous studies have shown that high resistivity refers to low moisture and vice versa. Therefore the ERI test result revealed the moisture condition in the cover for lysimeter 2. The first test was done 2 days after a rainfall event, and the second test was done 10 days after the same rainfall event. Figure 5-10 shows the results from the test. By observing lines 1, 2, and 3, we can visualize the moisture distribution in lysimeter 2. Line 1 is in the upslope, in a north-south direction; whereas line 2 is along the slope of the lysimeter, in an east- west direction; and line 3 is for the downslope location, in a north-south direction.

It can be observed that line 3 shows higher moisture content after two days of rainfall than line 1. This is because of the 2% gradient of the cell. Due to the bathtub-like structure of the lysimeters, the moisture settles in the middle section of the lysimeter, The perimeter side of the lysimeter is drier than the middle section. Line 2 shows the test result along the slope of the cell. It can be clearly observed that more moisture is perched up on one side of the cell. The lack of moisture at shallow depths shows that the top soil

dried up, which might have occurred due to the plants taking up water. The difference in the moisture between the days after the rainfall event is clearly visible in the shallow zone, where the plant roots were able to absorb the soil moisture from the shallow depths of the lysimeter after just 10 days. The growth of plant roots is necessary for removing the soil moisture more efficiently.

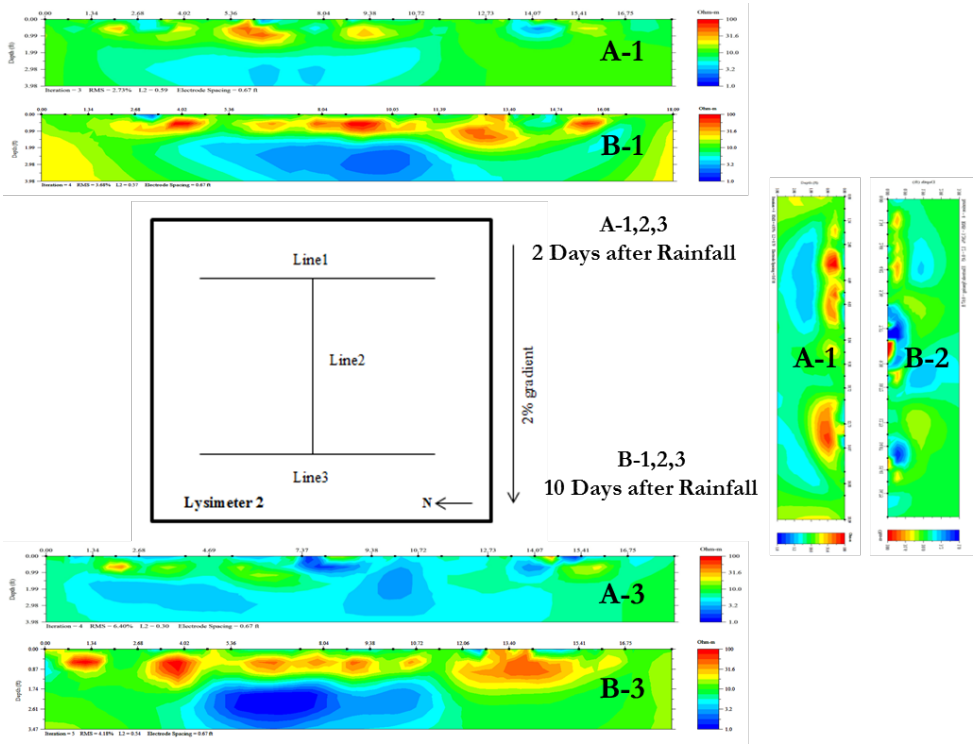

Figure 5-6 I Section investigation for moisture conditions in lysimeters

Relationship between ERI and Soil Moisture

Electrical resistivity and soil moisture for the lysimeters yielded an exponential relationship as shown by Hossain and Hossain, 2017[a]. The exponential relationship between ERI and MC has previously been observed in different studies (Ozcep et al. 2009, Kibria et al. 2012, Schnabel et al. 2012). Two separate models were proposed by Hossain and Hossain, 2017[a]: one distinctly for non-vegetated compacted clay cover soil ($R = e^{(-0.067\theta+4.593)}$, $R^2 = 0.92$) and the other one for vegetated clay cover soil ($R = e^{(-}$

$^{0.077\theta+5.837)}$, R^2 = 0.87). The exponential relationship was true for all of the lysimeters, and the r squared value was within the range of 0.87 to 0.92. Here, θ is the volumetric moisture content (%) and R is the electrical resistivity (Ohm-m) value after temperature correction at 25°C. The model was validated for soils with unit weight ranging from 103.5 pcf to 105.8 pcf. The range of moisture content was 3% to 60%, and the range for resistivity was 5 Ohm-m to 100 Ohm-m. It needs to be mentioned that the ET cover soil, at the time of this investigation, had root growth within 12 inches of the surface. To estimate the base layer moisture, which can be used to assess the rate of percolation, the equation for non-vegetated compacted clay can be employed at the base layer depth. To estimate the soil water storage in the ET cover lysimeter, both equations can be utilized and a reliable analysis can be carried out.

Excess Base Layer Moisture and Percolation

Rainfall was the only form of moisture applied to the ET lysimeters. Figure 5-7 shows the precipitation for the period of October 2014 to December 2016.

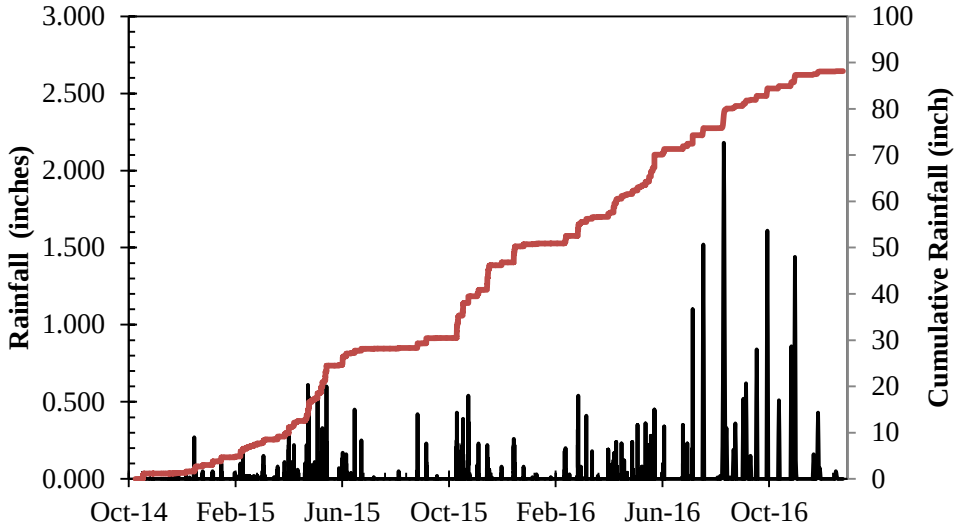

Figure 5-7 Rainfall events in the ET lysimeter from the beginning of operation (October 2014 to June 2015)

The rainfall events were lower during October 2014 to March 2015, and the cumulative rainfall was only 8.52 inch; however, during April and May 2015, there were frequent rainfall events. The cumulative rainfall increased to 22.48 inches by May 2015. The effects of these frequent rainfall events can be observed in the base layer moisture data. The soil moisture storage obtained from the soil sensor data is discussed in the following section. The moisture sensors placed at the deepest layer of the cover soil (30 and 39 inches), are considered as the base layer moisture of the cover soil. Figure 5-8 shows a plot for the base layer moisture storage, with the measured cumulative percolation for each lysimeter. After the construction period, the initial base layer moisture was considered to be at field capacity, which is in the range of 6.09 inches to 7.53 inches. The moisture storage is calculated using the average soil moisture content multiplied by 18 inches of the base layer soil. The amount of moisture in the base layer of the lysimeters fluctuated slightly during the period of October 2014 to February 2015, indicating that the impacts of precipitation and evapotranspiration were limited to the ET layer and the cover soil layer above the base layer. This proves the idea that the deeper soils in the base layer of the lysimeters were not affected by rainfall or evapotranspiration during this period.

From the figure, a direct correlation can be inferred between the percolation and the excess base layer moisture storage. The increase in moisture storage beyond the initial field capacity at the base layer was followed percolation for all of the lysimeters. Qualitative assessment of the percolation can be interpreted from the change in base layer moisture storage and cumulative percolation plot of the lysimeters. In summary, the cover soil stored and released water by evaporation and evapotranspiration for the first five months after construction. The base layer soil of all of the lysimeters exceeded the

field capacity which led to percolation from the lysimeters. This supports the idea that the base layer remained at or above the field capacity throughout the study period.

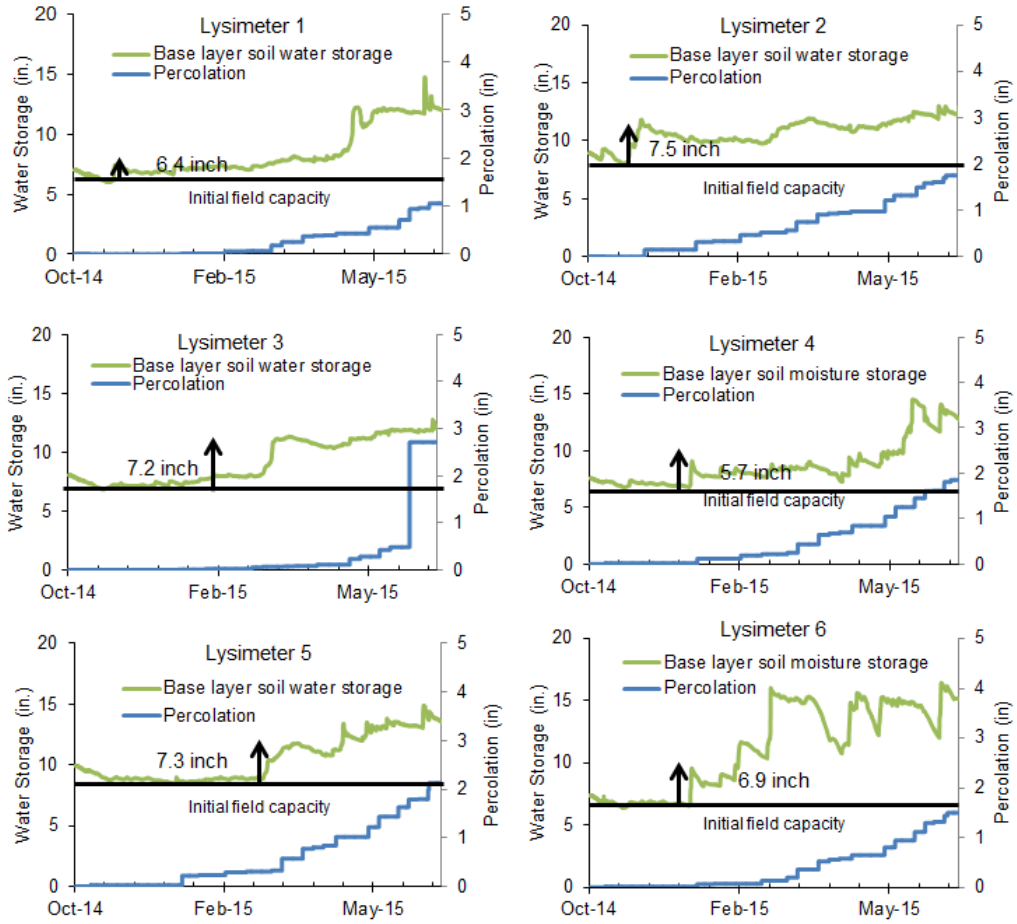

Figure 5-8 Moisture variation of the base layer in the ET lysimeters from October 2014 to June 2015

The observed soil moisture in the base layer, measured by the soil moisture sensors, matched the percolation curves in the lysimeters, suggesting that a rise in the ET layer moisture is followed by percolation from the base of the lysimeters. The only discrepancy was observed in lysimeter 5, where a significant rise in base layer moisture storage was observed in early March 2015. However, the percolation initiated from

January 2015. This might be attributed to the fact that the moisture sensors only provided discrete point information in the lysimeter.

Therefore, in this case, the small rise in the base layer moisture can be interpreted as the period in which percolation began. The data from the base layer provided reliable indications about the percolation of the ET lysimeters. The base layer soil moisture not only provided information about the percolation of the lysimeters, but also can also be related quantitatively with the percolation for a specific period of time. Figure 5-8 shows the plot of the base layer excess moisture with the daily percolation rate for the lysimeters. The excess base layer moisture storage is defined as moisture storage observed in the base layer, using the moisture sensors, during a given period minus the field capacity moisture of the respective lysimeters.

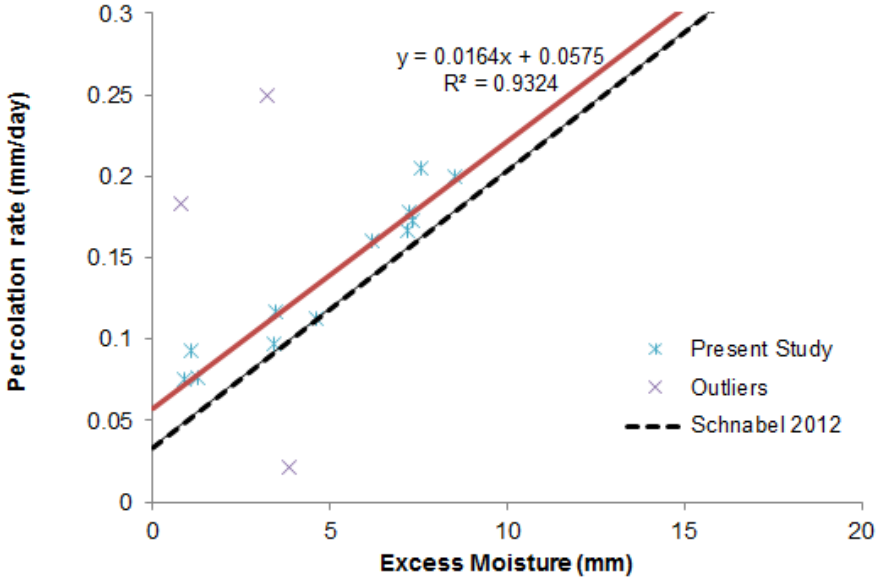

Figure 5-9 Relationship between base layer excess moisture and the rate of percolation for the ET lysimeter

The moisture content at the base layer of the lysimeters at field capacity was 6.09 inches, 7.53 inches, 7.1 inches, 6.3 inches, 7.3 inches, 6.65 inches, respectively, for

lysimeters 1, 2, 3, 4, 5 and 6. The field capacity moisture was obtained from the moisture sensor data at the base layer of the lysimeter for the period when there was no percolation. The plot for rate of percolation and base layer excess moisture shows a linear relationship, where an increase in the excess moisture led to the an increase in percolation rate.

The results of the present study are consistent with the work presented by Schnabel et al. They showed that the daily percolation rate of an ET lysimeter can be correlated with the base layer excess moisture by the equation y = 0.017x + 0.0334 (r squared = 0.917). The base layer moisture was predicted using an ERI correlation; however, there was no validation that the ERI produced the exact moisture amount at the base layer. In the present study, the direct correlation between the rate of percolation and excess moisture storage yielded the equation y = 0.0164x+0.0575 (r squared = 0.9324). The excess moisture in the base layer was measured using the soil moisture sensors installed in the ET cover lysimeters. This implies that the quantitative measurement of percolation can be related to the soil moisture sensor data. Another important observation in this study was that, in all cases, percolation began prior to the change in excess moisture (Figure 5-7). This observation is also reflected in the linear relationship shown above. When excess moisture is zero, the percolation rate is only 0.0575 mm/day. It should be noted that a few outlying points were omitted from the correlation shown in Figure 5-8. Those points were found for lysimeter 4, where the onset of percolation was seen before the rise in moisture in the base layer. At those points, the percolated water did not flow through the sensor, which may have been due to the preferential flow of water avoiding the sensor location.

Estimation of Percolation

One of the major functions of final covers in landfills is to control the cover soil moisture and percolation (Madalinski et al., 2003). ERI can be a very effective tool for estimating the soil water storage of an ET cover system. Spatial soil resistivity tests and application of the field scale models allows efficient estimation of soil moisture. Figure 5-10 shows the ERI profiles for the lysimeters for the month of January 2017. Base layer has been designated in the figure and using the average resistivity of the base layer the moisture content of the base layer is estimated. Consequently the base layer storage is calculated using the depth of base layer (18 inches). Initial base layer field capacity has already been calculated in the previous section and the field capacity is subtracted from the current base layer storage to find the excess base layer moisture. Rate of percolation is predicted using the relationship developed for excess moisture and percolation rate.

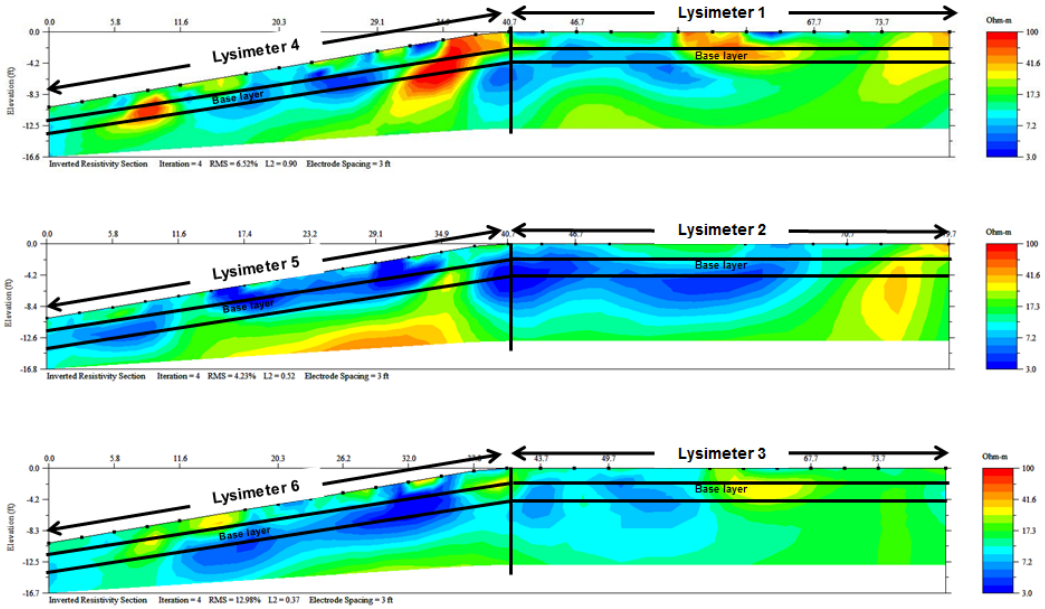

Figure 5-10 ERI profile of all the lysimeters for January 2017

The following section exhibits the step by step calculation of the percolation rate estimation for Lysimeter 1 for the month of January 2017:

Total depth of the cover soil = 4 ft

Base layer = Bottom 1.5 ft (18 inches) of the cover soil (2.5 ft to 4 ft from the top)

Step 1. Calculate average resistivity of the base layer using field ERI test (30th January, 2017) (Figure 5-11) (Base layer cross-section resistivity log considered at every 2 ft for the entire 40 ft lysimeter), Sample data at x=26 ft cross-section (Table 5-2): Resistivity within 2.5 ft to 4 ft (base layer) has been considered for all the cross sections.

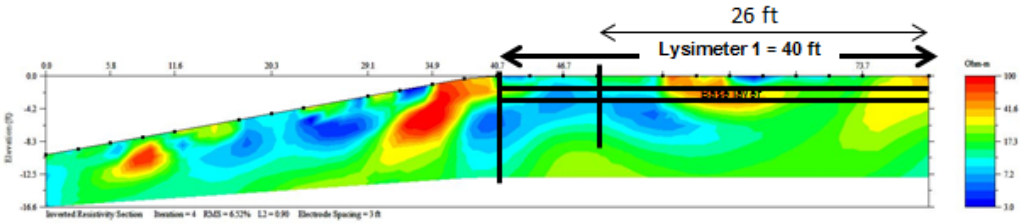

Figure 5-11 ERI profile of Lysimeter 1 for January 2017

Table 5-2 Resistivity log of lysimeter 1 cross-section (x= 26 feet) on 30th January, 2017

x = 26.000(Feet)	
Depth(Feet)	Resistivity(Ohm-m)
0	15.892
1.62	13.691
2.903	10.557
3.274	6.552
4.742	5.638
6.319	7.003
8.015	10.988
9.843	15.697
11.817	19.714
12.842	22.093

Average resistivity (for all the cross-sections) of the base layer = 11.243 Ohm-m

Step 2. Temperature correction required using: $\rho = \rho T * (1 + \alpha * (T - 25°C)$ (Samouelian et al. 2005), average soil temperature of base layer (2nd February, 2017) = 14°C and α = 0.0202

For ρT = 11.243 Ohm-m, $\boldsymbol{\rho}$ **= R = 8.745 Ohm-m**

Step 3. Base layer moisture predicted by the model: (non-vegetated clay)

$$R = e^{-0.067\theta + 4.593}$$

At R = 8.745 Ohm-m, Volumetric moisture content, θ = **36.18%**

Step 4. Base layer moisture stored = θ * depth of base layer (Hanson et al., 2007) = 0.3618*18 inches = **6.5124** inches.

Step 5. Initial base layer moisture storage = **6.4** inches (Figure 5-8)

Step 6. Excess base layer moisture = Base layer moisture stored - Initial base layer moisture storage = 6.5124-6.4 = 0.1124 inches = **2.886** mm

Step 7. Predicted percolation rate = 0.0164*excess moisture storage + 0.0575 (Figure 5-9) = 0.0164*2.886+0.0575 = **0.104834 mm/day**

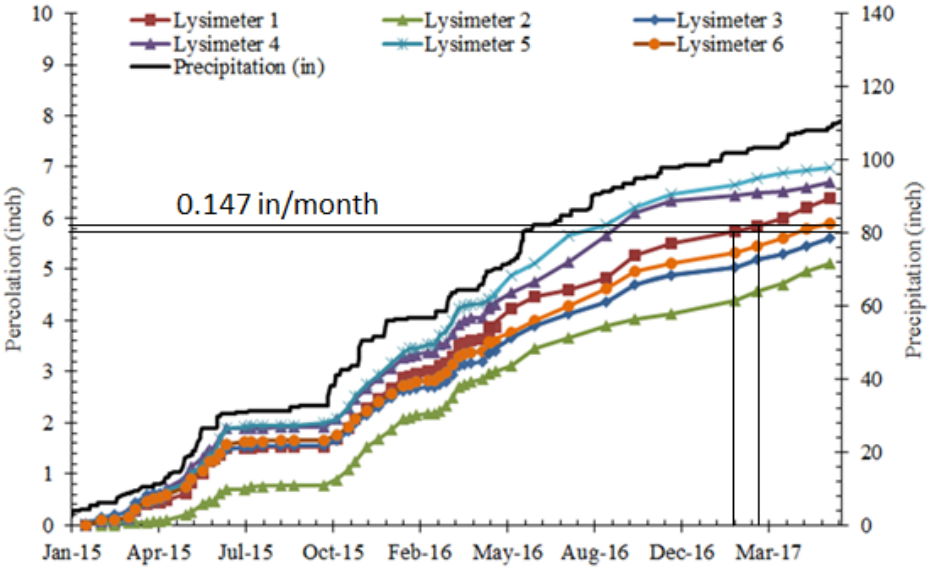

Figure 5-12 Observed cumulative percolation in the lysimeters

Step 8. Observed percolation rate from lysimeter percolation tanks = 0.147 in/month = **0.12446 mm/day**

Step 9. Percentage error = [(Predicted-Observed)/Observed]*100 = **16.72%**

Table 5-2 shows the calculated values of the predicted percolation rate of all the lysimeters for the month of January 2017 and the observed percolation rate obtained from the percolation tanks. The percentage errors for the predicted percolation rate were within the range of 12.6% to 27.3%. The use of this method to determine the percolation rate for ET cover system is a unique approach. In presence of an ERI and soil moisture model this method can determine the percolation rate without any existing lysimeter system or soil monitoring instrumentations.

Table 5-3 Rate of percolation predicted from the excess moisture

Lysimeter	Average resistivity of the base layer (Ohm-m)	Average soil moisture at the base layer predicted by the model (%)	Base layer moisture storage (in)	Field capacity (initial base layer stored moisture) (in)	Excess base layer moisture (mm)	Predicted percolation rate (mm/day)	Observed Percolation rate (mm/day)	Percentage Error (%)
1	8.745	36.18683	6.51363	6.4	2.886206	0.104834	0.125046	16.16393
2	5.331	43.57405	7.843328	7.5	8.720544	0.200517	0.159238	25.92242
3	6.321	41.03168	7.385702	7.2	4.716842	0.134856	0.18546	27.28555
4	12.3	31.09553	5.597196	5.7	-2.61122	0.014676	0.019538	24.88676
5	6.257	41.18357	7.413043	7.3	2.87128	0.104589	0.134815	22.42058
6	7.269	38.94599	7.010278	6.9	2.801062	0.103437	0.091831	12.63917

SUMMARY AND CONCLUSIONS

Evapotranspiration covers are becoming popular as a final cover alternative to conventional landfill covers. The lysimetry method is used commonly as a monitoring method for ET cover systems, however there are limitations on the use of lysimeter

method. In addition, indirect monitoring methods for ET cover systems are required to monitor the ET cover system efficiently. Current methods provide only discrete data, and they are expensive and time consuming. Hence, a non-destructive, efficient method is required to monitor the ET cover system both spatially and temporally. To fulfill this objective, several moisture sensors were placed in the ET cover base layer, and both qualitative and quantitative assessments were carried out to correlate the percolation rate of the lysimeters with the moisture storage data of the ET cover lysimeters. The linear trend obtained was $y = 0.0239x+0.0642$ (r squared = 0.934), where y is the percolation rate (mm/day) and x is the excess base layer moisture (mm). The establishment of the correlation suggested that estimation of the base layer moisture may be an alternative method for monitoring the ET cover percolation. The model was validated with observed percolation from the lysimeters and promising results were obtained. Thus, the quantitative relationship between soil moisture storage and percolation rate suggested that ERI might be used as a tool for estimating percolation in ET cover lysimeters.

Chapter 6

SUMMARY AND CONCLUSIONS

The final cover system is an essential component of landfills because it is vital to minimize infiltration of water into the waste, to quarantine the environment from the buried waste, and to reduce landfill gas emissions. Conventional cover systems have been a typical solution for the landfill authorities until recently. However, alternative landfill covers, such as evapotranspiration (ET) covers, are being increasingly used as final cover systems due to their cost effectiveness and nature-friendly performance. Nonetheless, comprehensive analyses of the performance of alternative covers performance in the field have not been investigated in detail. The lysimetry method is used as a monitoring method for small-scale ET cover systems installed in the landfills; however, indirect monitoring methods are required to monitor them efficiently. Monitoring evapotranspiration cover performance requires limiting percolation of the cover system within specified guidelines to ensure an efficient soil water storage system. Tools currently available to understand moisture in the ET cover soil only provide discrete point data, and they are expensive and time consuming. This led to the development of this study, which strived to establish an alternative, non-destructive, efficient method with which to monitor the ET cover system, both spatially and temporally.

To fulfill this objective, several moisture sensors were placed at different depths in the six ET cover lysimeters in the City of Denton landfill, Texas, USA. Simultaneous monitoring was also carried out, using electrical resistivity, in an attempt to develop a field scale statistically significant relationship between cover soil moisture and electrical resistivity. Electrical resistivity has been used as a tool in several studies to estimate soil moisture; however, the application of this method has been very limited in ET cover systems. Therefore the competence of soil resistivity for soil moisture estimation was

tested at different scales. Soil moisture sensors and soil resistivity measurements were conducted in six ET cover lysimeters, and the data from the analysis was grouped by lysimeter, depth, and soil condition (compacted clay and vegetated clay). Based on the results, two one-parameter models were proposed for moisture estimation, using electrical resistivity. For compacted non-vegetated clay, the model is [$R = e^{(-0.067\theta+4.593)}$, $R^2 = 0.92$]; for vegetated clay cover soil, the model is [$R = e^{(-0.077\theta+5.837)}$, $R^2 = 0.87$] where, R is resistivity in Ohm-m and θ is volumetric moisture content (%) and the range of this model is 1-100 Ohm-m for electrical resistivity and 10-60% for soil moisture. Both field scale models were validated using field scale datasets. The percentage of error was less than 5% for both models.

The development of the two models for non-vegetated and vegetated clay covers led to an in-depth investigation to determine the factors that resulted in the differences of the models and that might influence the performance of the conventional and evapotranspiration covers. Based on the comparative study of the surfaces and subsurfaces of the vegetated and non-vegetated landfill cover systems, in terms of physical and chemical property variations of cover soil, a few factors were identified as significant. The presence of plant roots in the ET cover soil leads to a decrease in soil compaction due to the presence of preferential paths along the plant root system. In addition, the presence of plant roots means that the root mass density of the plant increases the soil resistivity. For the above reasons, two different models were developed for the non-vegetated and vegetated clay cover systems. Further model validation was carried out, using a two-parameter multiple linear regression model, which resulted in a maximum variation of 20% for non-vegetated clay. For vegetated clay covers, the factors were added to the model.

In an attempt to extend the use of the field scale models beyond estimating the soil moisture storage, a further investigation was carried out, using the base layer soil moisture. A linear trend was obtained between the base layer soil moisture and the rate of percolation. The linear trend obtained was y = 0.0239x+0.0642 (r squared = 0.934), where y is the percolation rate (mm/day) and x is the excess base layer moisture (mm). The establishment of the correlation suggested that estimation of the base layer moisture may be an alternative method for monitoring the ET cover percolation. The model was validated with observed percolation from the lysimeters and promising results were obtained. Thus, the quantitative relationship between soil moisture storage and percolation rate suggested that ERI might be used as a tool for estimating percolation in ET cover lysimeters. The installation of sensors or moisture-measuring devices in the ET cover lysimeters is expensive, and the instruments depreciate with time. Alternative techniques, such as electrical resistivity imaging (ERI), can provide the moisture content in the ET cover lysimeters. The current field scale study successfully correlated the soil moisture sensor data with the ERI results. ERI results and soil moisture sensor data were analyzed for a period of more than two years, and a logarithmic model was developed to estimate the moisture content. The establishment of the model was validated with previous studies, and the quantitative relationship between the soil moisture content and the percolation rate suggested that ERI is a viable tool for estimating percolation in ET cover lysimeters.

APPENDIX A

ERI PROFILES OF ET LYSIMETERS

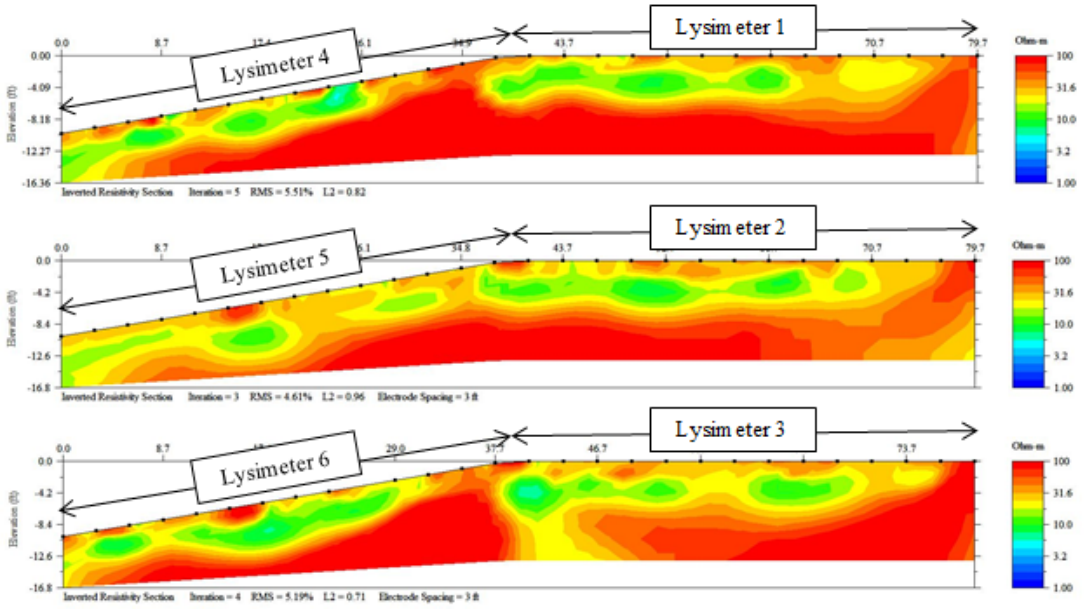

January 2015

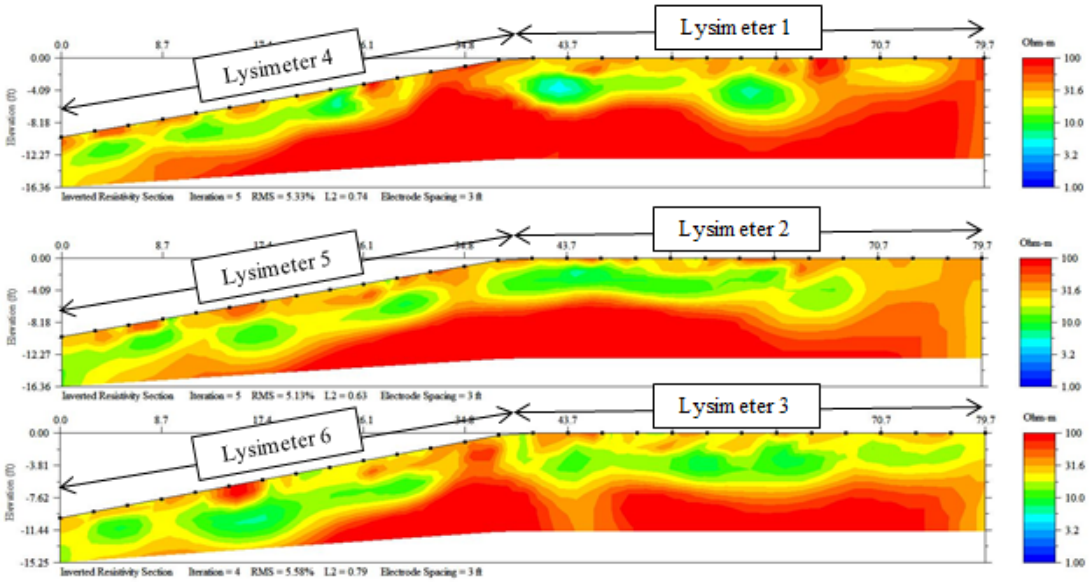

March 2015

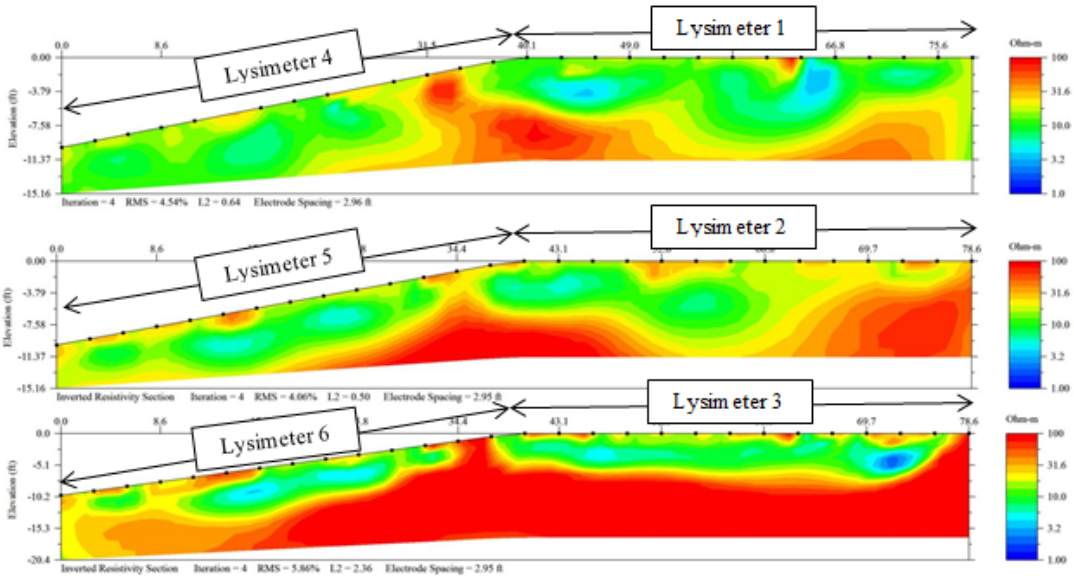

May 2015

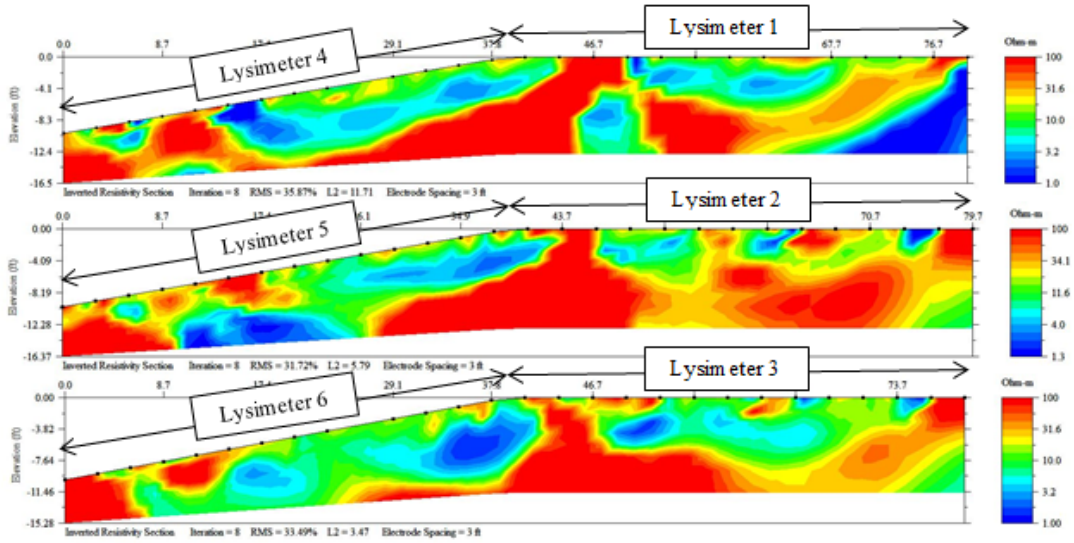

July 2015

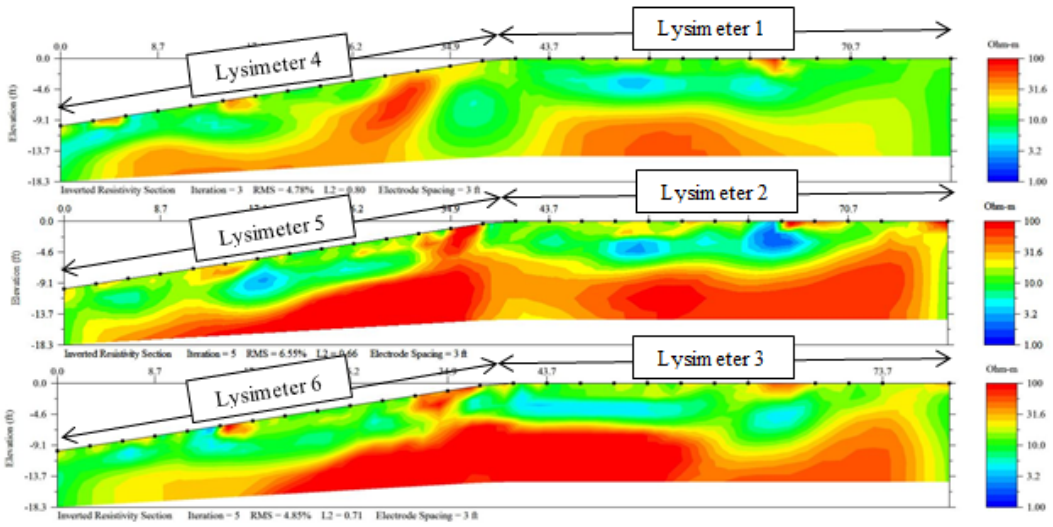

September 2015

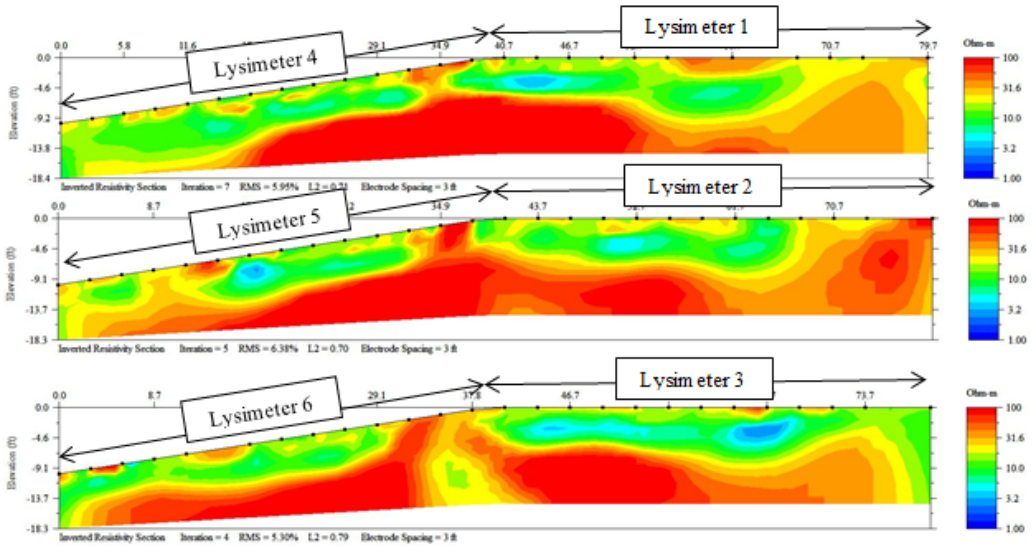

November 2015

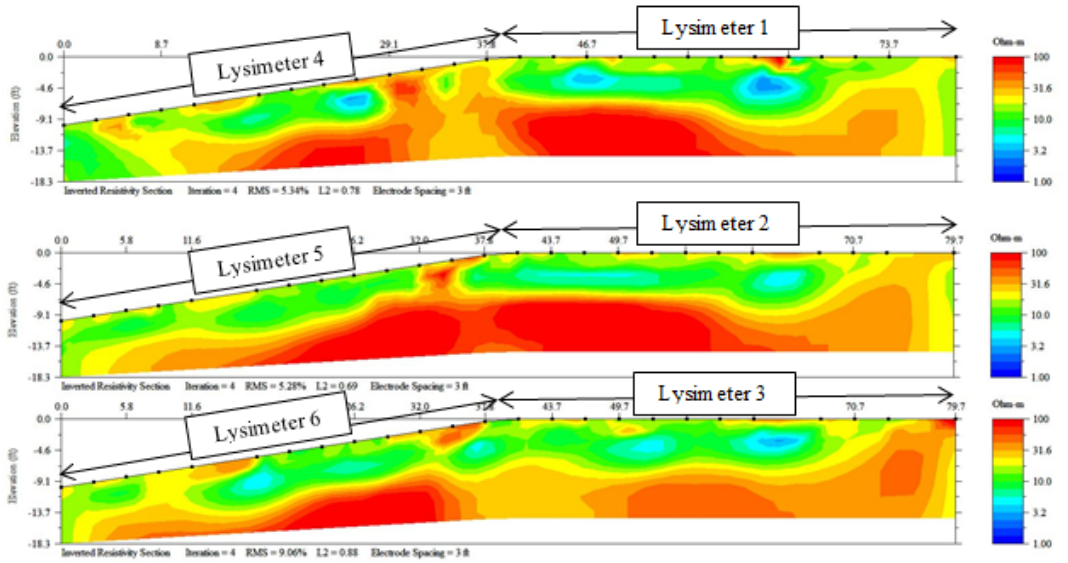

January 2016

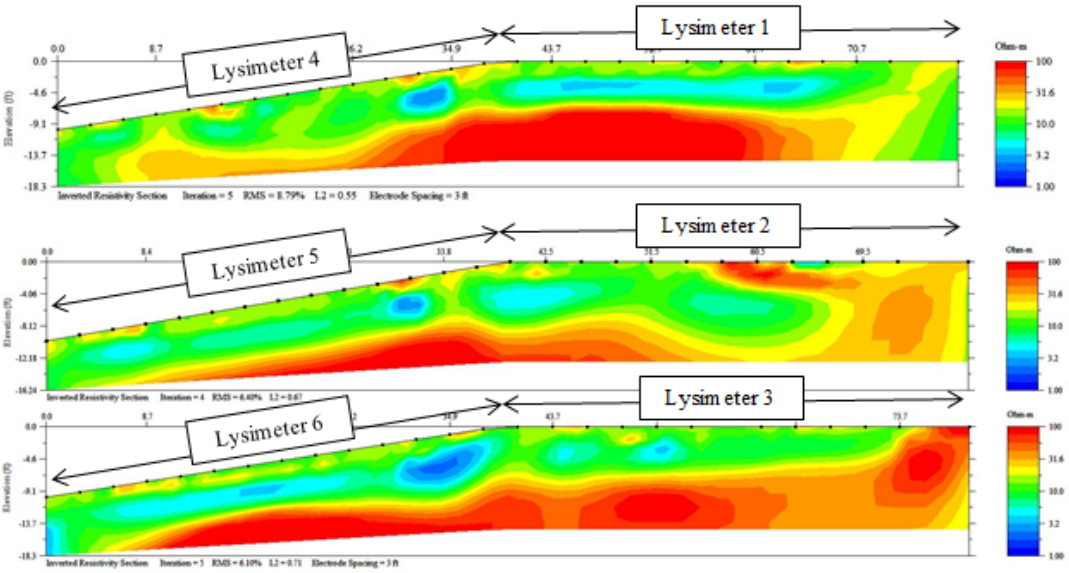

March 2016

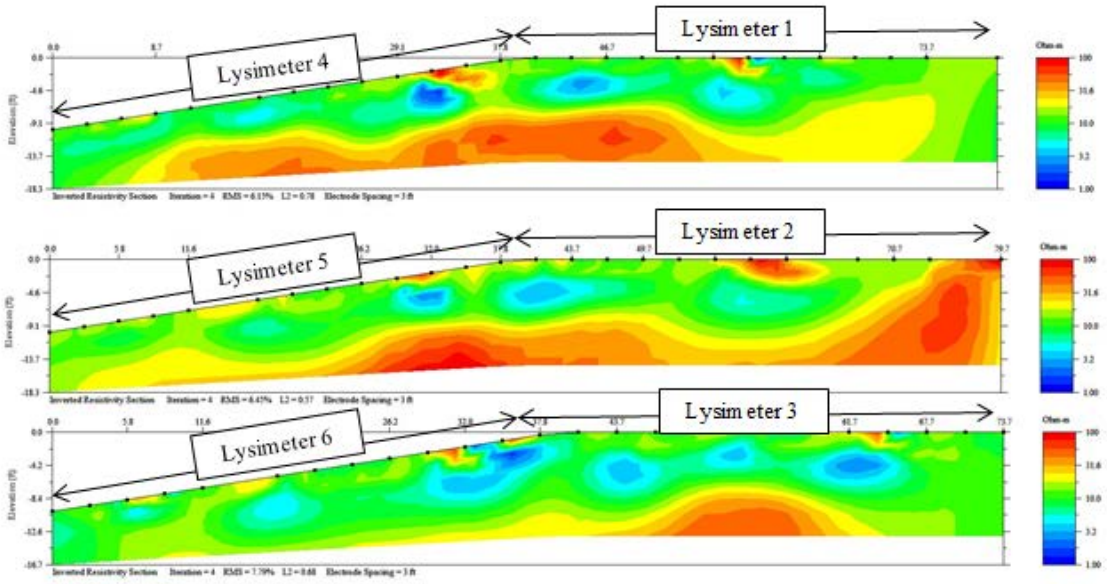

May 2016

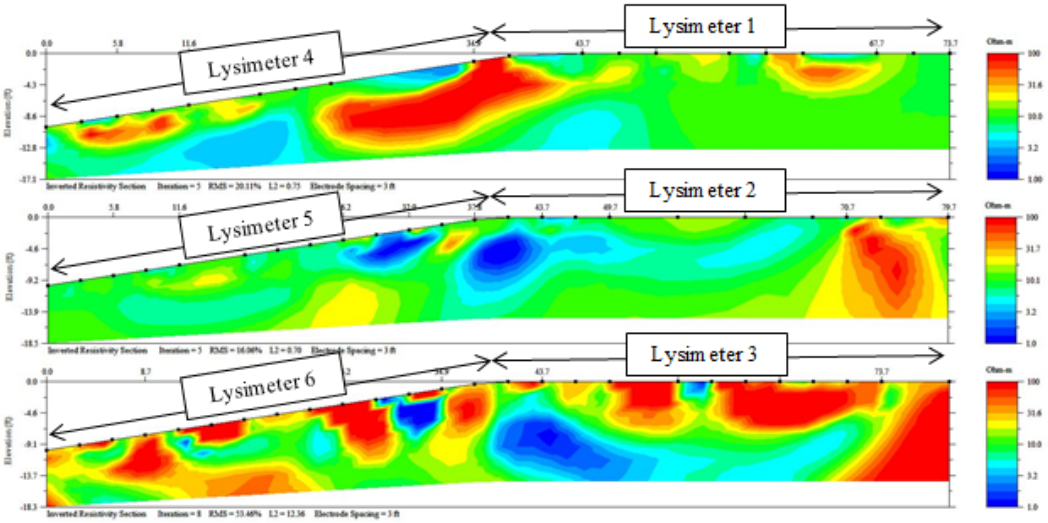

July 2016

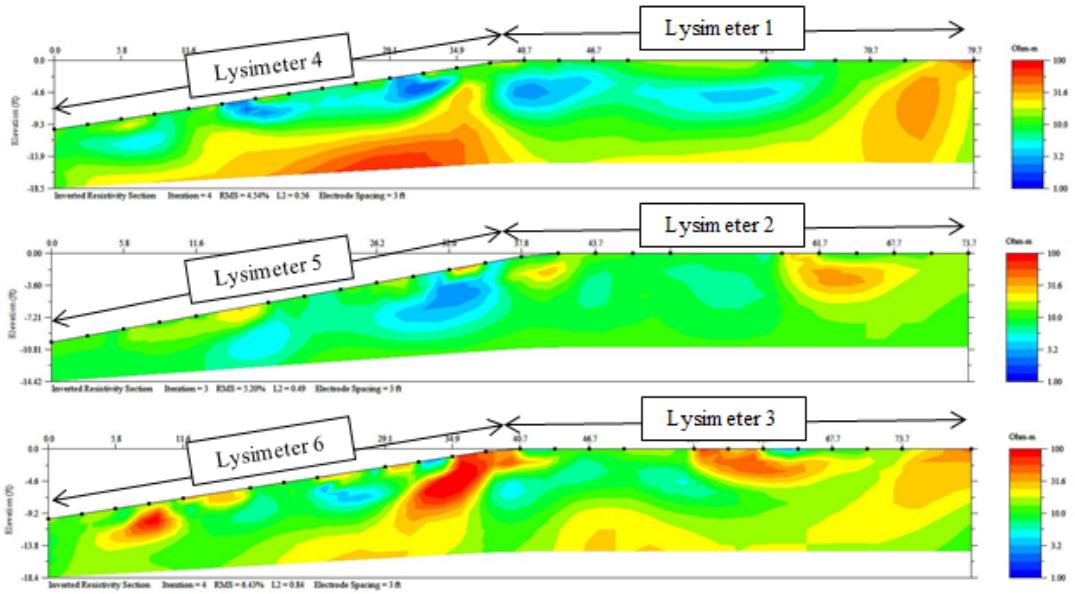

September 2016

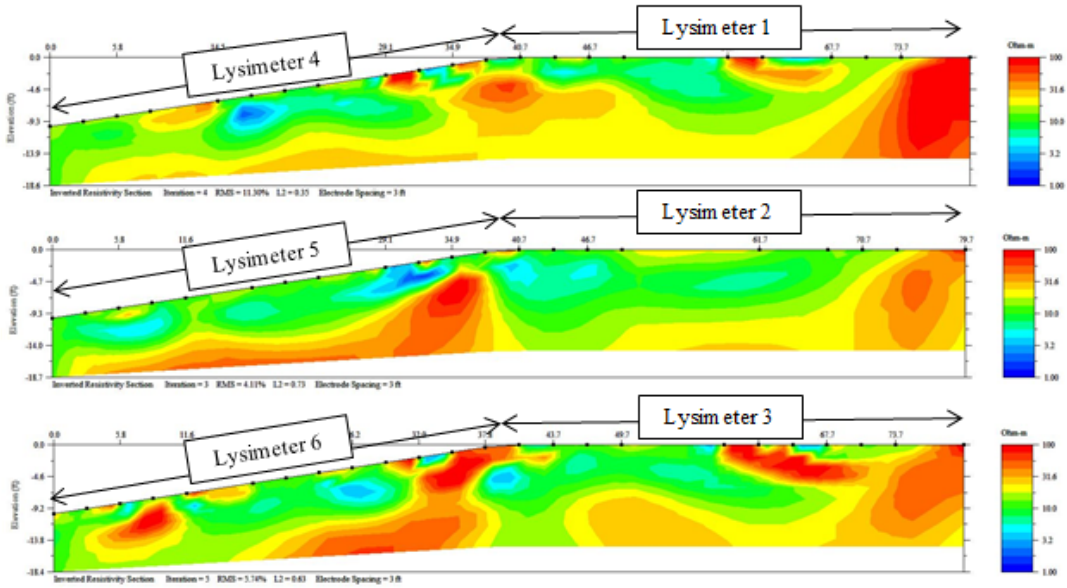

November 2016

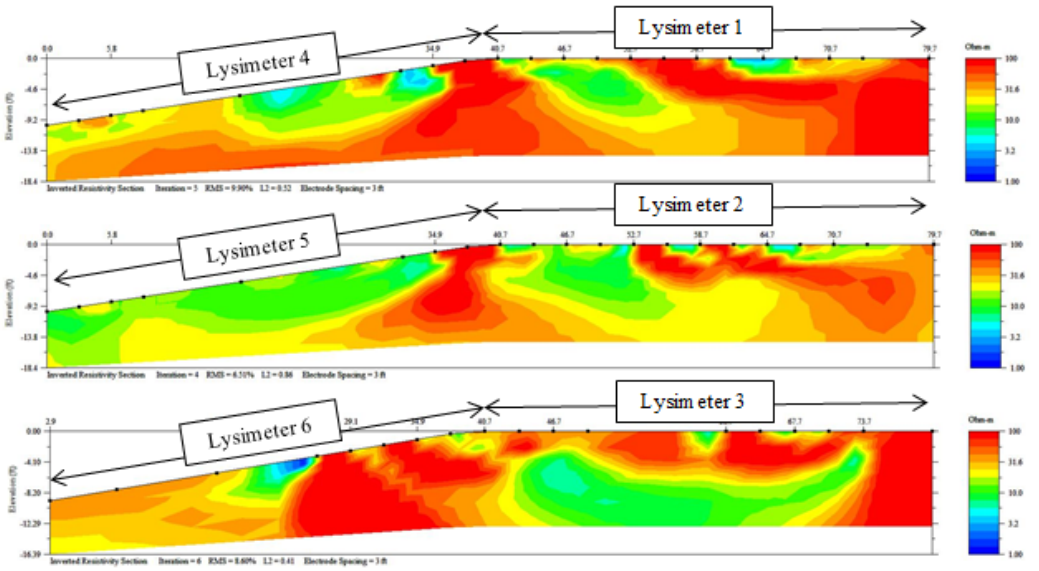

January 2017

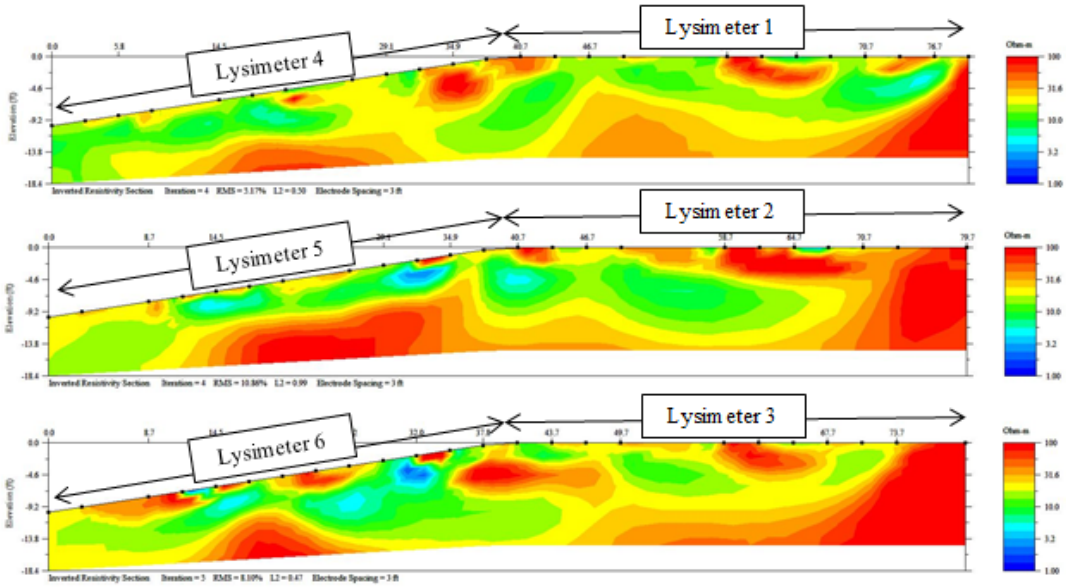

March 2017

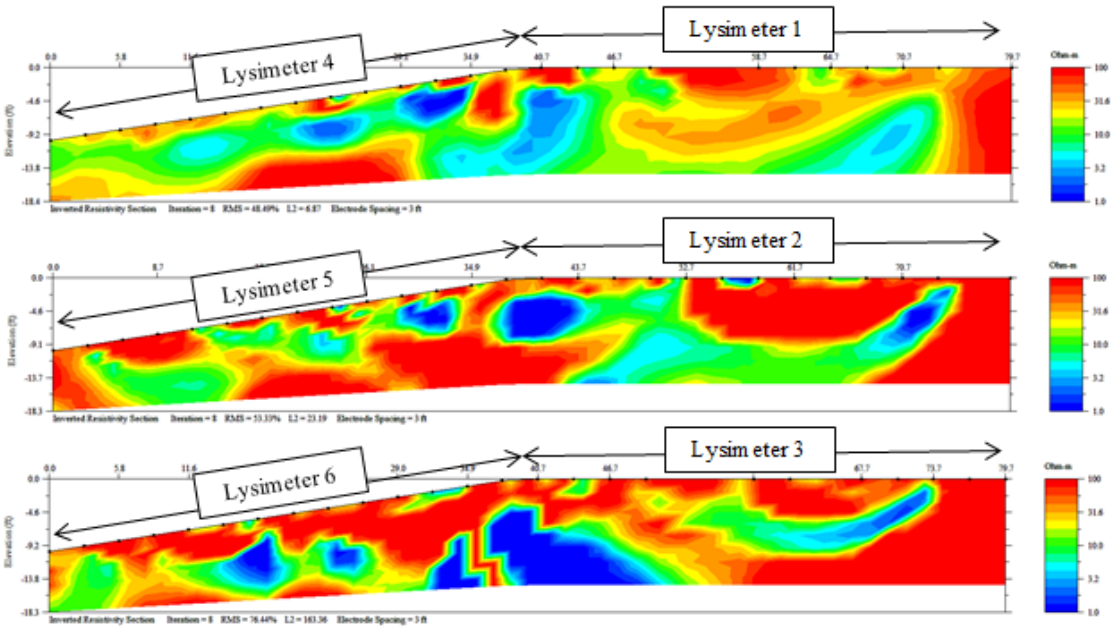
Lysimeter 4
Lysim eter 1
Lysimeter 5
Lysim eter 2
Lysimeter 6
Lysim eter 3

May 2017

REFERENCES

Aaltonen, J. (2001). Seasonal resistivity variations in some different Swedish soils. European Journal of Environmental and Engineering Geophysics, 6(1), 33-45.

Abu-Hassanein, Z. S., Benson, C. H., and Blotz, L. R. (1996). “Electrical resistivity of compacted clays.” Journal of Geotechnical Engineering, 122(5), 397-406.

Advanced Geosciences, Inc., (2004). Instruction Manual for Earth Imager 2D Version 1.7.4. Resistivity and IP Inversion Software 2004. P.O. Box 201087, Austin, Texas 78720.

Aizebeokhai, A. P. (2010). "2D and 3D geoelectrical resistivity imaging: Theory and field design." Scientific Research and Essays, 5(23), 3592-3605.

Albright, W., Benson, C., Gee, G., Roesler, A., Abichou, T., Apiwantragoon, P., Lyles, B. and Rock, S. (2004). “Field water balance of landfill final covers.” J. Environ. Qual., 33, 2317-2332.

Albright, W. H., Benson, C. H., Gee, G. W., Abichou, T., McDonald, E. V., Tyler, S. W., & Rock, S. A. (2006). Field performance of a compacted clay landfill final cover at a humid site. Journal of Geotechnical and Geoenvironmental Engineering, 132(11), 1393-1403.

Albright, W. H., Benson, C. H., & Waugh, W. J. (2010, August). Water balance covers for waste containment: principles and practice. American Society of Civil Engineers.

Al Hagrey, S.A., Meissner, R., Werban, U., Rabbel, W., Ismaeil, A., 2004. Hydro-, biogeophysics. Lead. Edge 23 (7), 670–674.

Al Hagrey, S. A., & Michaelsen, J. (2002). Hydrogeophysical soil study at a drip irrigated orchard, Portugal. European Journal of Environment and Engineering Geophysics, 7, 75-93.

al Hagrey, S.A. (2007). Geophysical imaging of root-zone, trunk, and moisture heterogeneity. J. Exp. Bot. 58:839–854.

Amato, M., Bitella, G., Rossi, R., Gómez, J. A., Lovelli, S., & Gomes, J. J. F. (2009). Multi-electrode 3D resistivity imaging of alfalfa root zone. European Journal of Agronomy, 31(4), 213-222.

Amato, M., Basso, B., Celano, G., Bitella, G., Morelli, G., & Rossi, R. (2008). In situ detection of tree root distribution and biomass by multi-electrode resistivity imaging. Tree physiology, 28(10), 1441-1448.

Amato, M., & Ritchie, J. T. (2002). Spatial distribution of roots and water uptake of maize (L.) as affected by soil structure. Crop Science, 42(3), 773-780.

Ankeny, M.D., L.M. Coons, N. Majumdar, J. Kelsey, and M. Miller. 1997. Performance and Cost Considerations for landfill Caps in Semi-Arid Climates. In: Reynolds, T.D., and R.C. Morris (eds), Landfill Capping in the Semi-Arid West: Problems, Perspectives, and Solutions. Environmental Science and Research Foundation, Idaho Falls, ID.

Archie, G.E., 1942. The electrical resistivity log as an aid in determining some reservoir characteristics. Trans. Am. Inst. Miner. Metall. Petrol. Eng. 146, 54–62.

Arjwech, R. (2011). “Electrical resistivity imaging for unknown bridge foundation depth determination.” Ph.D. Dissertation, Texas A & M University, College Station, TX.

Arulanandan, K. (1969). Hydraulic and electrical flows in clays. Clays Clay Minerals, 17, 63-76.

Arriaga, F. J., Lowery, B., & Raper, R. (2011). Soil Penetrometers and Penetrability. In Encyclopedia of Agrophysics (pp. 757-760). Springer Netherlands.

ASTM. “Annual book of standards, volume 04.08, soil and rock.” West Conshohocken, PA

Attia al Hagrey, S. (2007). Geophysical imaging of root-zone, trunk, and moisture heterogeneity. Journal of Experimental Botany, 58(4), 839-854.

Barnswell, K. D. and Dwyer, D. F. (2011). “Assessing the Performance of Evapotranspiration Covers for Municipal Solid Waste Landfills in Northwestern Ohio.” J. Environ. Engr., 137(4), 301-305.

Bedient, P.B., Huber, W.C., and Vieux, B.E. (2008). Hydrology and Floodplain Analysis, Prentice-Hall, Inc., Upper Saddle River, NJ.

Benson, C. H., & Khire, M. V. (1995). Earthen covers for semi-arid and arid climates. Geotechnical Special Publication, (53), 201-217.

Benson, C., Abichou, T., Olson, M., and Bosscher, P. (1995). “Winter effects on hydraulic conductivity of compacted clay.” J. Geotech. Eng., 121(1), 69-79.

Benson, C., Abichou, T., Albright, W., Gee, G., and Roesler, A. (2001). “Field evaluation of alternative earthen final covers.” Int. J. Phytoremediation, 3(1), 1-21.

Benson, C. H., Albright, W. H., Roesler, A. C., and Abichou, T. (2002). “Evaluation of Final Cover Performance: Field Data from the Alternative Cover Assessment Program (ACAP).” Proc. WM ’02 Conference, February 24-28, 2002: pp. 1-18.

Benson, C. and Bareither, C. (2012). Designing Water Balance Covers for Sustainable Waste Containment: Transitioning State of the Art to State of the Practice. Geotechnical Engineering State of the Art and Practice: pp. 1-33

Besson, A., Cousin, I., Dorigny, A., Dabas, M., and King, D. (2008). “The temperature correction for the electrical resistivity measurements in undisturbed soil samples: Analysis of the existing conversion models and proposal of a new model.” Soil Science, 173(10), 707-720.

Bews, B.E., Barbour, S.L., and Wickland, B. (1999). “Lysimeter design in theory and practice.” Tailings and Mine Waste’99, 13-21.

Binley, A., Peter Winship, L., West, J., Pokar, M., Middleton, R., 2002. Seasonal variation of moisture content in unsaturated sandstone inferred from borehole radar and resistivity profiles. J. Hydrol. 267 (3–4), 160–172.

Bottraud, JC, Bornand, M., & Servat, E. (1984). Resistivity measurements applied to soil mapping. *Soil Science* , *4* , 279-294.

Bourennane, H., Nicoullaud, B., Couturier, A., Pasquier, C., Mary, B., & King, D. (2012). Geostatistical filtering for improved soil water content estimation from electrical resistivity data. Geoderma, 183, 32-40.

Brunet, P., Clément, R., Bouvier, C., 2009. Monitoring soil water content and deficit using Electrical Resistivity Tomography (ERT) – a case study in the Cevennes area, France. J. Hydrol. 380 (1–2), 146–153.

Brocca, L., Morbidelli, R., Melone, F., Moramarco, T., 2007. Soil moisture spatial variability in experimental areas of central Italy. J. Hydrol. 333, 356–373.

Bryson, L. S. (2005). "Evaluation of geotechnical parameters using electrical resistivity measurements." Proc., Earthquake Engineering and Soil Dynamics, GSP 133, Geo-Frontiers 2005, ASCE, Reston, VA.

Calamita, G., Brocca, L., Perrone, A., Piscitelli, S., Lapenna, V., Melone, F., & Moramarco, T. (2012). Electrical resistivity and TDR methods for soil moisture estimation in central Italy test-sites. Journal of Hydrology, 454, 101-112.

Campbell, C. S. (2001). Response of the ECH2O soil moisture probe to variation in water content, soil type, and solution electrical conductivity. Decagon Devices Inc.

Campbell, R.B., Bower, C.A., Richard, L.A., 1948. Change in electrical conductivity with temperature and the relation with osmotic pressure to electrical conductivity and ion concentration for soil extracts. Soil Sci. Soc. Am. Proc. 13, 33–69

Charts, L. I. (1986). Schlumberger Well Services. *Houston, TX (1989, 1991, 1994, and 1997)*.

Chibueze Okpoli, C. (2013). Application of 2D electrical resistivity tomography in landfill site: a case study of Iku, Ikare Akoko, Southwestern Nigeria. *Journal of Geological Research*, *2013*.

Chittoori, B. and Puppala, A. J. (2011). “Quantitative estimation of clay mineralogy in fine grained soils.” *Journal of Geotechnical and Geoenvironmental Engineering*, 137(11), 997-1007.

Cobos, D. R., & Chambers, C. (2010). Calibrating ECH2O soil moisture sensors. Application Note, Decagon Devices, Pullman, WA.

Coleman, D. C., Crossley, D. A., & Hendrix, P. F. (2004). *Fundamentals of soil ecology*. Academic press.

Cosenza, P., Marmet, E., Rejiba, F., Cui, Y.J., Tabbagh, A., Charlery, Y., 2006. Correlations between geotechnical and electrical data: a case study at Garchy in France. J. Appl. Geophys. 60 (3–4), 165–178.

Croney, D., Coleman, J., and Currer, E. (1951). "The electrical resistance method of measuring soil moisture." *British Journal of Applied Physics,* 2 (4), 85-91.

Dahlin, T., & Zhou, B. (2004). A numerical comparison of 2D resistivity imaging with 10 electrode arrays. *Geophysical prospecting*, *52*(5), 379-398.

DeVries, B. (2016). “Hydraulic performance evaluation of evapotranspiration cover systems”, Ph.D. Dissertation, University of Texas at Arlington.

Dey, A., & Morrison, H. F. (1979). Resistivity modeling for arbitrarily shaped three-dimensional structures. *Geophysics*, *44*(4), 753-780.

Di, S., Jing-fang, X., De-xin, G., An-zhi, W., Jia-bing, W., & Feng-hui, Y. (2010). Soil water characteristic curves at different soil depths in a broad-leaved Korean pine forest in Changbai Mountains. YingyongShengtaiXuebao, 21(6).

Duble, R. L. (2007). Bermuda grass: The sports turf of the South.

Dugas, W. A., Reicosky, D. C., and Kiniry, J. R. (1997).“Chamber and micrometeorological measurement of CO2 and H2O fluxes for three C4 grasses. “Agricultural and Forest Meteorology, 83, 113-133.

Duiker, S. W. (2002).Diagnosing soil compaction using a penetrometer (soil compaction tester). Agronomy Facts, 63(4).

Dunn, R. J. (1995). Landfill Closures: Environmental Protection and Land Recovery. ASCE.

Dwyer, S. F. (2003). Water balance measurements and computer simulations of landfill covers (Doctoral dissertation, The University of New Mexico).

Entin, J.K., Robock, A., Vinnikov, K.Y., Hollinger, S.E., Li, S., Namkai, A., 2000. Temporal and spatial scales of observed soil moisture variations in the extratropics. J. Geophys. Res. 105, 865–877.

Friedman, S. P. (2005). “Soil properties influencing apparent electrical conductivity: a review.” Computers and electronics in agriculture, 46(1), 45-70. Application note, Washington, DC.

Fukue, M., Minato, T., Horibe, H., Taya, N., 1999. The micro structures of clay given by resistivity measurements. Eng. Geol. 54, 43–53.

Garcia, C. A., Johnson, M. J., Andraski, B. J., Halford, K. J., and Mayers, C. J. (2008). “Portable chamber measurements of evapotranspiraton at the Amargosa Desert Research Site near Beatty, Nye County, Navada, 2003-06.”U.S. Geological Survey, Reston, VA.

Gee., G. and Hillel, D. (1988). “Groundwater Recharge in Arid Regions: Review and Critique of Estimation Methods,” J. of Hydrological Processes, 2, 255-266.

Goldenberg, M., & Reddy, K. R. Sustainability Assessment of Conventional and Alternate Landfill Cover Systems. In *Geotechnical Frontiers 2017* (pp. 323-332).

Goyal, V.C., Gupta, P.K., Seth, S.M., Singh, V.N., 1996. Estimation of temporal changes in soil moisture using resistivity method. Hydrol. Process. 10 (9), 1147–1154.

Gupta, S.C., Hanks, R.J., 1972. Influence of water content on electrical conductivity of the soil. Soil Sci. Soc. Am. Proc. 36, 855–857.

Hakonson, T. E., L. Karr, and B. Harre. (1997) "A water balance study of infiltration control landfill cover designs at Marine Corp Base, Hawaii." Landfill Capping in the Semi-Arid West: Problems, Perspectives, and Solutions. Proceedings of the Environmental Science and Research Foundation Conference.

Hanlon, E. A., &Bartos, J. M. (1993). Soil pH and electrical conductivity: a country extension soil laboratory manual. Circular (USA). no. 1081.

Hauser, V. L. (2008). Evapotranspiration covers for landfills and waste sites. Boca Raton, FL: C RC Press.

Hauser, V. L., D. M. Gimon, D. E. Hadden, and B. L. Weand. 1999. Survey of Air Force Landfills, Their Characteristics, and Remediation Strategies. Air Force Center for Environmental Excellence (AFCEE), Brooks AFB, TX. Available at: http://www.afcee.brooks.af.mil/er/ert/landfill.htm.

Hauser, V. L., and D. M. Gimon. 2001. Vegetated Landfill Covers and Phytostabilization-The potential for Evapotranspiration-Based Remediation at Air Force Bases. Air Force Center for Environmental Excellence (AFCEE), Brooks AFB, TX. Available at: http://www.afcee.brooks.af.mil/er/ert/landfill.htm

Hossain, J. (2012). “Geohazard potential of rainfall induced slope failure on expansive clay.” *Ph.D. Dissertation,* University of Texas at Arlington, TX.

Hymer, D.C., Moran, M.S., Keefer, T.O., 2000. Soil moisture evaluation using a hydrologic model and calibrated sensor network. Soil Sci. Soc. Am. J. 64, 319–326.

Jakobsen, B. F., & Dexter, A. R. (1987). Effect of soil structure on wheat root growth, water uptake and grain yield. A computer simulation model. *Soil and Tillage Research*, *10*(4), 331-345.

Jackson, T. J. (1993). III. Measuring surface soil moisture using passive microwave remote sensing. *Hydrological processes*, *7*(2), 139-152.

Jayawickreme, D. H., Van Dam, R. L., & Hyndman, D. W. (2008). Subsurface imaging of vegetation, climate, and root-zone moisture interactions. Geophysical Research Letters, 35(18).

Jones, C. A. (1983). Effect of soil texture on critical bulk densities for root growth. *Soil Science Society of America Journal*, *47*(6), 1208-1211.

Kalinski, R.J., Kelly, W.E., 1993. Estimating water content of soils from electrical resistivity. ASTM Geotech. Test. J. 16 (3), 323–329.

K. A. Olsson and B. Cockrof, Structure, Managing Belowground, Encyclopedia of Soil Science, 2002

Kibria, G. (2014). *Evaluation of physico-mechanical properties of clayey soils using electrical resistivity imaging technique*. The University of Texas at Arlington.

Kibria, G., & Hossain, M. S. (2012). Investigation of geotechnical parameters affecting electrical resistivity of compacted clays. Journal of Geotechnical and Geoenvironmental Engineering, 138(12), 1520-1529.

Kibria, G., Hossain, M. S., Hossain, J., & Khan, M. S. (2012). Determination of moisture content and unit weight of clayey soil using resistivity imaging (RI). Proceedings of GeoCongress, 398-3.

Kibria, G., & Hossain, M. S. (2015). Investigation of degree of saturation in landfill liners using electrical resistivity imaging. Waste Management, 39, 197-204.

Kizito, F., Campbell, C. S., Campbell, G. S., Cobos, D. R., Teare, B. L., Carter, B., &Hopmans, J. W. (2008). Frequency, electrical conductivity and temperature analysis of a low-cost capacitance soil moisture sensor. Journal of Hydrology, 352(3), 367-378.

Koerner, R. M., & Daniel, D. E. (1997). *Final covers for solid waste landfills and abandoned dumps*. Thomas Telford.

Koide, R. T., Robichaux, R. H., Morse, S. R., & Smith, C. M. (2000). Plant water status, hydraulic resistance and capacitance. In Plant physiological ecology (pp. 161-183). Springer Netherlands.

Lapenna, V., Lorenzo, P., Perrone, A., Piscitelli, S., Rizzo, E., Sdao, F., 2005. 2D electrical resistivity imaging of some complex landslides in Lucanian Apennine (Southern Italy). Geophysics 70 (3), B11–B18.

Lazzari, L. (2008). *Study of spatial variability of soil root zone properties using electrical resistivity technique* (Doctoral dissertation, Ph. D. Thesis. University of Basilicata, Potenza, Italy).

Liang, C. H. E. N., YIN, Z. Z., & ZHANG, P. (2007). Relationship of resistivity with water content and fissures of unsaturated expansive soils. Journal of China University of Mining and Technology, 17(4), 537-540.

Licht, L., Aitchison, E., Schnabel, W., English, M., & Kaempf, M. (2001). Landfill capping with woodland ecosystems. Practice Periodical of Hazardous, Toxic, and Radioactive Waste Management, 5(4), 175-184.

Loke, M. H. (2000). Electrical imaging surveys for environmental and engineering studies. A practical guide to 2-D and 3-D surveys.

Loke, M. H. (2001, January). Constrained time-lapse resistivity imaging inversion. In *Symposium on the Application of Geophysics to Engineering and Environmental Problems 2001*(pp. EEM7-EEM7). Society of Exploration Geophysicists.

Loperte, A., A. Satriani., L. Lazzari, M. Amato, G. Celano, V. Lapenna and G. Morelli. 2006. 2D and 3D high resolution geoelectrical tomography for non-destructive determination of the spatial variability of plant root distribution: laboratory experiments and field measurements. Geophys. Res. Abstr. Wien 8:06749.

Lowery, B., & Morrison, J. E. (2002).Soil penetrometers and penetrability. Methods of Soil Analysis: Part 4: Physical Methods.

Madalinski, K. L., Gratton, D. N., & Weisman, R. J. (2003). Evapotranspiration covers: An innovative approach to remediate and close contaminated sites. Remediation Journal, 14(1), 55-67.

Malusis, M. A., & Benson, C. H. (2006). Lysimeters versus water-content sensors for performance monitoring of alternative earthen final covers. Geotechnical Special Publication, 147(1), 741.

Manzur, S. R., Hossain, M. S., Kemler, V., & Khan, M. S. (2016). Monitoring extent of moisture variations due to leachate recirculation in an ELR/bioreactor landfill using resistivity imaging. Waste Management.

McBean, E.A., F.A. Rovers, and G.J. Farquhar. 1995. Solid Waste Landfill Engineering and Design. Prentice Hall PTR, Englewood Cliffs, NJ.

McCarter, W.J., 1984. The electrical resistivity characteristics of compacted clays. Geotechnique 34, 263–267.

McLean, E. O. (1982). Soil pH and lime requirement. Methods of soil analysis. Part 2. Chemical and microbiological properties, (methodsofsoilan2), 199-224.

McLoed, M. K., Daniel, H., Faulkner, R., and Murison, R. (2004). “Evaluations of an enclosed portable chamber to measure crop and pasture actual evapotranspiration at small scale.” Agricultural Water Management, 67, 15-34.

Meheni, Y., Guérin, R., Benderitter, Y., & Tabbagh, A. (1996). Subsurface DC resistivity mapping: approximate 1-D interpretation. *Journal of Applied Geophysics*, *34*(4), 255-269.

Melchior, S. (2002, April). Field studies and excavations of geosynthetic clay barriers in landfill covers. In Clay Geosynthetics Barriers, Proceedings of the international symposium IS Nuremberg (pp. 321-330).

Mitchell, J., and Soga, K. (2005). "Fundamentals of soil behavior.” *John Wiley and Sons, Inc.,* Hoboken, NJ.

Michot, D., Benderitter, Y., Dorigny, A., Nicollaud, B., King, D., Tabbagh, A., 2003. Spatial and temporal monitoring of soil water content with an irrigated corn crop cover using surface electrical resistivity tomography. Water Resour. Res. 39 (5), 1138.

Mualem, Y., Friedman, S.P., 1991. Theoretical prediction of electrical conductivity in saturated and unsaturated soil. Water Resour. Res. 27 (10), 2771–2777.

Muchingami, I., Nel, J., Xu, Y., Steyl, G., & Reynolds, K. (2013). On the use of electrical resistivity methods in monitoring infiltration of salt fluxes in dry coal ash dumps in Mpumalanga, South Africa. Water SA, 39(4), 00-00.

Chik, Z., Murad, O. F., & Rahmad, M. (2016). Dependency of dry density of soil on water content in the measurement of electrical resistivity of soil. *Journal of Engineering Research and Technology*, *2*(2).

Ng, C. W. W., & Zhan, L. T. (2007). Comparative study of rainfall infiltration into a bare and a grassed unsaturated expansive soil slope. Soils and foundations, 47(2), 207-217.

Nijland, W., Van der Meijde, M., Addink, E. A., & De Jong, S. M. (2010). Detection of soil moisture and vegetation water abstraction in a Mediterranean natural area using electrical resistivity tomography. Catena,81(3), 209-216.

Nyhan, J. W., Hakonson, T. E., & Drennon, B. J. (1990). A water balance study of two landfill cover designs for semiarid regions. *Journal of Environmental Quality*, *19*(2), 281-288.

Oldenburg, D. W., & Li, Y. (1994). Inversion of induced polarization data. *Geophysics*, *59*(9), 1327-1341.

Ozcep, F., Tezel, O., & Asci, M. (2009). Correlation between electrical resistivity and soil-water content: Istanbul and Golcuk. International Journal of Physical Sciences, 4(6), 362-365.

Pazdirek, O., & Blaha, V. (1996, June). Examples of resistivity imaging using ME-100 resistivity field acquisition system. In *58th EAGE Conference and Exhibition*.

Paglis, C. M. (2013). Application of electrical resistivity tomography for detecting root biomass in coffee trees. International Journal of Geophysics, 2013.

Panissod, C., Michot, D., Benderitter, Y., & Tabbagh, A. (2001). On the effectiveness of 2D electrical inversion results: an agricultural case study. *Geophysical Prospecting*, *49*(5), 570-576.

Pozdnyakova, L.A., 1999. Electrical Properties of Soils. Ph.D. Thesis, University of Wyomins, USA

Reicosky, D. C., Sharratt, B. S., Ljungkull, J. E., and Baker, D. G. (1983).“Comparison of alfalfa evapotranspiration measured by a weighing lysimeter and a portable chamber. “Agricultural Meteorology, 28, 205-211.

Rhoades, J.D., Raats, P.A.C., Prather, R.J., 1976. Effect of liquid phase electrical conductivity, water content, and surface conductivity on bulk soil electrical conductivity. Soil Sci. Soc. Am. J. 40, 651–655.

Rimi, F., Macolino, S., & Ziliotto, U. (2012). Rooting characteristics and turf grass quality of three Bermuda grass cultivars and a zoysia grass. *Acta Agriculturae Scandinavica, Section B-Soil & Plant Science*, *62*(sup1), 24-31.

Rinaldi, V. A., and Cuestas, G. A. (2002). "Ohmic conductivity of a compacted silty clay." *J. Geotechnical and Geoenvironmental Engineering,* 128 (10), 824- 835.

Robinson, D.A., Campbell, S.C., Hpmans, J.W., Hornbuckle, B.K., Jones, S.B., Knight, R., Odgen, F., Selker, J., Wendroth, O., 2008a. Soil moisture measurement for ecological and hydrological watershed-scale observatories: a review. Vadose Zone J. 7, 359–389.

Rock, S., Myers, B., and Fiedler, L. (2012). “Evapotranspiration (ET) covers.” International Journal of Phytoremediation, 14(S1), 1-25.

Sadek, M.S. (1993). “A comparative study of the electrical and hydraulic conductivities of compacted clay.” *Ph.D. Dissertation*, University of California, Berkeley, CA.

Samouëlian, A., Cousin, I., Richard, G., Tabbagh, A., & Bruand, A. (2003). Electrical resistivity imaging for detecting soil cracking at the centimetric scale. *Soil Science Society of America Journal*, *67*(5), 1319-1326.

Samouëlian, A., Cousin, I., Tabbagh, A., Bruand, A., & Richard, G. (2005). Electrical resistivity survey in soil science: a review. Soil and Tillage research, 83(2), 173-193.

Santamarina, J. C., Klein, K.A. and Fam, M.A. (2001). "Soil and Waves: Particulate material behavior, characterization and monitoring." *John Wiley and Sons*, NY.

Sauchelli, V. (1969). Trace elements in agriculture. Trace elements in agriculture.

Schnabel, W. E., Munk, J., Abichou, T., Barnes, D., Lee, W., & Pape, B. (2012). Assessing the performance of a cold region evapotranspiration landfill cover using lysimetry and electrical resistivity tomography. International journal of phytoremediation, 14(sup1), 61-75.

Schwartz, B. F., Schreiber, M. E., & Yan, T. (2008). Quantifying field-scale soil moisture using electrical resistivity imaging. Journal of Hydrology, 362(3), 234-246.

Seladji, S., Cosenza, P., Tabbagh, A., Ranger, J., & Richard, G. (2010). The effect of compaction on soil electrical resistivity: a laboratory investigation. European journal of soil science, 61(6), 1043-1055.

Seneviratne, S. I., Lüthi, D., Litschi, M., & Schär, C. (2006). Land-atmosphere coupling and climate change in Europe. *Nature*, *443*(7108), 205.

Sharma, P. V. (1997). Environmental and engineering geophysics. Cambridge university press.

Shevnin, V., Mousatov, A., Ryjov, A., and Delgado-Rodriquez, O. (2007). “Estimation of clay content in soil based on resistivity modelling and laboratory measurements.” Geophysical Prospecting, 55(2), 265-275.

Skempton, A. W. (1953). The colloidal activity of clays. Selected Papers on Soil Mechanics, 106-118.

Smith, J. L., & Doran, J. W. (1996). Measurement and use of pH and electrical conductivity for soil quality analysis. Methods for Assessing Soil Quality. Soil Science Society of America (SSSA). Special Publication, (49).

Stannard, D. I. (1988). “Use of a hemispherical Chamber for measurement of evapotranspiration.”U.S. Geological Survey, Reston, VA.

Stannard, D. I. and Weltz, M. A. (2006).“Partitioning evapotranspiration in sparsely vegetated rangeland using a portable chamber. “Water Resources Research, 42, 1-13.

Stormont, J. C., & Morris, C. E. (1998). Method to estimate water storage capacity of capillary barriers. *Journal of Geotechnical and Geoenvironmental Engineering*, *124*(4), 297-302.

Suter, G. W., Luxmoore, R. J., & Smith, E. D. (1993). Compacted soil barriers at abandoned landfill sites are likely to fail in the long term. *Journal of Environmental Quality*, *22*(2), 217-226.

Squillace, M., Babb, E., Kean, B., & Snider, C. (2012). Evapotranspiration Landfill Cover Systems Provide a Natural, Cost-Effective, High-Performance Solution. Burns & McDonnell Publication.

Tabbagh, A., and Cosenza, P. (2007). Effect of microstructure on the electrical conductivity of clay-rich systems. *Physics and Chemistry of the Earth, Parts A/B/C*, *32*(1), 154-160.

Thomas, G. W. (1996). Soil pH and soil acidity. *Methods of Soil Analysis Part 3—Chemical Methods*, (methodsofsoilan3), 475-490.

Topp, G. C., Davis, J. L., & Annan, A. P. (1980). Electromagnetic determination of soil water content: Measurements in coaxial transmission lines. Water resources research, 16(3), 574-582.

Texas Commission on Environmental Quality (TCEQ) (2012). "Guidance for Requesting a Water Balance Alternative Final Cover for a Municipal Solid Waste Landfill." Waste Permits Division, Texas Commission on Environmental Quality, Austin, TX.

Twum, E. K., & Nii-Annang, S. (2015). Impact of soil compaction on bulk density and root biomass of Quercus petraea L. at Reclaimed Post-Lignite Mining Site in Lusatia, Germany. Applied and Environmental Soil Science, 2015.

U.S. Environmental Protection Agency (USEPA) (2011). "Fact Sheet on Evapotranspiration Landfill Cover Systems for Waste Containment." Solid Waste and Emergency Response, U.S. Environmental Protection Agency, Cincinnati, OH.

U.S. Environmental Protection Agency (USEPA) (2006). "Evapotranspiration Landfill Cover Systems FactSheet." Solid Waste and Emergency Response, U.S. Environmental Protection Agency, Cincinnati, OH.

Vachaud, G., Passerat de Silans, A., Balabanis, P., & Vauclin, M. (1985). Temporal stability of spatially measured soil water probability density function. Soil Science Society of America Journal, 49(4), 822-828.

Van Quang, P., & Jansson, P. E. (2012).Soil penetration resistance and its dependence on soil moisture and age of the raised-beds in the Mekong Delta, Vietnam.

Voronin, A. D. (1986). The basics of soil physics.

Walker, J. P., Willgoose, G. R., & Kalma, J. D. (2004). In situ measurement of soil moisture: a comparison of techniques. Journal of Hydrology, 293(1), 85-99.

Walker, J.P., Houser, P.R., 2002. Evaluation of the OhmMapper instrument for soil moisture measurement. Soil Sci. Soc. Am. J. 66, 728–734.

Western, A. W., Blöschl, G., & Grayson, R. B. (1998). Geostatistical characterization of soil moisture patterns in the Tarrawarra catchment. Journal of Hydrology, 205(1-2), 20-37.

Xiaojun, L. I. U. S. Z. H. A. F. (2006). LABORATORY MEASUREMENT TECHNIQUES OF THE ELECTRICAL RESISTIVITY OF SOILS [J]. Journal of Engineering Geology, 2, 012.

Xu, J. M., Tang, C., & Chen, Z. L. (2006). The role of plant residues in pH change of acid soils differing in initial pH. Soil Biology and Biochemistry, 38(4), 709-719.

Yukselen, Y., and Kaya, A. (2006). Prediction of cation exchange capacity from soil index properties. Clay Minerals, 41(4), 827-837.

Zhu, J.J., Kang, H.Z., Gonda, Y., 2007. Application of Wenner configuration to estimate soil water content in pine plantations on sandy land. Pedosphere 17, 801–812

Zhou, Q.Y., Shimada, J., Sato, A., 2001. Three-dimensional spatial and temporal monitoring of soil water content using electrical resistivity tomography. Water Resour. Res. 37, 273–285.

BIOGRAPHICAL INFORMATION

Md Ishtiaque Hossain was born in Dhaka, Bangladesh on August 04, 1989. He graduated with a Bachelor of Science in Civil Engineering from Bangladesh University of Engineering and Technology in March 2013. He started his career as a lecturer in the Civil Engineering Department of Stamford University Bangladesh in August 2013, and joined the University of Texas at Arlington in spring 2014 for graduate studies, where he is currently pursuing his Ph.D. degree. He had the opportunity to work as graduate research assistant under Dr. Sahadat Hossain. The author's research interests include electrical properties of landfill cover soil, geophysical testing, landfill fugitive emission, application of numerical modeling in geotechnical engineering, non-destructive testing, and geotechnical aspects of municipal solid waste (MSW).